Supporting Information for

A Versatile Modification Strategy to Enhance Polyethylene Properties through Solution-State Peroxide Modifications

Utku Yolsal,[a] Thomas J. Neal,[a] James A. Richards,[b] John R. Royer,[b] Jennifer A. Garden*[a]

[a]*EaStCHEM School of Chemistry, The University of Edinburgh, Joseph Black Building, David Brewster Road, Edinburgh, EH9 3FJ, Scotland, United Kingdom*
[b]*School of Physics and Astronomy, University of Edinburgh, King's Buildings, Peter Guthrie Tait Road, Edinburgh, EH9 3FD, Scotland, United Kingdom*

** Corresponding author: j.garden@ed.ac.uk*

Table of Contents

1 Nuclear Magnetic Resonance (NMR) Spectroscopy Results of Injection Moulding HDPE (IMPE) 2

2 Linear Rheological Characterisation of the Commercial and Modified Samples 4

3 Nonlinear Rheology 40

4 Size Exclusion Chromatograms of the Modified Samples 44

5 Differential Scanning Calorimetry (DSC) Results of the Modified Samples 48

6 Wide Angle and Small Angle X-Ray Scattering (WAXS and SAXS) Results 57

7 NMR Spectroscopy Results of the Modified Samples 59

8 Small Molecule Reactivity Studies on n-Dodecane 62

9 FT-IR Analysis 63

10 References 63

1 Nuclear Magnetic Resonance (NMR) Spectroscopy Results of Injection Moulding HDPE (IMPE)

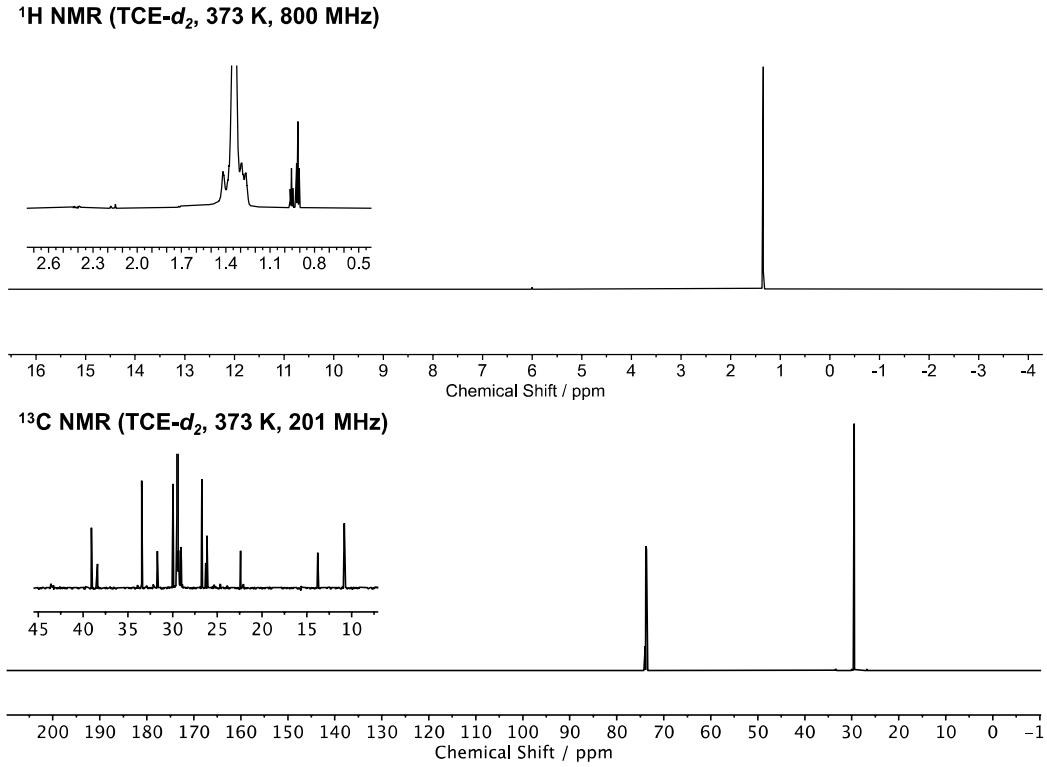

Figure S1: ^{1}H and ^{13}C NMR spectra of **IMPE**.

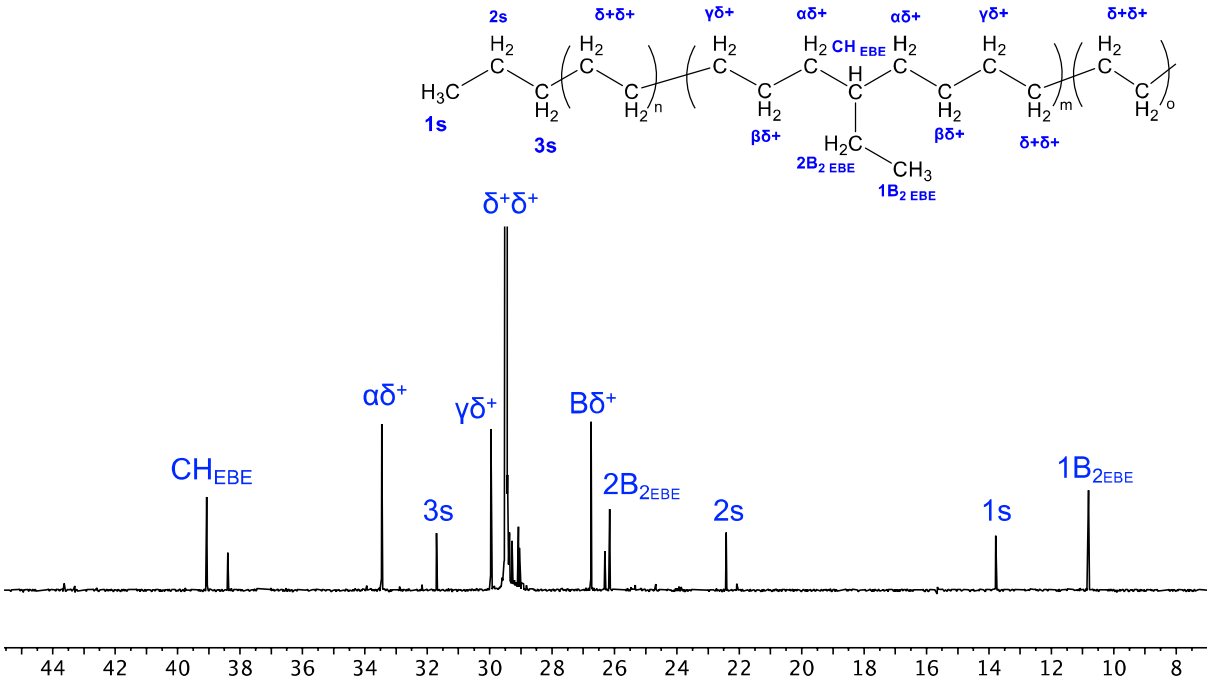

Figure S2: Assignment of the ^{13}C NMR spectrum of **IMPE** in accordance with literature.[1]

Table S1: A summary of the ^{13}C NMR spectrum results for **IMPE**.

^{13}C Peak (ppm)	Integral[a]	Moiety	Origin monomer
10.8	4.26	CH_3	Butene
13.8	2.00	CH_3	Ethylene
22.4	1.96	CH_2	Ethylene
26.2	4.10	CH_2	Butene
26.8	7.89	CH_2	Ethylene
29.5	1270.45	CH_2	Ethylene
30	7.93	CH_2	Ethylene
31.7	2.03	CH_2	Ethylene
33.5	8.04	CH_2	Butene and Ethylene[b]
39.1	3.98	CH	Butene

[a] The integral value of 1s peak was set to 2 as an ideal polymer chain would have two CH_3 end groups. [b] 4.02 area under signal each.

Calculation S1: Estimating the 1-butene comonomer content in **IMPE** in accordance with the ^{13}C NMR results.

1-Butene mol% = (Sum of Peak Integrals Originating from 1-Butene Monomer) / (Sum of All Integrals) * 100

1-Butene mol% = 1.2 mol%

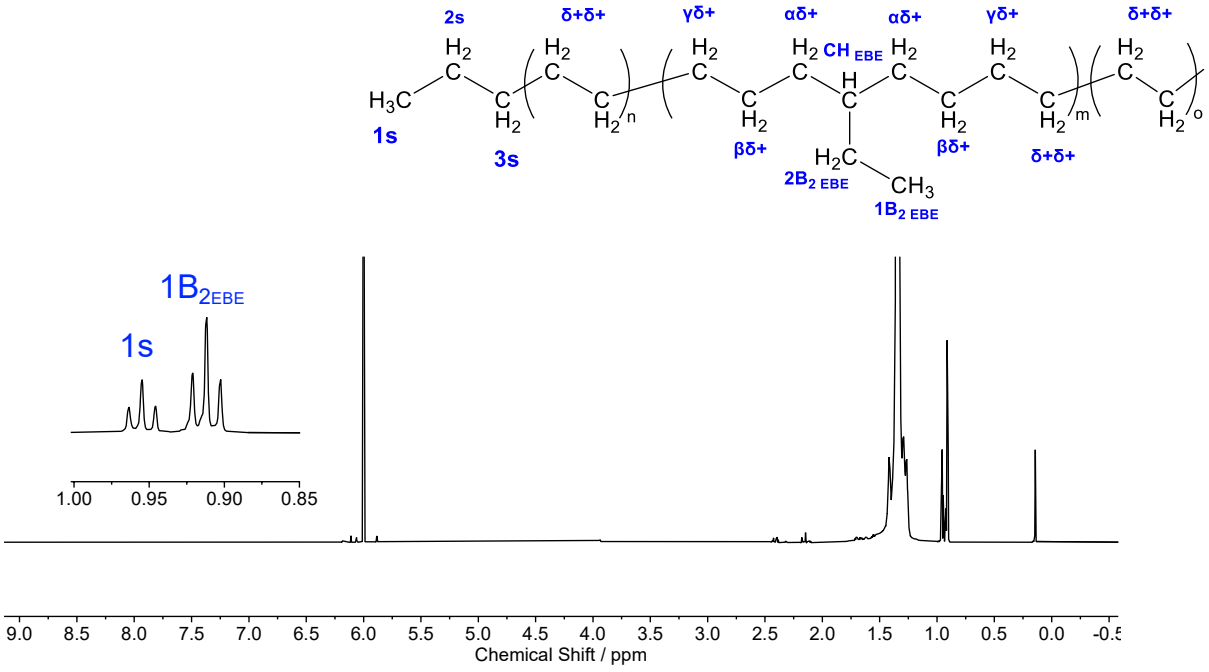

Figure S3: Assignment of the ^{1}H NMR spectrum of **IMPE** in accordance with literature.[1] The peak at 6.0 ppm originates from the NMR solvent.

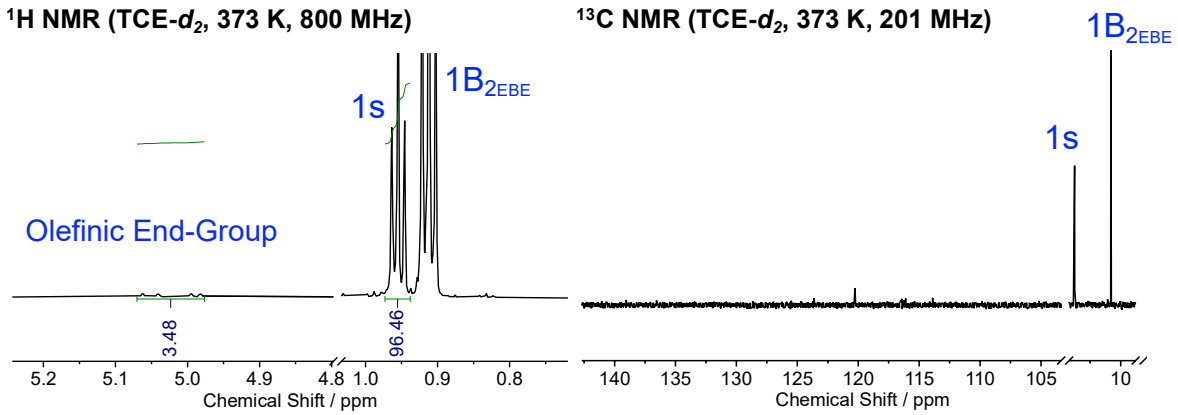

Figure S4: Investigating for the presence of olefinic end-groups in **IMPE**. While a small amount of olefinic units were identified in the proton NMR, it was not possible to identify any olefinic carbons with ^{13}C NMR spectroscopy. This figure shows that the amount of any olefin end-group is very low, and most chains are fully saturated.

2 Linear Rheological Characterisation of the Commercial and Modified Samples

- **IMPE**

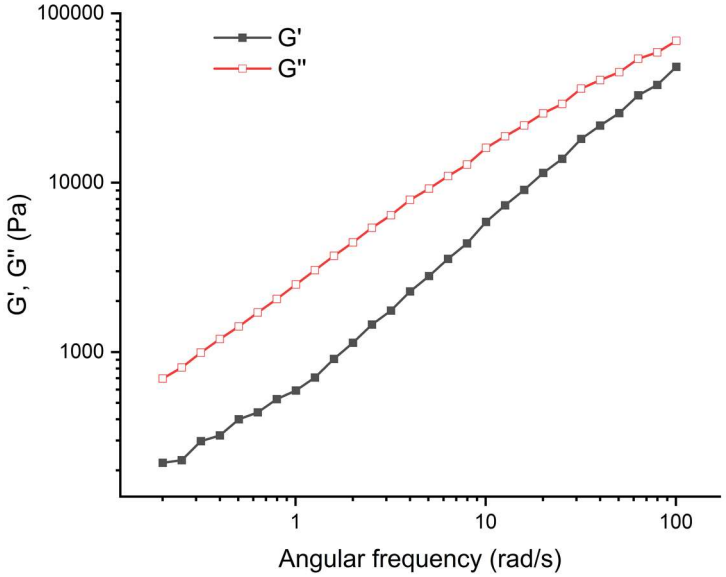

Figure S5: Frequency dependencies of the dynamic moduli (at 1% amplitude, 190 °C) for the injection-moulding grade polymer.

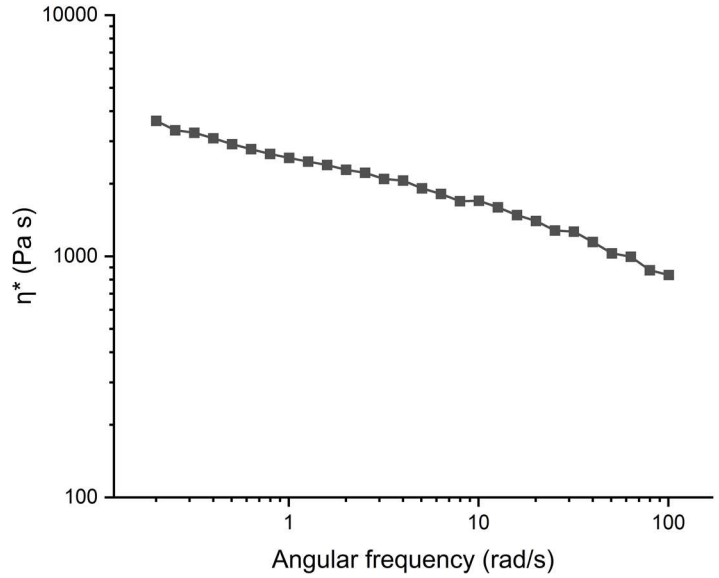

Figure S6: Frequency dependency of the complex viscosity (at 1% amplitude, 190 °C) for the injection-moulding grade polymer.

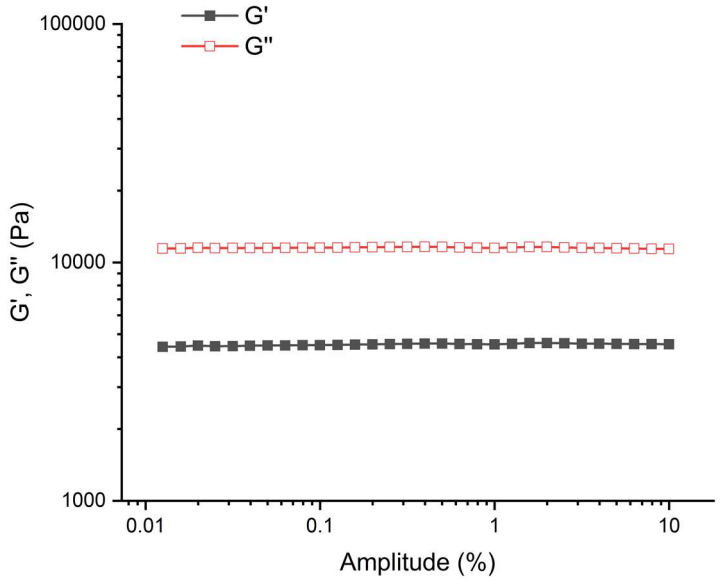

Figure S7: The amplitude sweep test (at 1 Hz, 190 °C) on **IMPE** showing how dynamic moduli behave as a function of amplitude (strain), confirming the earlier frequency sweep measurement was performed at the linear viscoelastic regime (LVER).

- **Blow Moulding HPDE (BMPE)**

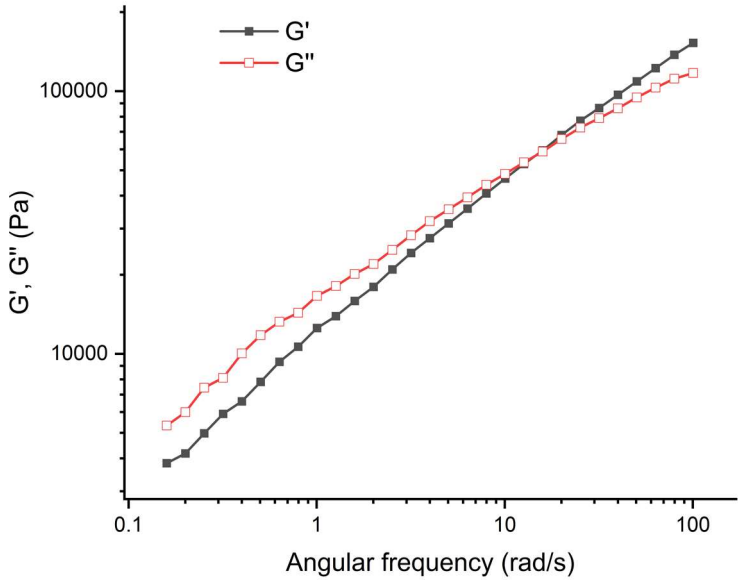

Figure S8: Frequency dependencies of the dynamic moduli (at 1% amplitude, 190 °C) for the blow-moulding grade polymer.

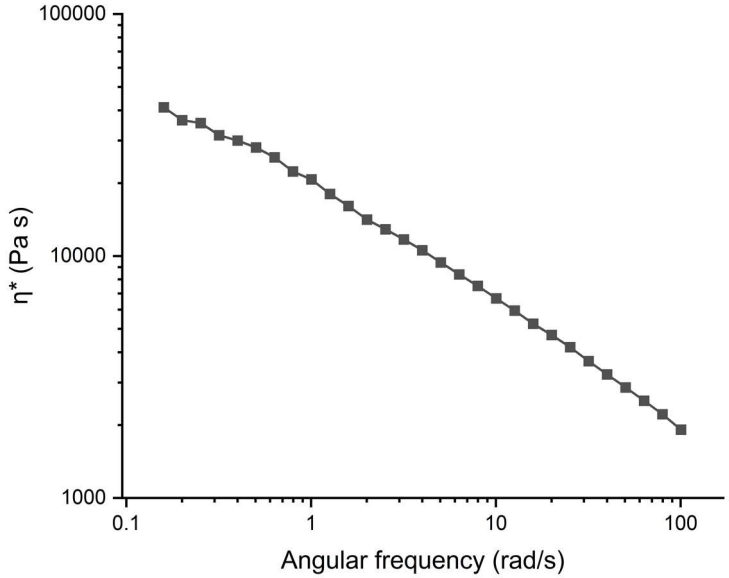

Figure S9: Frequency dependency of the complex viscosity (at 1% amplitude, 190 °C) for the blow-moulding grade polymer.

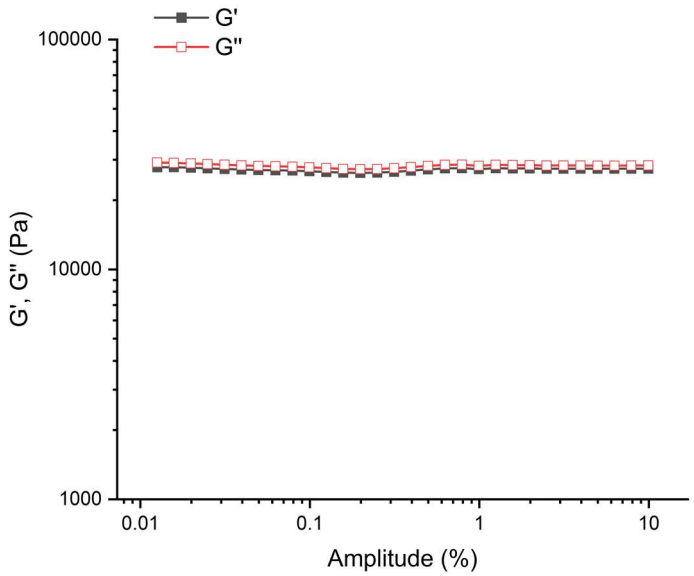

Figure S10: The amplitude sweep test (at 1 Hz, 190 °C) on **BMPE** showing how dynamic moduli behave as a function of amplitude, confirming the earlier frequency sweep measurement was performed at the LVER.

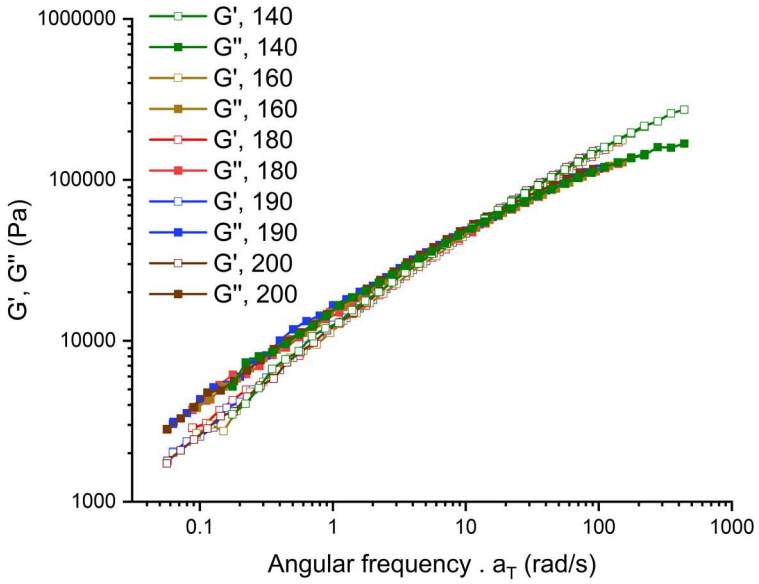

Figure S11: Time-temperature superposition (TTS) of the frequency dependencies of the dynamic moduli at the reference temperature of 190 °C (all at 1% amplitude). The shift factors (a_T) were determined as 0.9 at 200 °C, 1.4 at 180 °C, 1.5 at 160 °C and 2.2 at 140 °C.

- **M1**

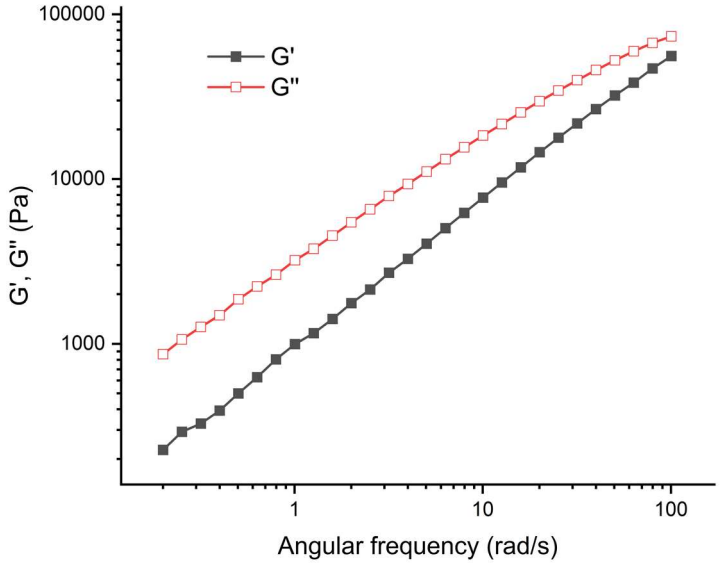

Figure S12: Frequency dependencies of the dynamic moduli (at 1% amplitude, 190 °C) for **M1**.

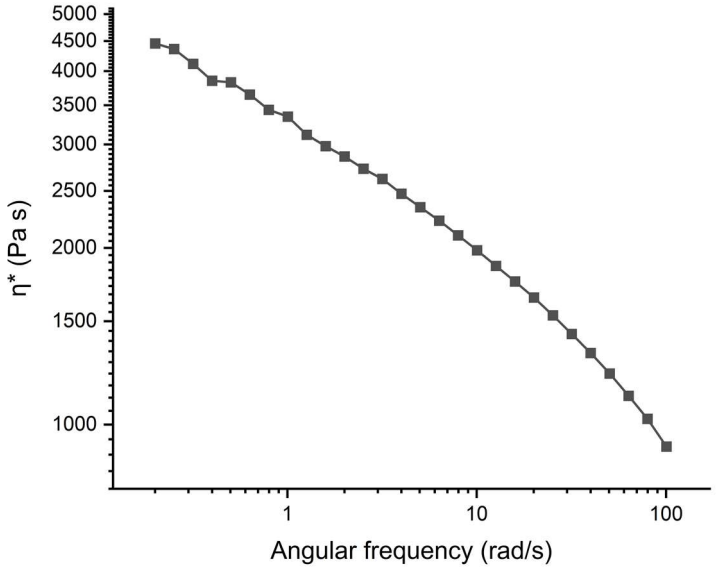

Figure S13: Frequency dependency of the complex viscosity (at 1% amplitude, 190 °C) for **M1**.

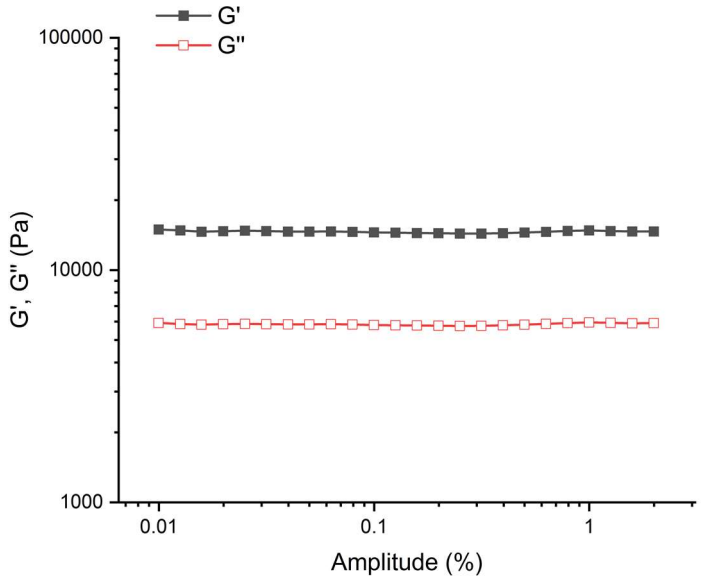

Figure S14: The amplitude sweep test (at 1 Hz, 190 °C) on **M1** showing how dynamic moduli behave as a function of amplitude, confirming the earlier frequency sweep measurement was performed at the LVER.

- **M2**

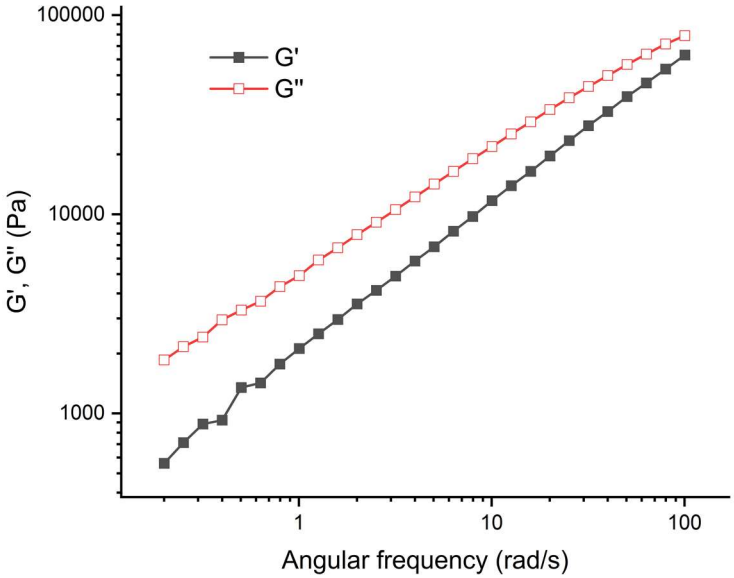

Figure S15: Frequency dependencies of the dynamic moduli (at 1% amplitude, 190 °C) for **M2**.

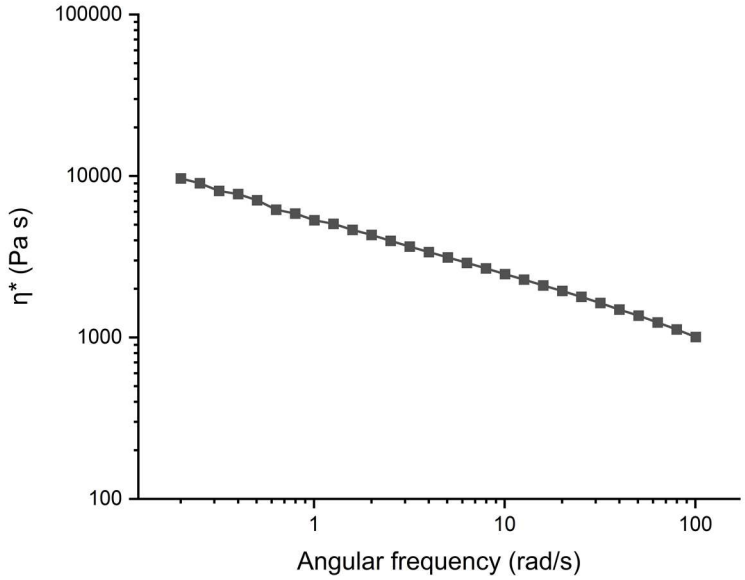

Figure S16: Frequency dependency of the complex viscosity (at 1% amplitude, 190 °C) for **M2**.

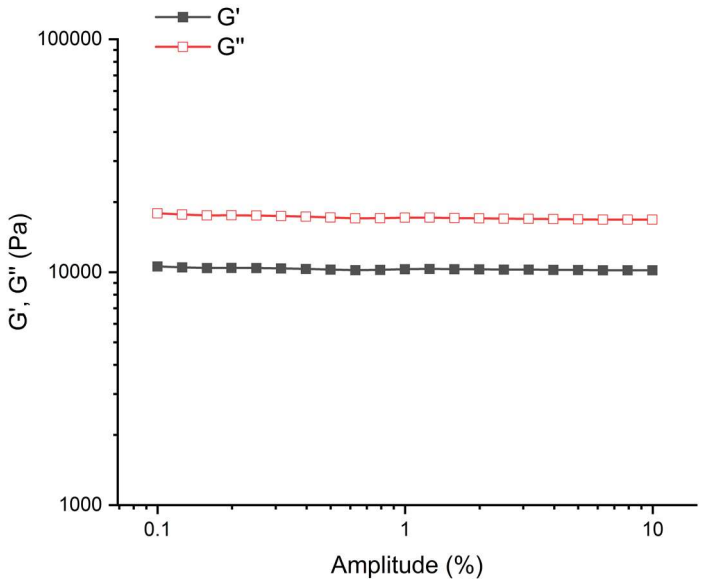

Figure S17: The amplitude sweep test (at 1 Hz, 190 °C) on **M2** showing how dynamic moduli behave as a function of amplitude, confirming the earlier frequency sweep measurement was performed at the LVER.

- **M3**

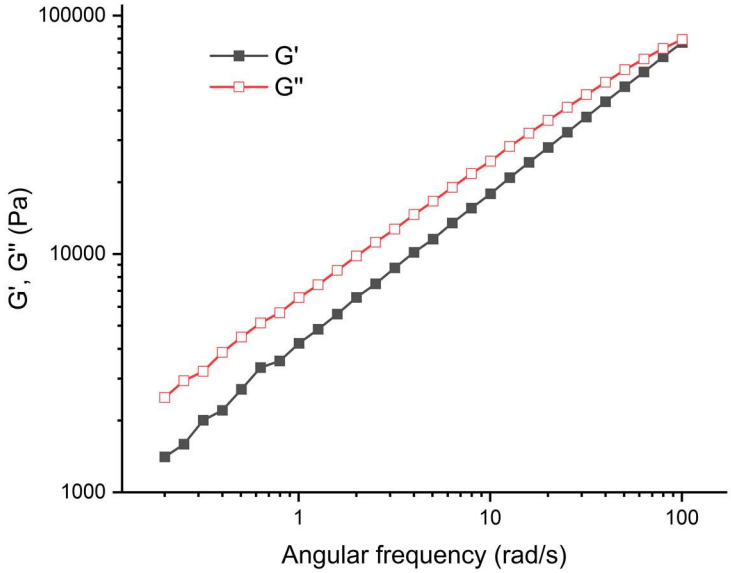

Figure S18: Frequency dependencies of the dynamic moduli (at 1% amplitude, 190 °C) for **M3**.

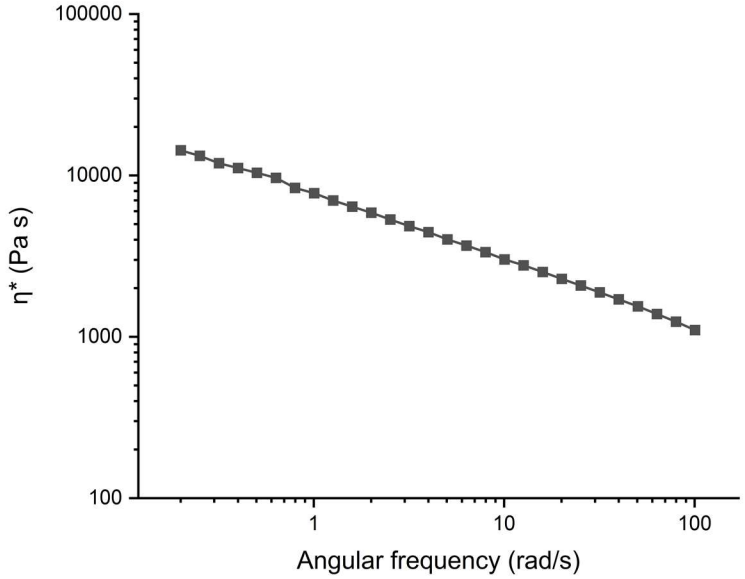

Figure S19: Frequency dependency of the complex viscosity (at 1% amplitude, 190 °C) for **M3**.

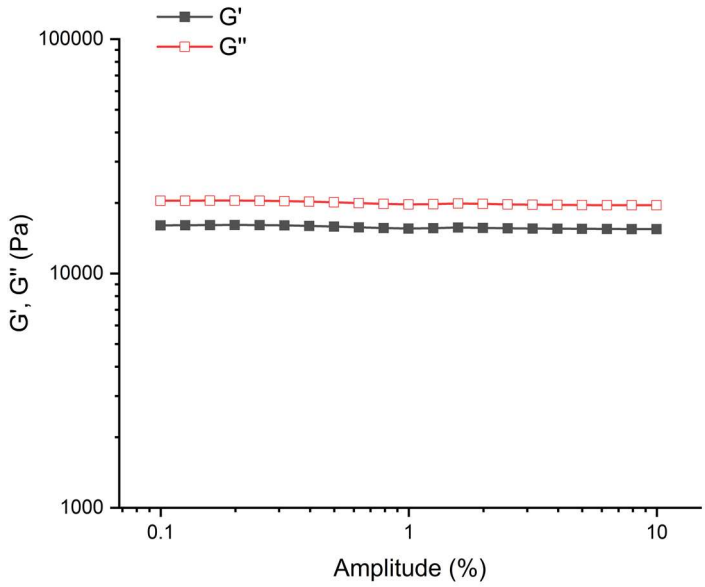

Figure S20: The amplitude sweep test (at 1 Hz, 190 °C) on **M3** showing how dynamic moduli behave as a function of amplitude, confirming the earlier frequency sweep measurement was performed at the LVER.

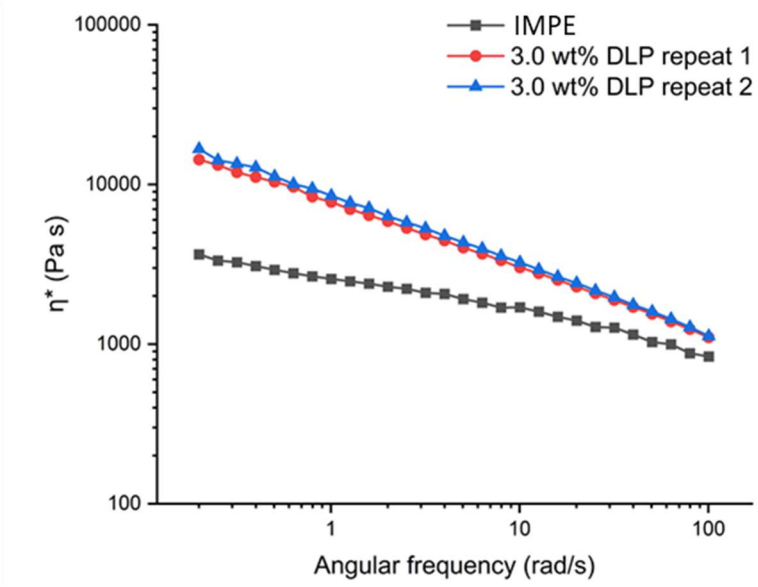

Figure S21: Frequency dependencies of the complex viscosity values for two separately prepared samples using the same experimental conditions (at 1% amplitude, 190 °C). The error on each data point was less than 5% on average.

- **M4**

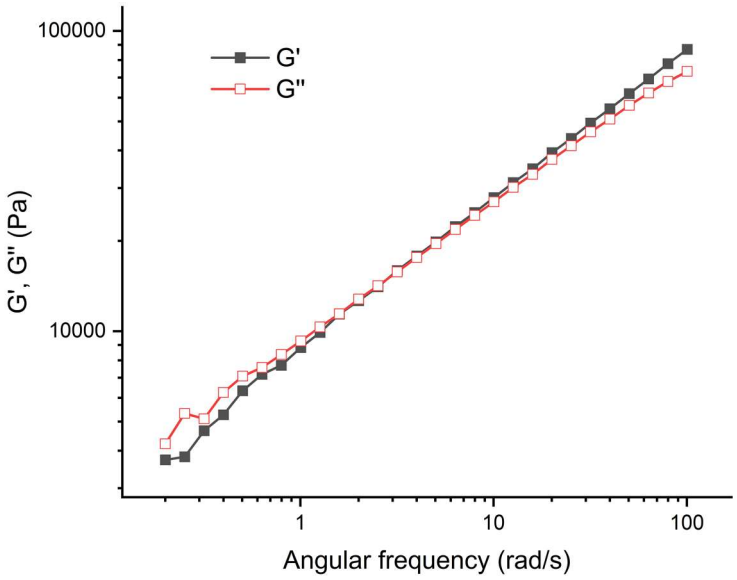

Figure S22: Frequency dependencies of the dynamic moduli (at 1% amplitude, 190 °C) for **M4**.

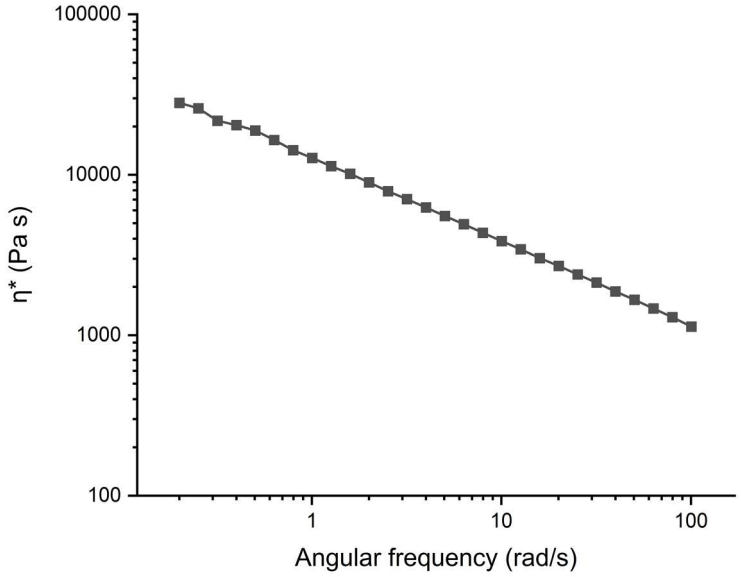

Figure S23: Frequency dependency of the complex viscosity (at 1% amplitude, 190 °C) for **M4**.

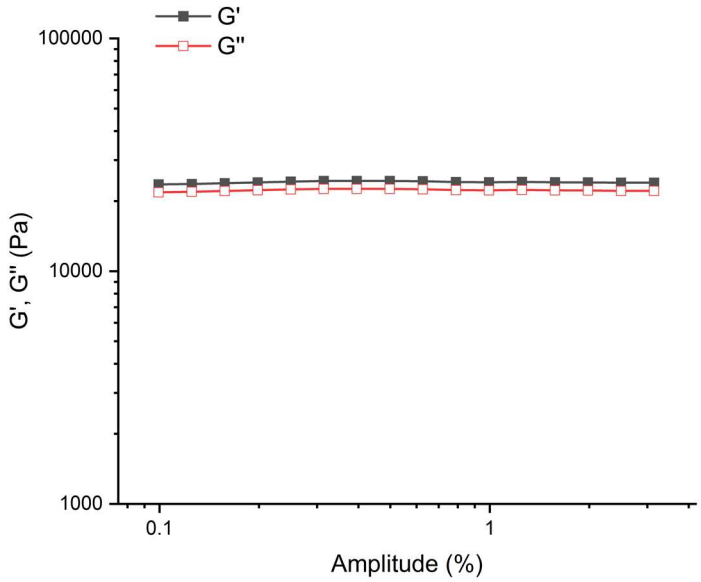

Figure S24: The amplitude sweep test (at 1 Hz, 190 °C) on **M4** showing how dynamic moduli behave as a function of amplitude, confirming the earlier frequency sweep measurement was performed at the LVER.

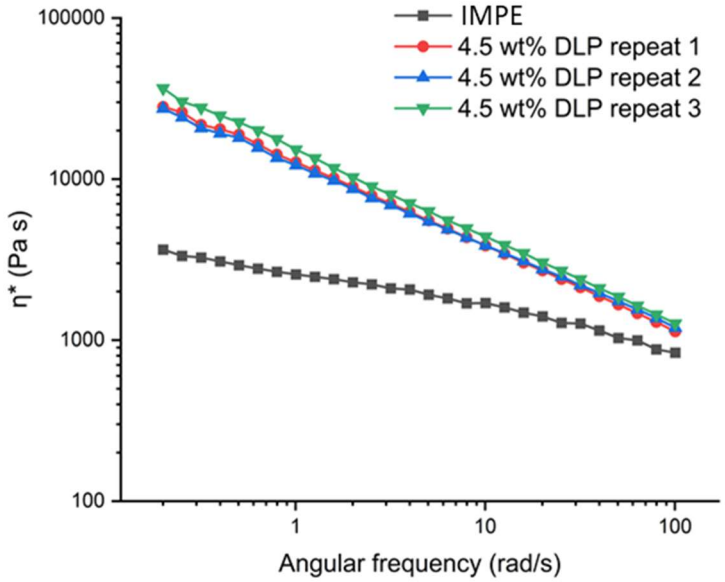

Figure S25: Frequency dependencies of the complex viscosity values for three separately prepared samples using the same experimental conditions (at 1% amplitude, 190 °C). The error on each data point was less than 5% on average.

- **M5**

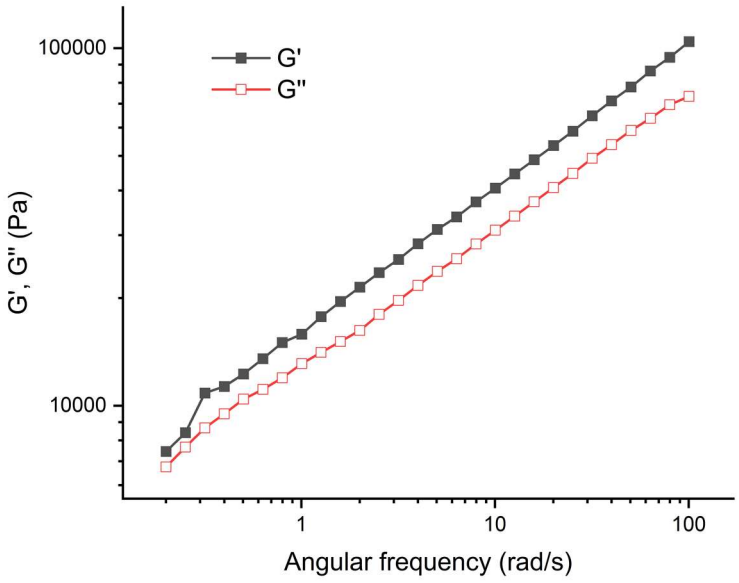

Figure S26: Frequency dependencies of the dynamic moduli (at 1% amplitude, 190 °C) for **M5**.

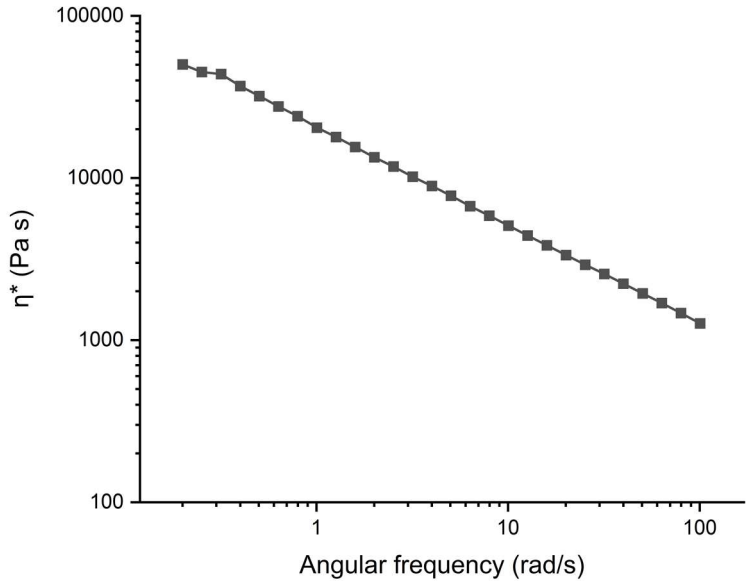

Figure S27: Frequency dependency of the complex viscosity (at 1% amplitude, 190 °C) for **M5**.

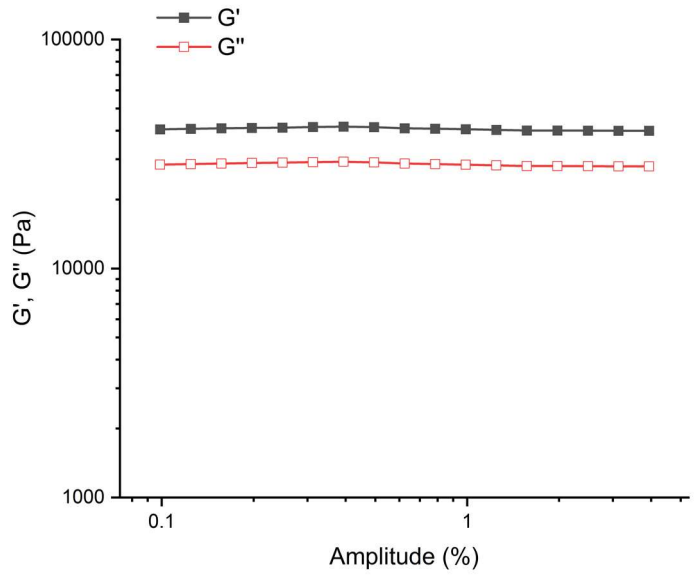

Figure S28: The amplitude sweep test (at 1 Hz, 190 °C) on **M5** showing how dynamic moduli behave as a function of amplitude, confirming the earlier frequency sweep measurement was performed at the LVER.

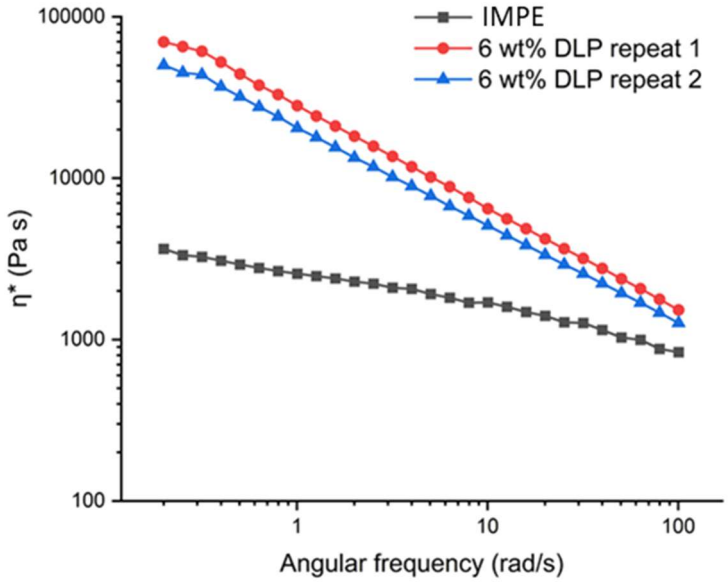

Figure S29: Frequency dependencies of the complex viscosity values for two separately prepared samples using the same experimental conditions (at 1% amplitude, 190 °C). The error on each data point was less than 10% on average.

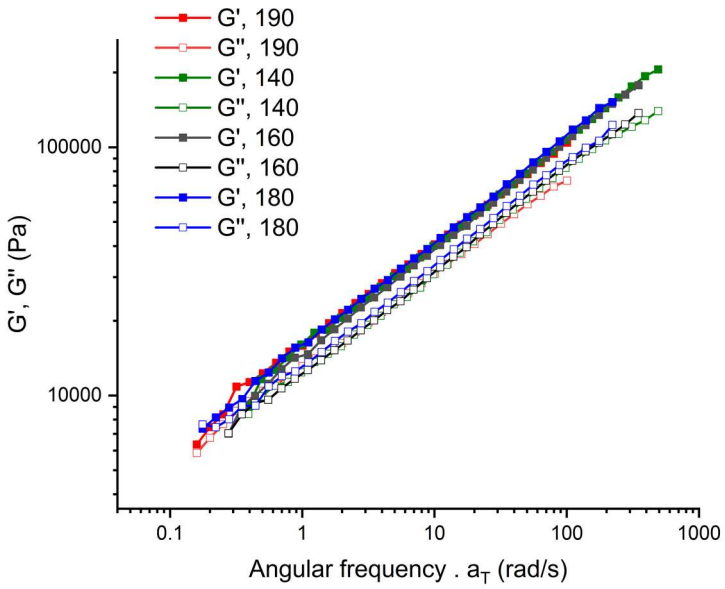

Figure S30: TTS of the frequency dependencies of the dynamic moduli at the reference temperature of 190 °C (all at 1% amplitude). The shift factors (a_T) were determined as 1.4 at 180 °C, 2.2 at 160 °C and 3.1 at 140 °C.

- **M6**

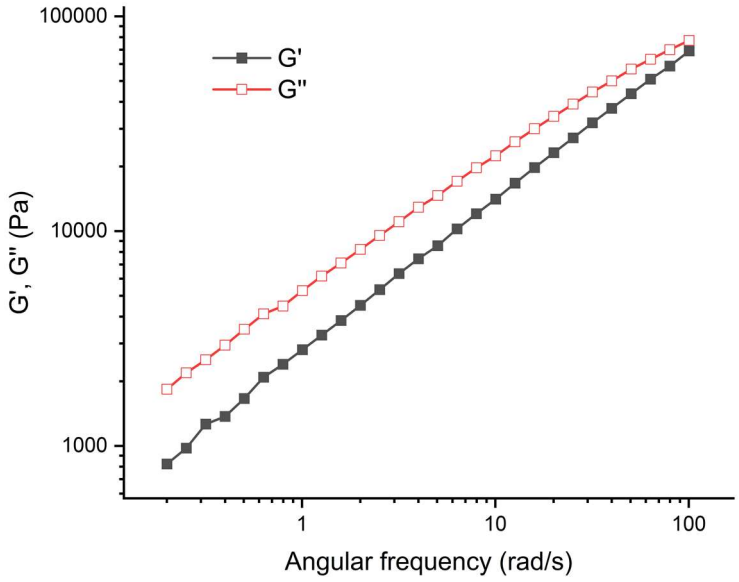

Figure S31: Frequency dependencies of the dynamic moduli (at 1% amplitude, 190 °C) for **M6**.

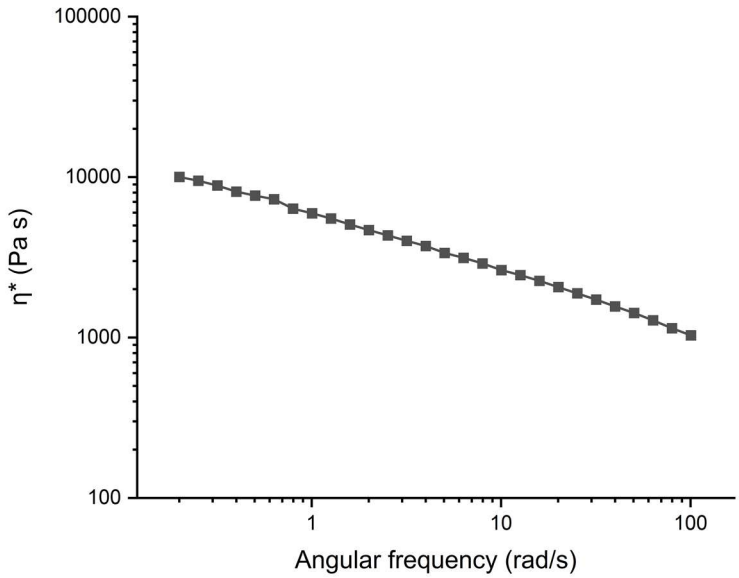

Figure S32: Frequency dependency of the complex viscosity (at 1% amplitude, 190 °C) for **M6**.

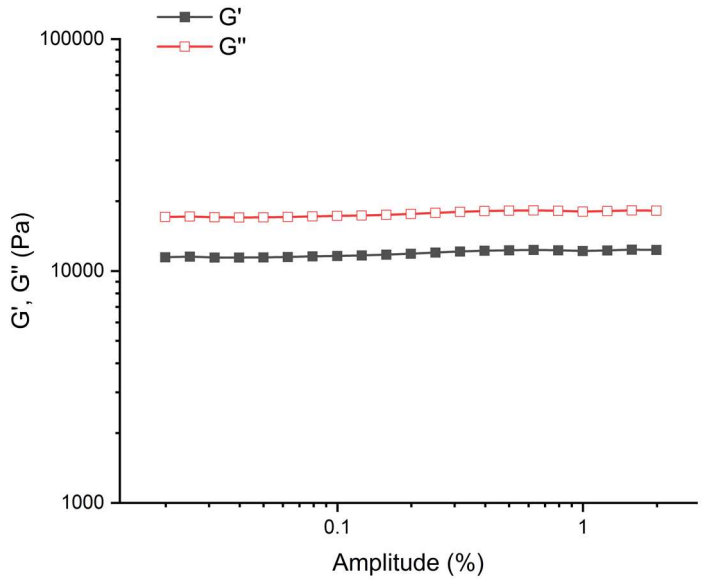

Figure S33: The amplitude sweep test (at 1 Hz, 190 °C) on **M6** showing how dynamic moduli behave as a function of amplitude, confirming the earlier frequency sweep measurement was performed at the LVER.

- **M7**

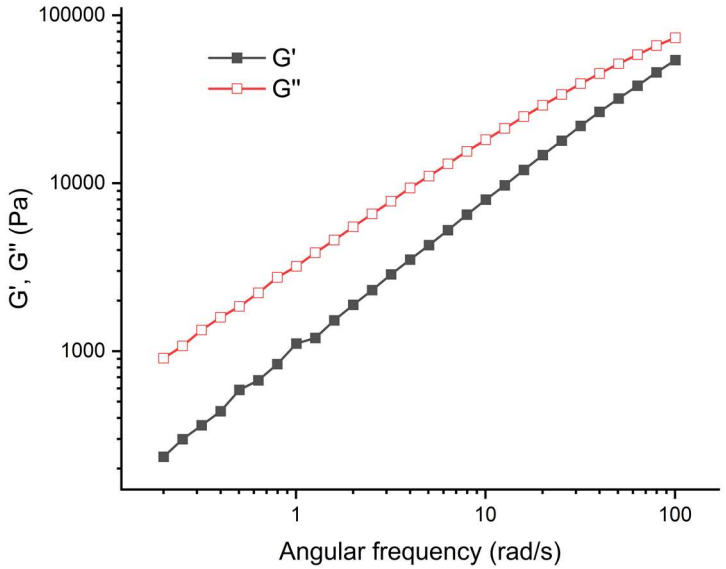

Figure S34: Frequency dependencies of the dynamic moduli (at 1% amplitude, 190 °C) for **M7**.

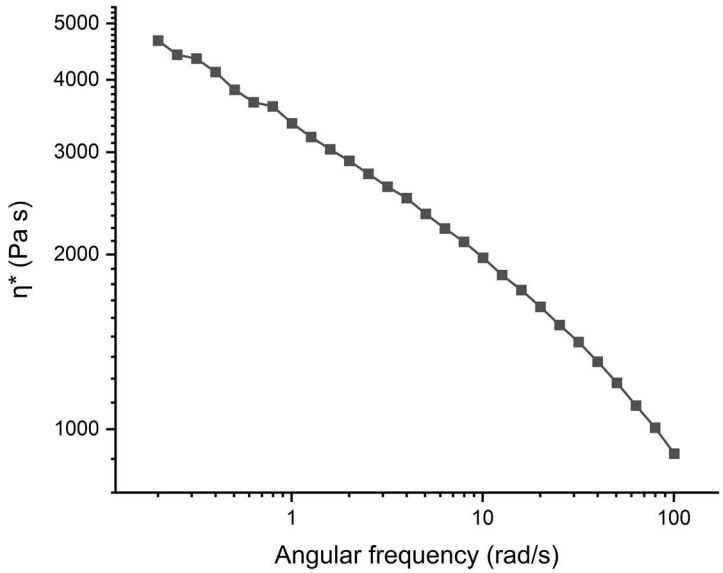

Figure S35: Frequency dependency of the complex viscosity (at 1% amplitude, 190 °C) for **M7**.

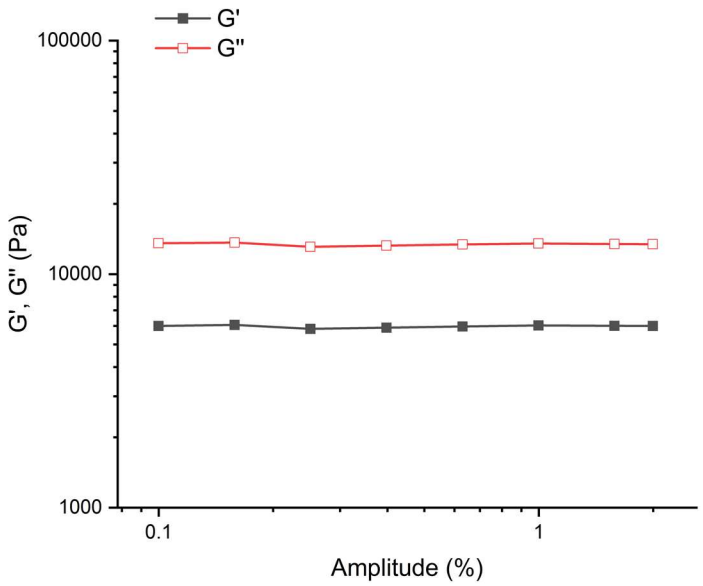

Figure S36: The amplitude sweep test (at 1 Hz, 190 °C) on **M7** showing how dynamic moduli behave as a function of amplitude, confirming the earlier frequency sweep measurement was performed at the LVER.

- **M8**

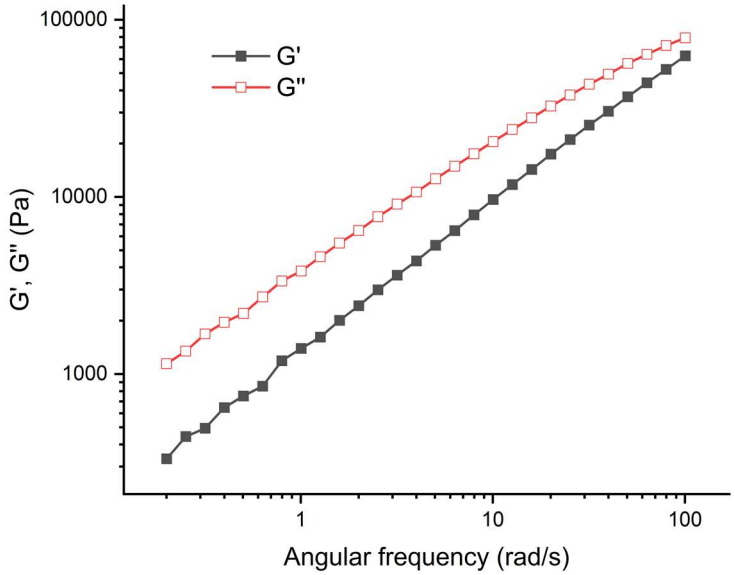

Figure S37: Frequency dependencies of the dynamic moduli (at 1% amplitude, 190 °C) for **M8**.

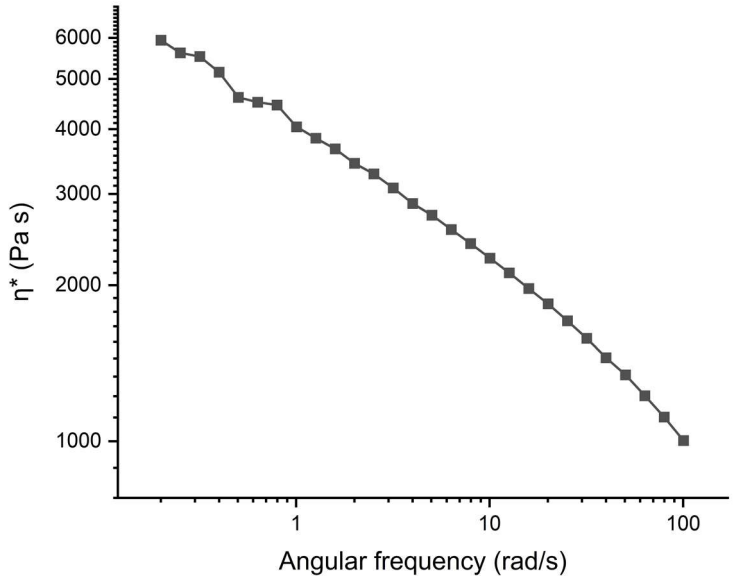

Figure S38: Frequency dependency of the complex viscosity (at 1% amplitude, 190 °C) for **M8**.

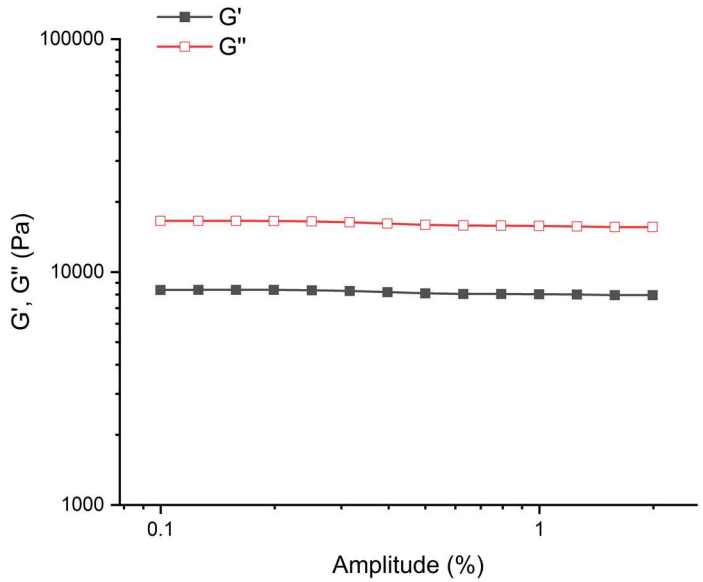

Figure S39: The amplitude sweep test (at 1 Hz, 190 °C) on **M8** showing how dynamic moduli behave as a function of amplitude, confirming the earlier frequency sweep measurement was performed at the LVER.

- **M9**

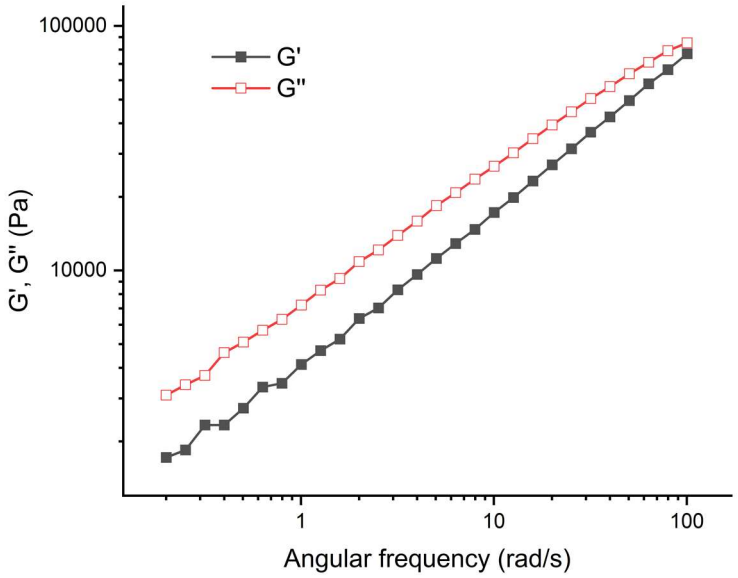

Figure S40: Frequency dependencies of the dynamic moduli (at 1% amplitude, 190 °C) for **M9**.

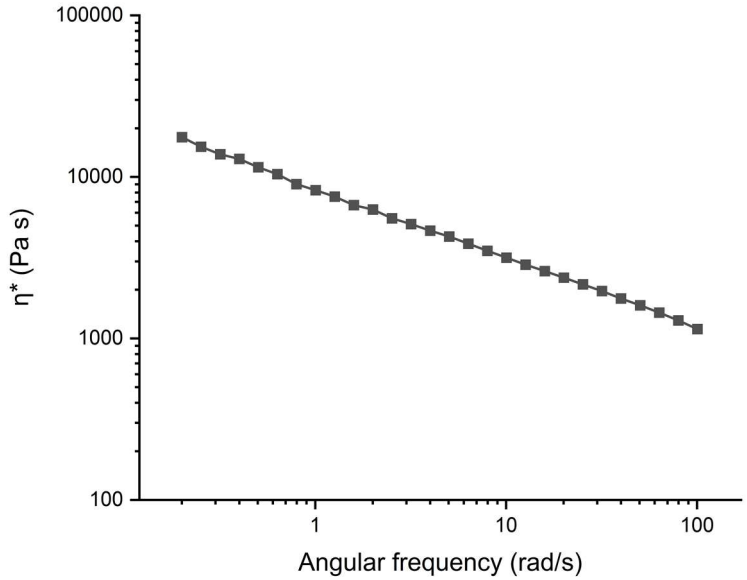

Figure S41: Frequency dependency of the complex viscosity (at 1% amplitude, 190 °C) for **M9**.

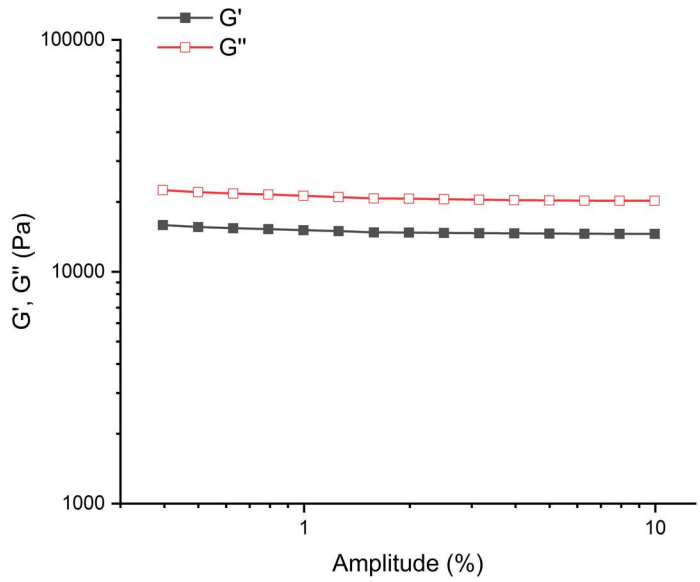

Figure S42: The amplitude sweep test (at 1 Hz, 190 °C) on **M9** showing how dynamic moduli behave as a function of amplitude, confirming the earlier frequency sweep measurement was performed at the LVER.

- **M10**

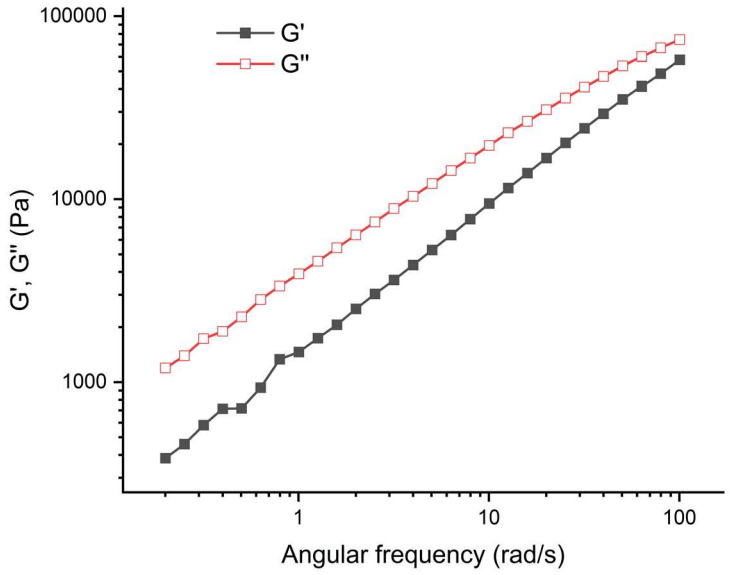

Figure S43: Frequency dependencies of the dynamic moduli (at 1% amplitude, 190 °C) for **M10**.

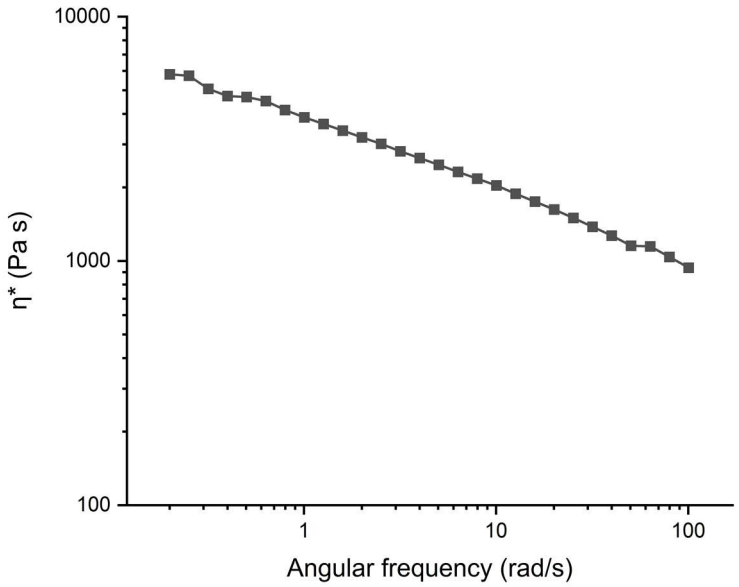

Figure S44: Frequency dependency of the complex viscosity (at 1% amplitude, 190 °C) for **M10**.

- **M11**

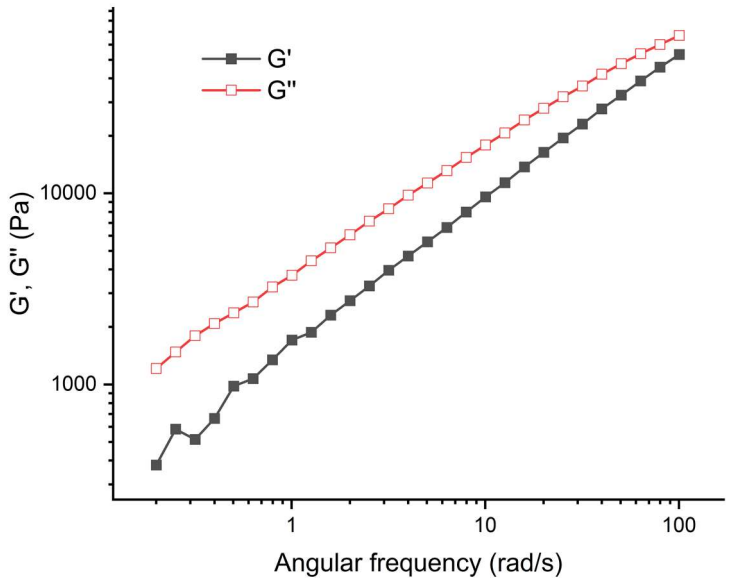

Figure S45: Frequency dependencies of the dynamic moduli (at 1% amplitude, 190 °C) for **M11**.

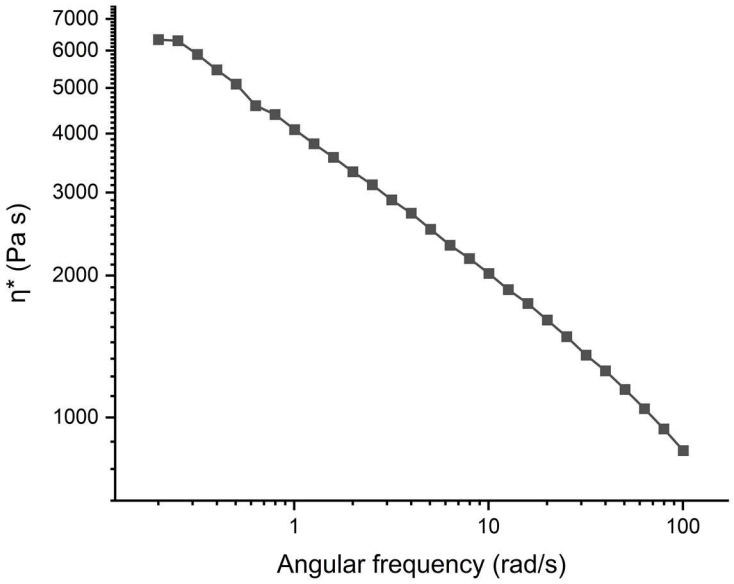

Figure S46: Frequency dependency of the complex viscosity (at 1% amplitude, 190 °C) for **M11**.

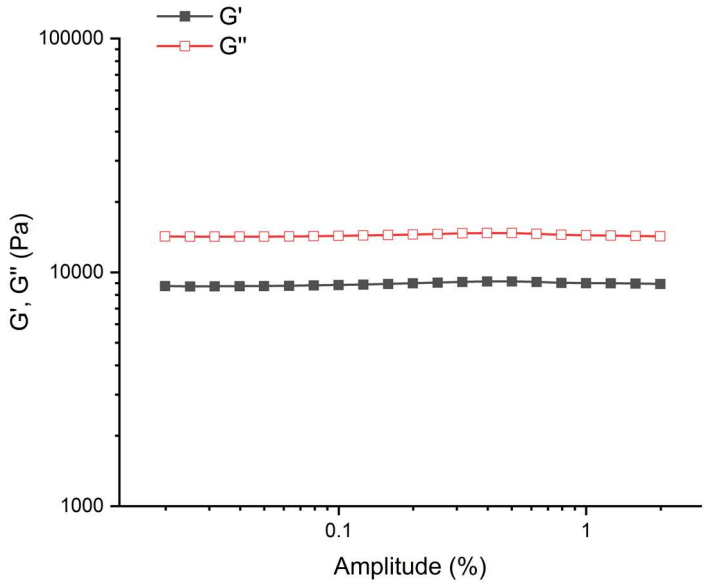

Figure S47: The amplitude sweep test (at 1 Hz, 190 °C) on **M11** showing how dynamic moduli behave as a function of amplitude, confirming the earlier frequency sweep measurement was performed at the LVER.

- **M12**

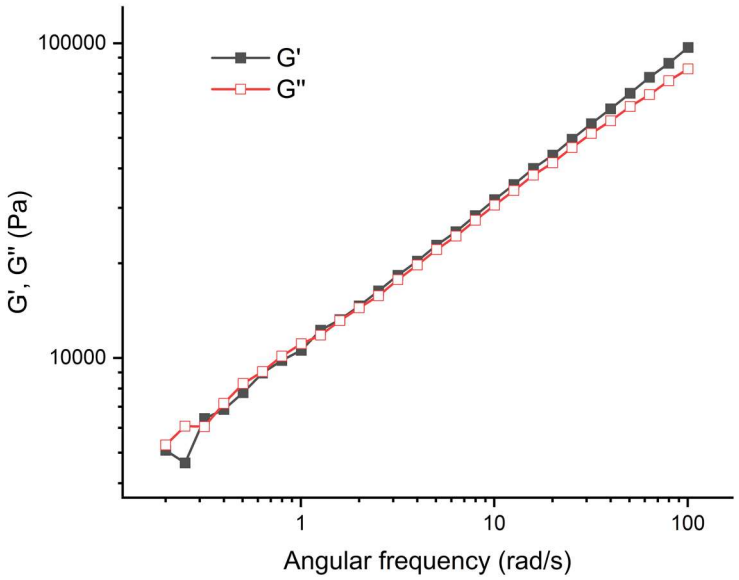

Figure S48: Frequency dependencies of the dynamic moduli (at 1% amplitude, 190 °C) for **M12**.

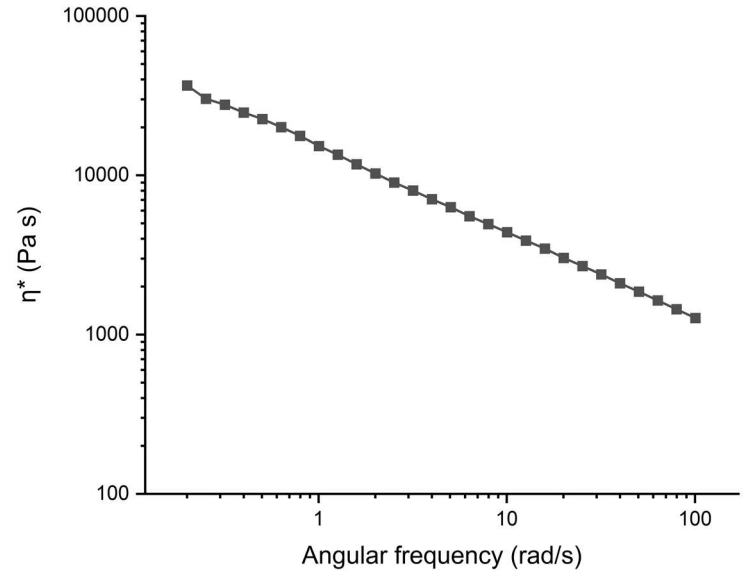

Figure S49: Frequency dependency of the complex viscosity (at 1% amplitude, 190 °C) for **M12**.

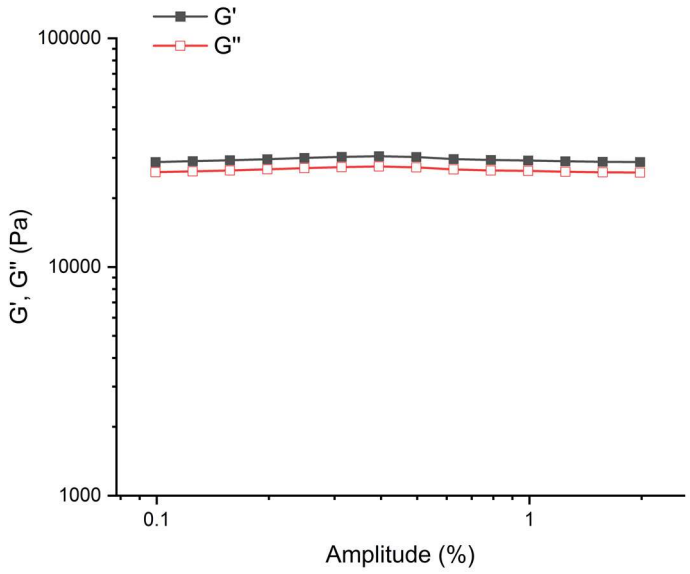

Figure S50: The amplitude sweep test (at 1 Hz, 190 °C) on **M12** showing how dynamic moduli behave as a function of amplitude, confirming the earlier frequency sweep measurement was performed at the LVER.

- **M13**

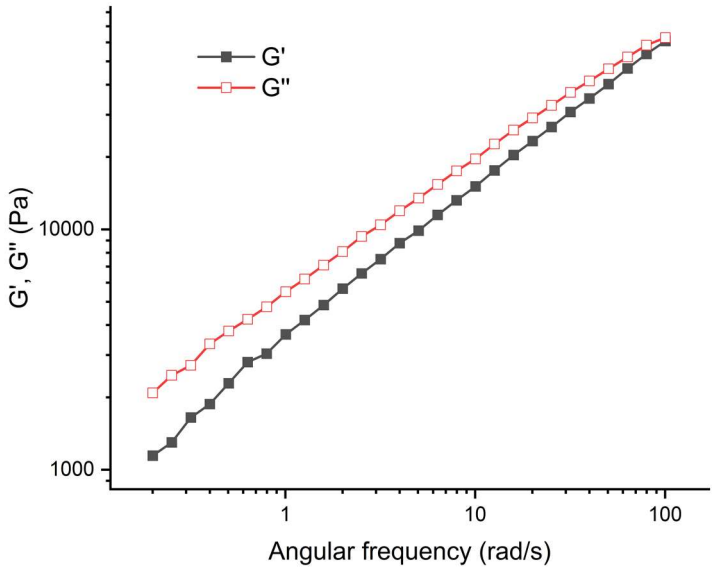

Figure S51: Frequency dependencies of the dynamic moduli (at 1% amplitude, 190 °C) for **M13**.

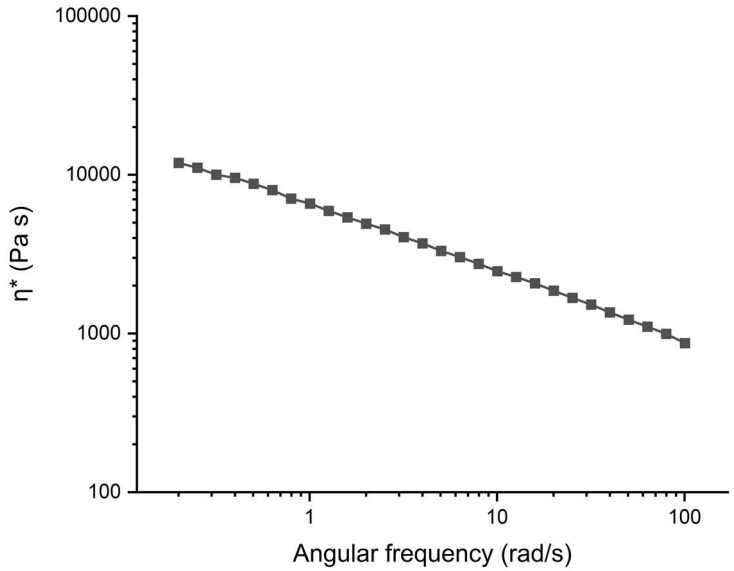

Figure S52: Frequency dependency of the complex viscosity (at 1% amplitude, 190 °C) for **M13**.

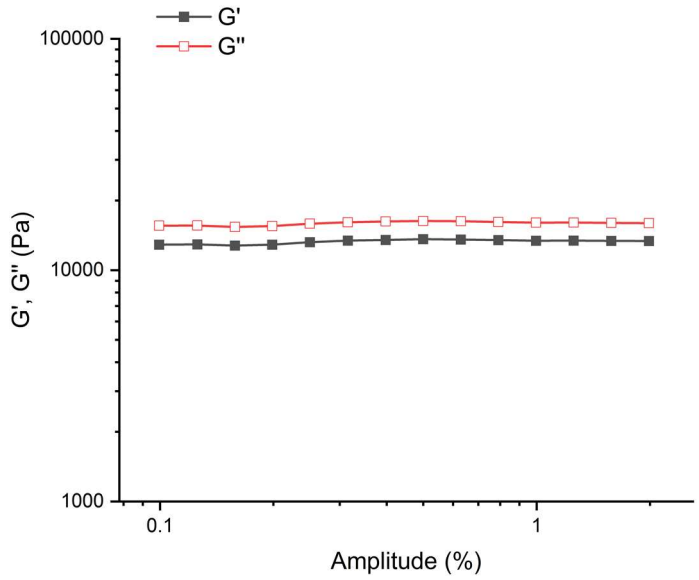

Figure S53: The amplitude sweep test (at 1 Hz, 190 °C) on **M13** showing how dynamic moduli behave as a function of amplitude, confirming the earlier frequency sweep measurement was performed at the LVER.

- **M14**

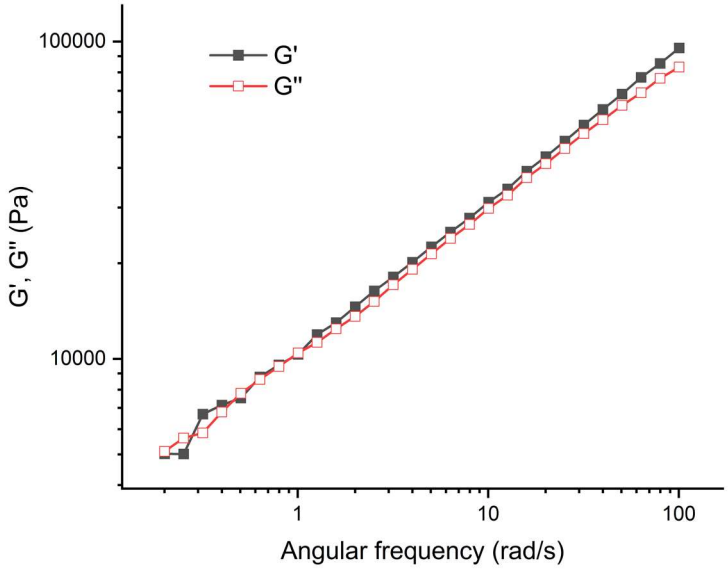

Figure S54: Frequency dependencies of the dynamic moduli (at 1% amplitude, 190 °C) for **M14**.

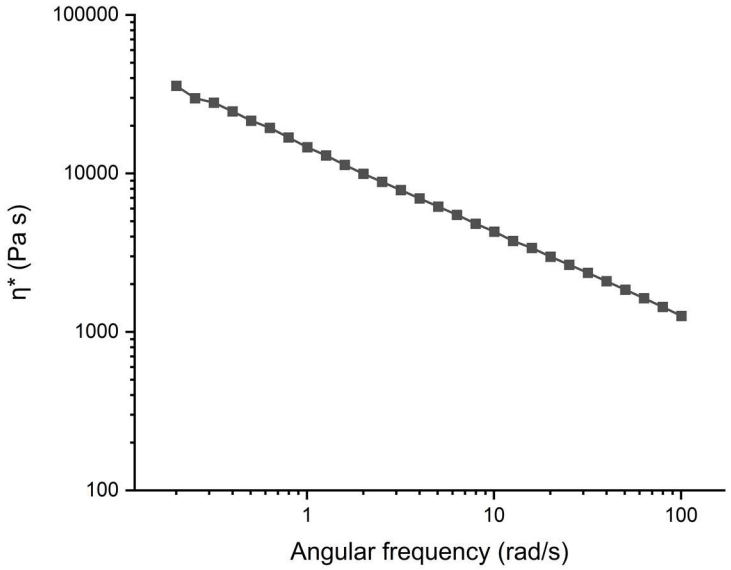

Figure S55: Frequency dependency of the complex viscosity (at 1% amplitude, 190 °C) for **M14**.

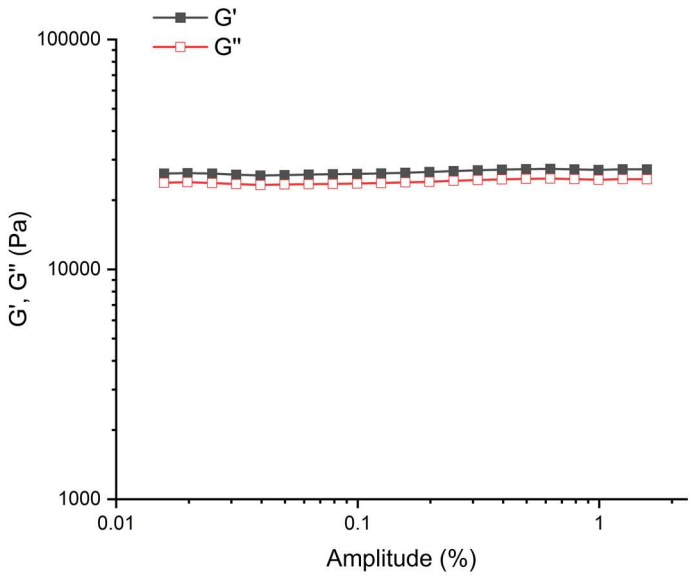

Figure S56: The amplitude sweep test (at 1 Hz, 190 °C) on **M14** showing how dynamic moduli behave as a function of amplitude, confirming the earlier frequency sweep measurement was performed at the LVER.

- **M15**

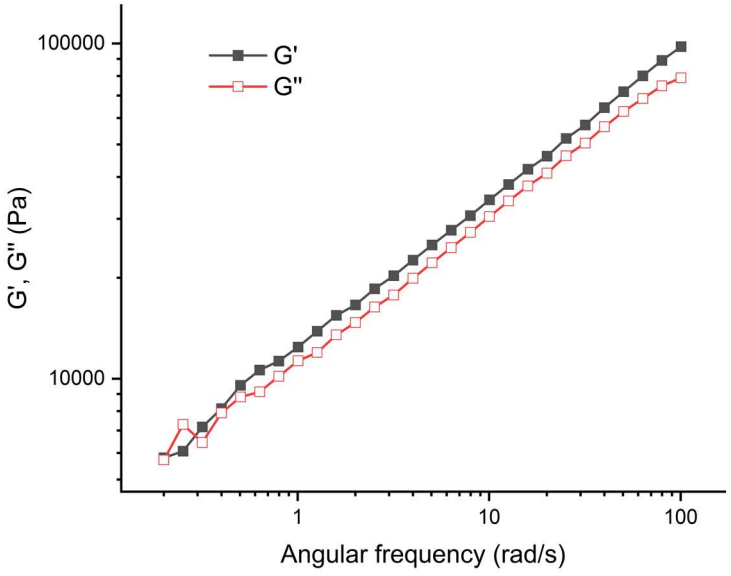

Figure S57: Frequency dependencies of the dynamic moduli (at 1% amplitude, 190 °C) for **M15**.

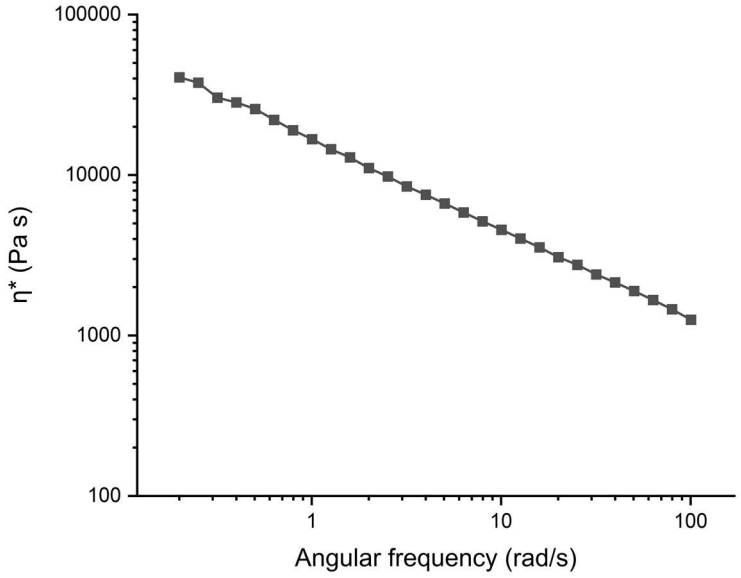

Figure S58: Frequency dependency of the complex viscosity (at 1% amplitude, 190 °C) for **M15**.

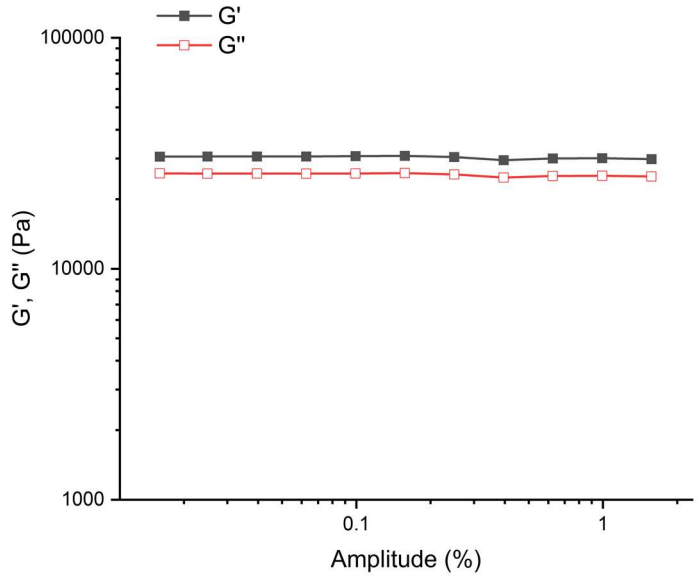

Figure S59: The amplitude sweep test (at 1 Hz, 190 °C) on **M15** showing how dynamic moduli behave as a function of amplitude, confirming the earlier frequency sweep measurement was performed at the LVER.

- **M16**

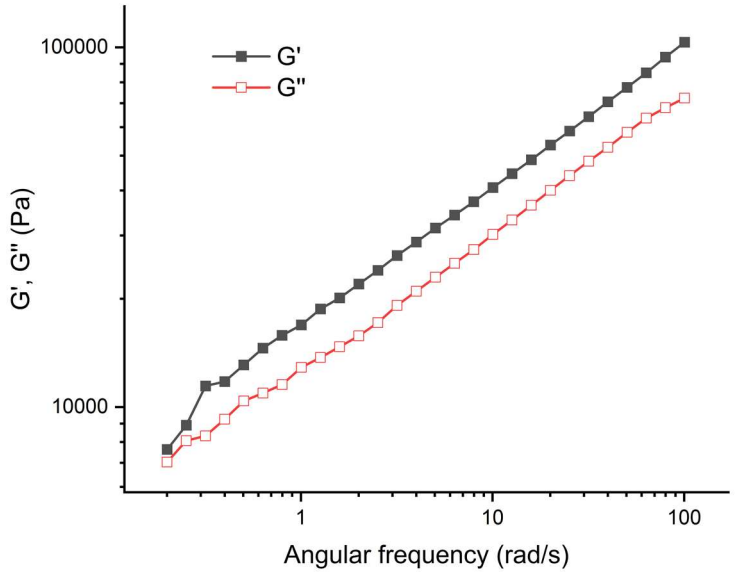

Figure S60: Frequency dependencies of the dynamic moduli (at 1% amplitude, 190 °C) for **M16**.

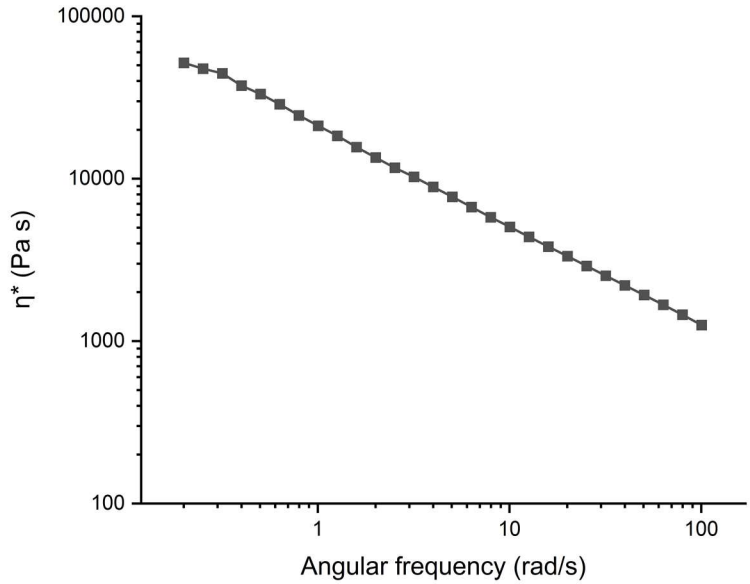

Figure S61: Frequency dependency of the complex viscosity (at 1% amplitude, 190 °C) for **M16**.

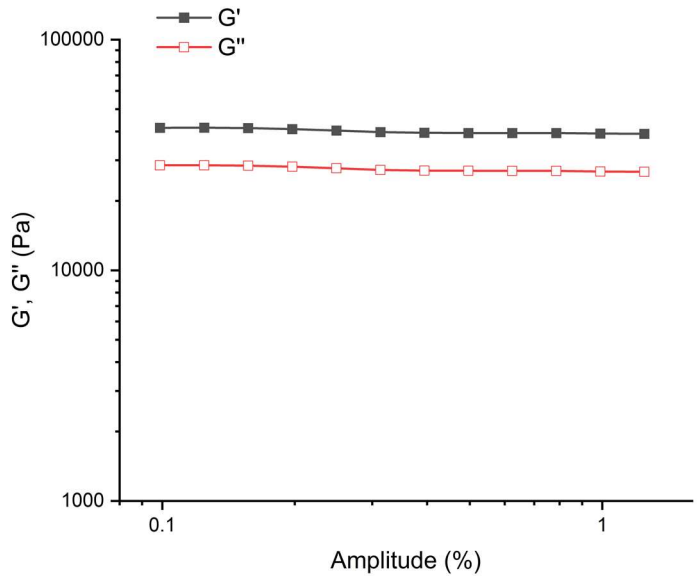

Figure S62: The amplitude sweep test (at 1 Hz, 190 °C) on **M16** showing how dynamic moduli behave as a function of amplitude, confirming the earlier frequency sweep measurement was performed at the LVER.

- **M17**

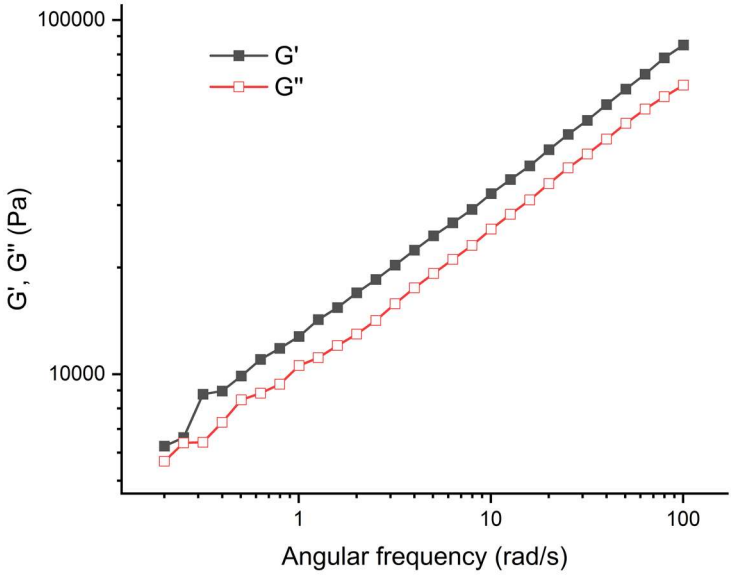

Figure S63: Frequency dependencies of the dynamic moduli (at 1% amplitude, 190 °C) for **M17**.

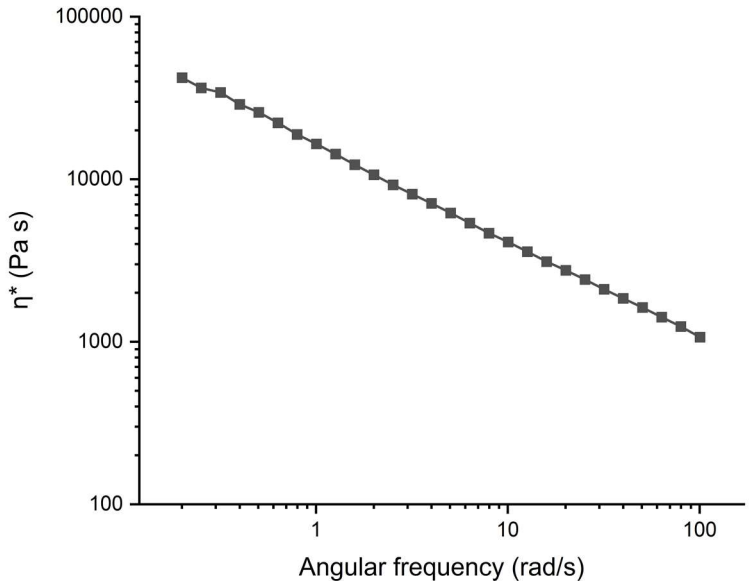

Figure S64: Frequency dependency of the complex viscosity (at 1% amplitude, 190 °C) for **M17**.

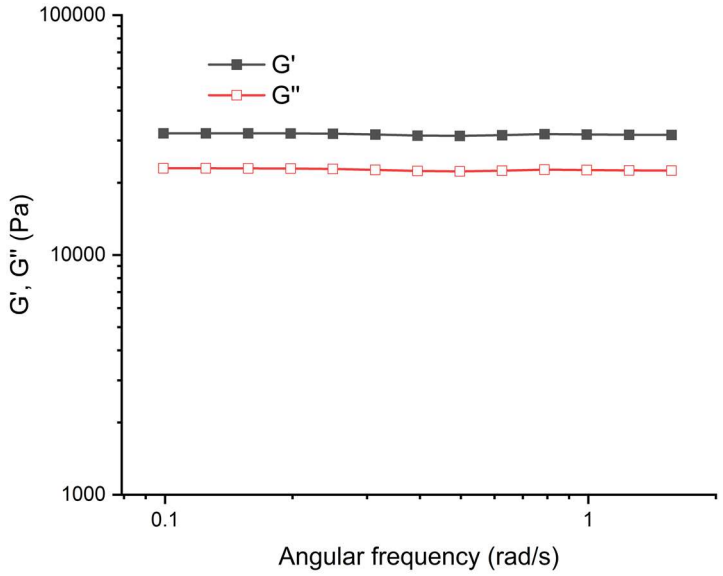

Figure S65: The amplitude sweep test (at 1 Hz, 190 °C) on **M17** showing how dynamic moduli behave as a function of amplitude, confirming the earlier frequency sweep measurement was performed at the LVER.

- **M18**

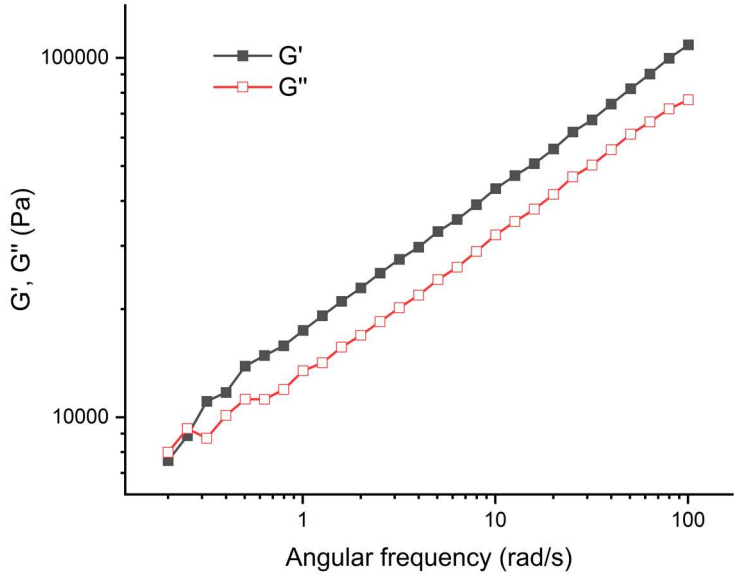

Figure S66: Frequency dependencies of the dynamic moduli (at 1% amplitude, 190 °C) for **M18**.

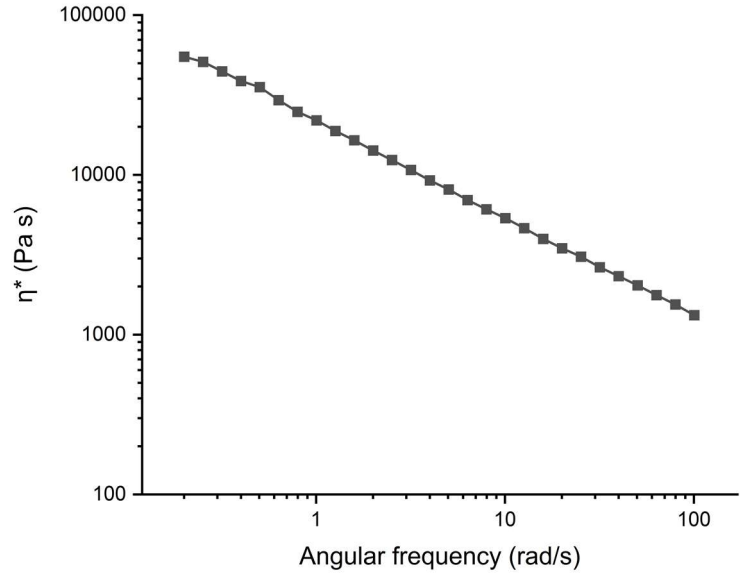

Figure S67: Frequency dependency of the complex viscosity (at 1% amplitude, 190 °C) for **M18**.

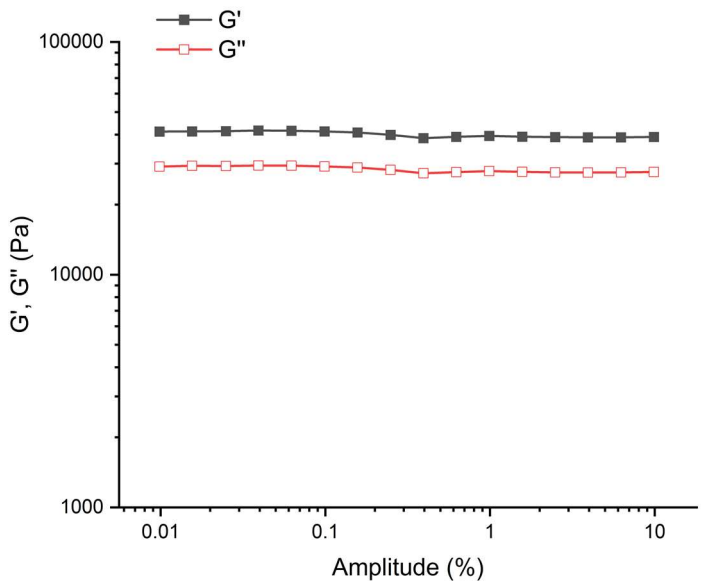

Figure S68: The amplitude sweep test (at 1 Hz, 190 °C) on **M18** showing how dynamic moduli behave as a function of amplitude, confirming the earlier frequency sweep measurement was performed at the LVER.

- **M19**

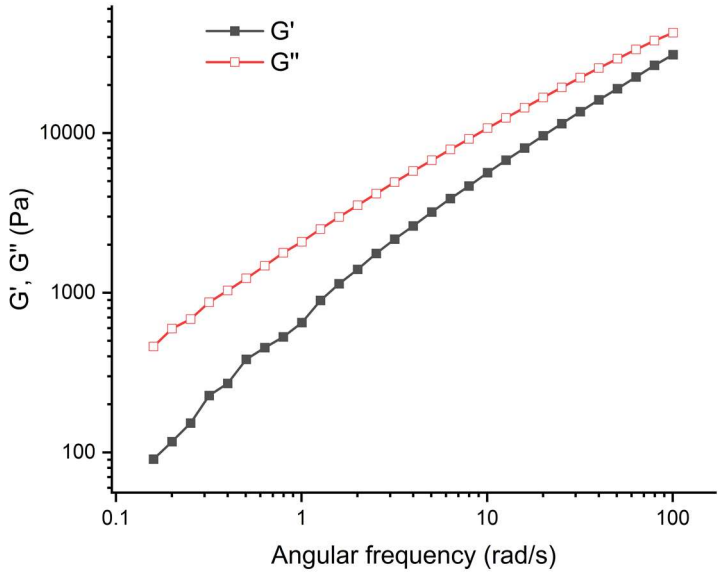

Figure S69: Frequency dependencies of the dynamic moduli (at 1% amplitude, 190 °C) for **M19**.

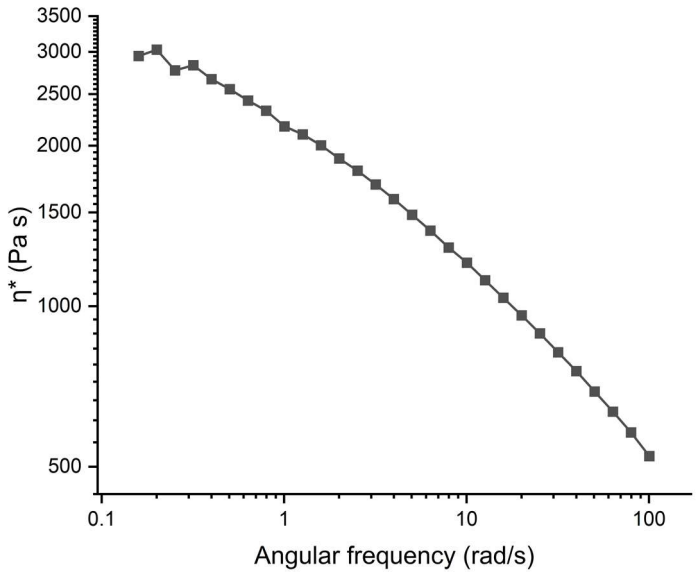

Figure S70: Frequency dependency of the complex viscosity (at 1% amplitude, 190 °C) for **M19**.

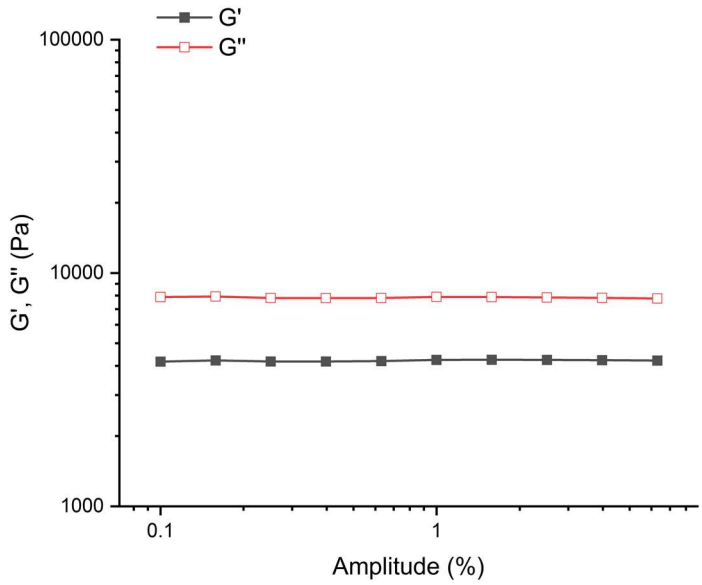

Figure S71: The amplitude sweep test (at 1 Hz, 190 °C) on **M19** showing how dynamic moduli behave as a function of amplitude, confirming the earlier frequency sweep measurement was performed at the LVER.

- **M20**

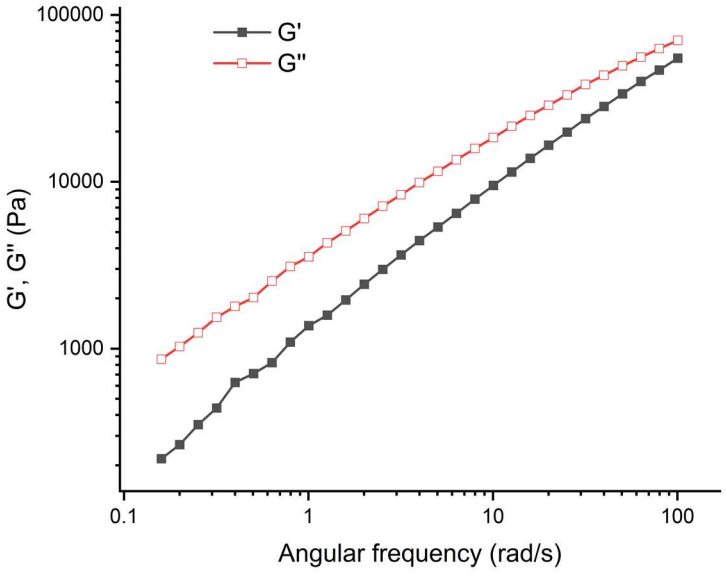

Figure S72: Frequency dependencies of the dynamic moduli (at 1% amplitude, 190 °C) for **M20**.

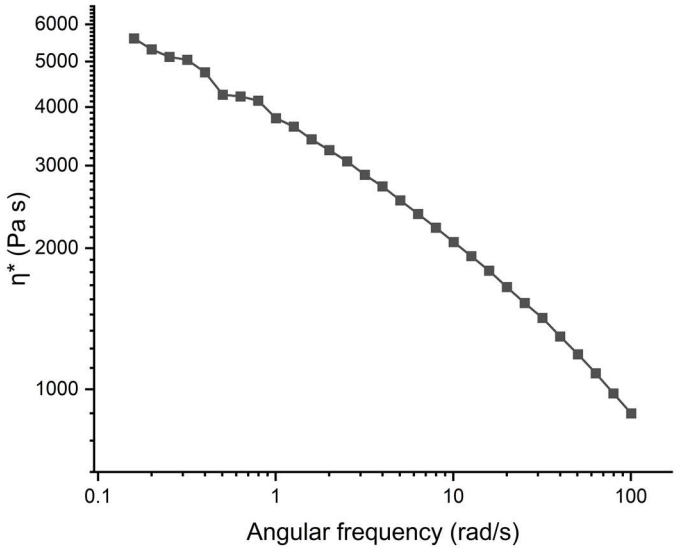

Figure S73: Frequency dependency of the complex viscosity (at 1% amplitude, 190 °C) for **M20**.

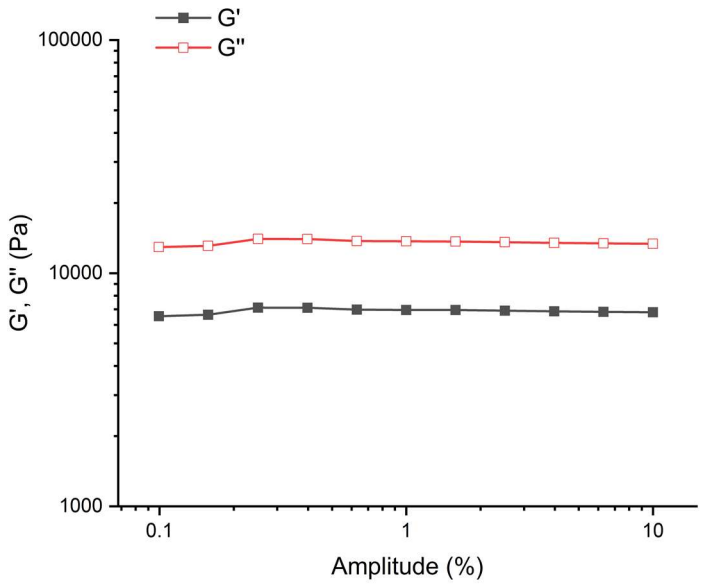

Figure S74: The amplitude sweep test (at 1 Hz, 190 °C) on **M20** showing how dynamic moduli behave as a function of amplitude, confirming the earlier frequency sweep measurement was performed at the LVER.

- **Comparison of IMPE, M1, M19 and M20**

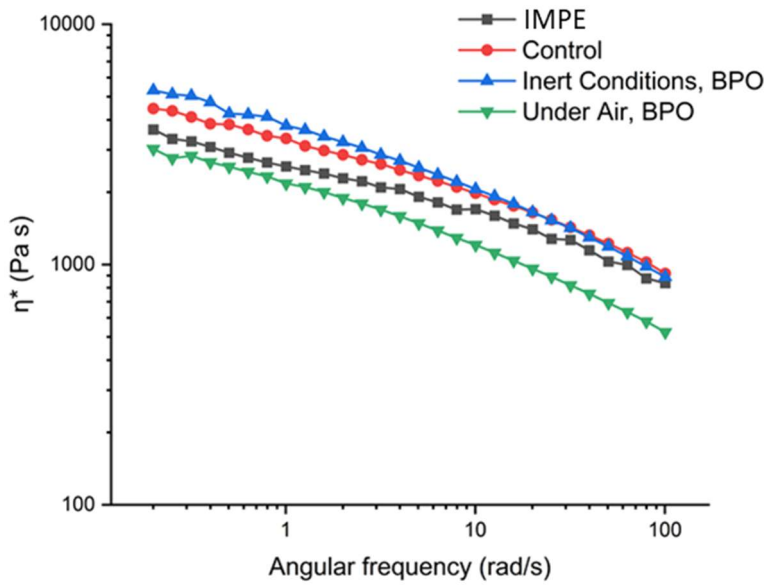

Figure S75: Frequency dependencies of the complex viscosity values (at 1% amplitude, 190 °C) for **IMPE**, **M1**, **M19** and **M20**.

3 Nonlinear Rheology

- **BMPE**

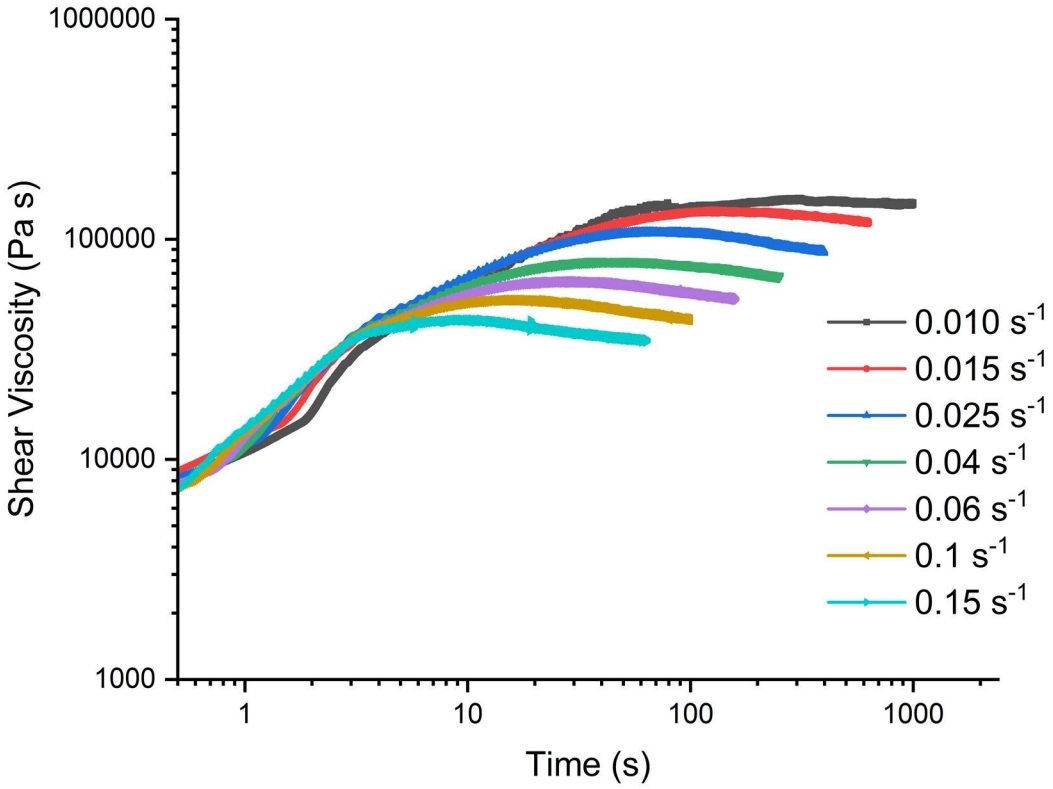

Figure S76: Step-shear non-linear rheology test on **BMPE** (at 190 °C) at different shear rates.

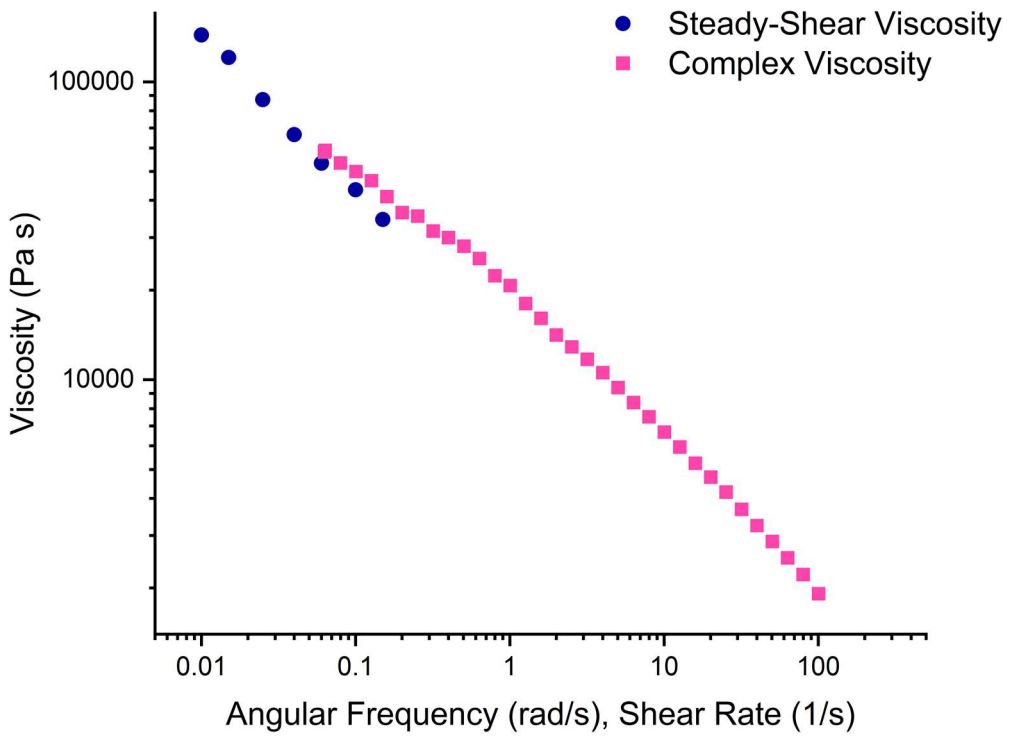

Figure S77: Dynamic viscosity (pink) and steady-state shear viscosity (blue) for **BMPE** to test the Cox-Merz rule.

- **M3**

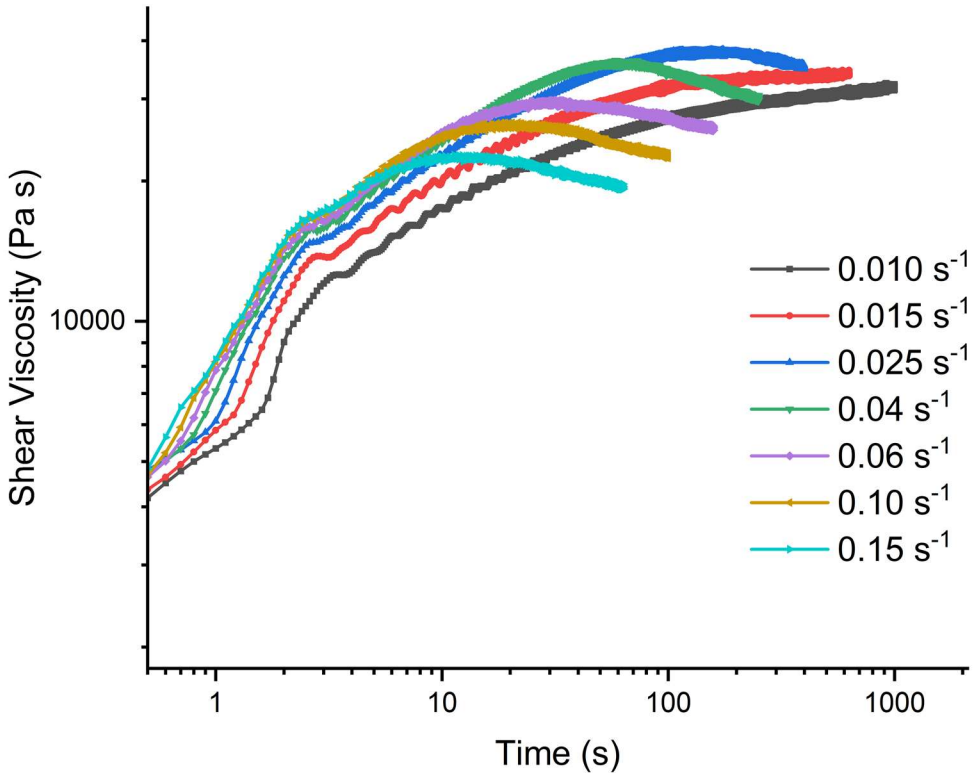

Figure S78: Step-shear non-linear rheology test on **M3** (at 190 °C) at different shear rates.

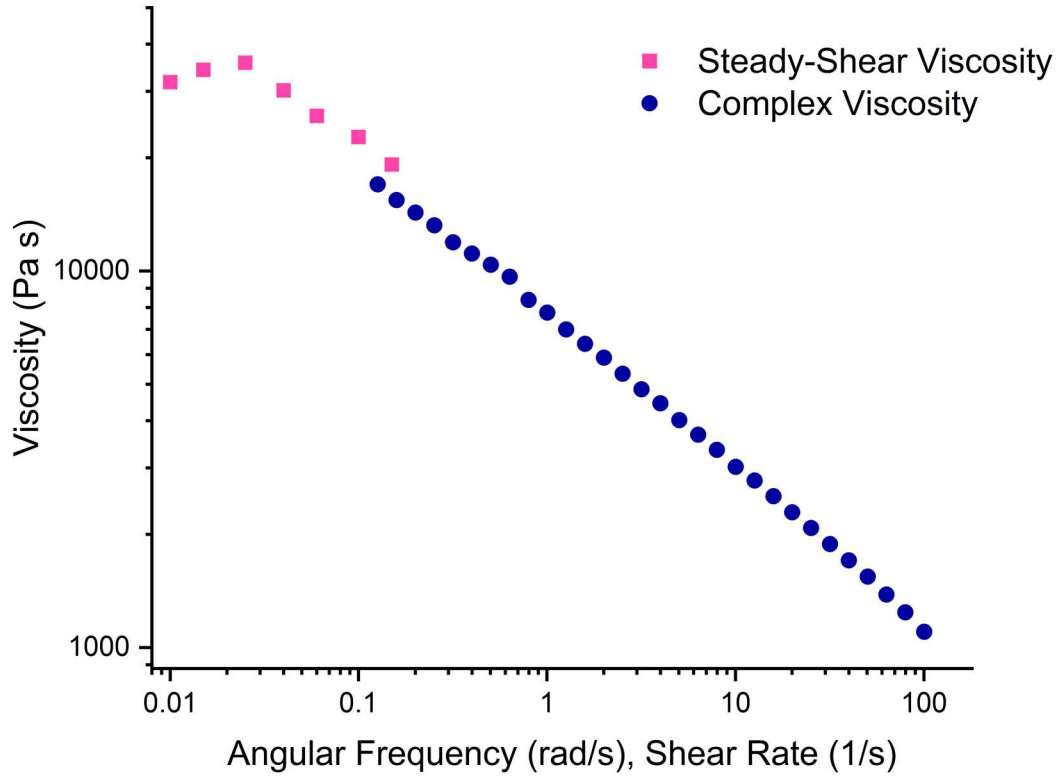

Figure S79: Dynamic viscosity (pink) and steady-state shear viscosity (blue) for **M3** to test the Cox-Merz rule.

- **M4**

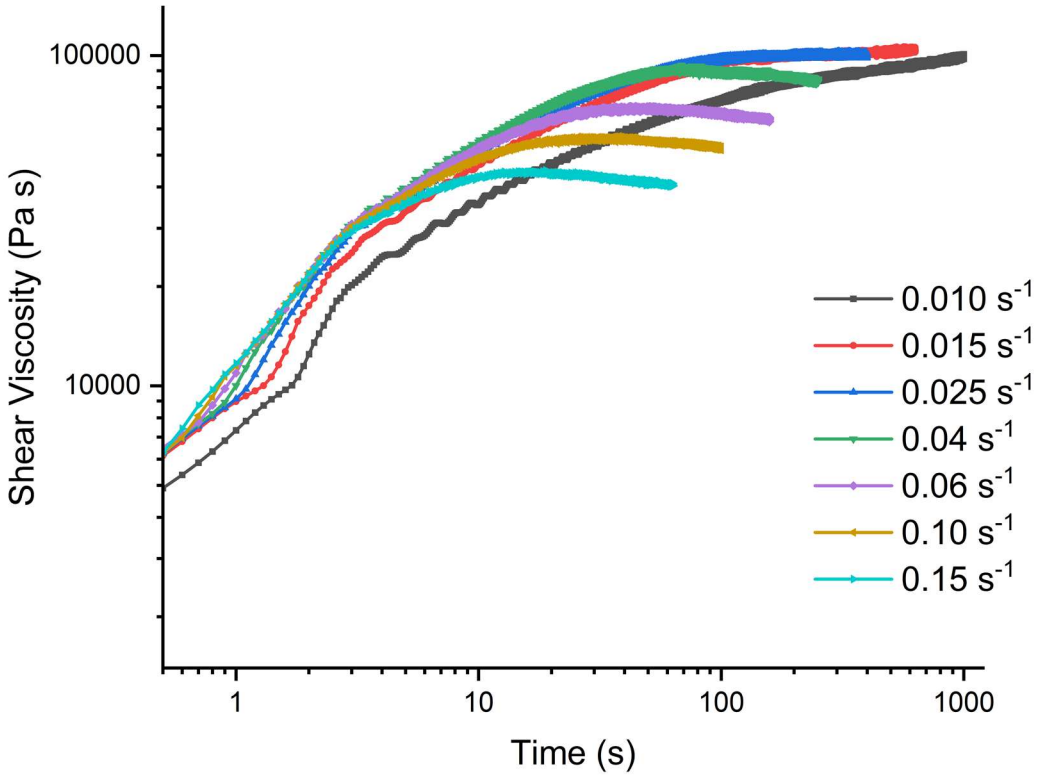

Figure S80: Step-shear non-linear rheology test on **M4** (at 190 °C) at different shear rates.

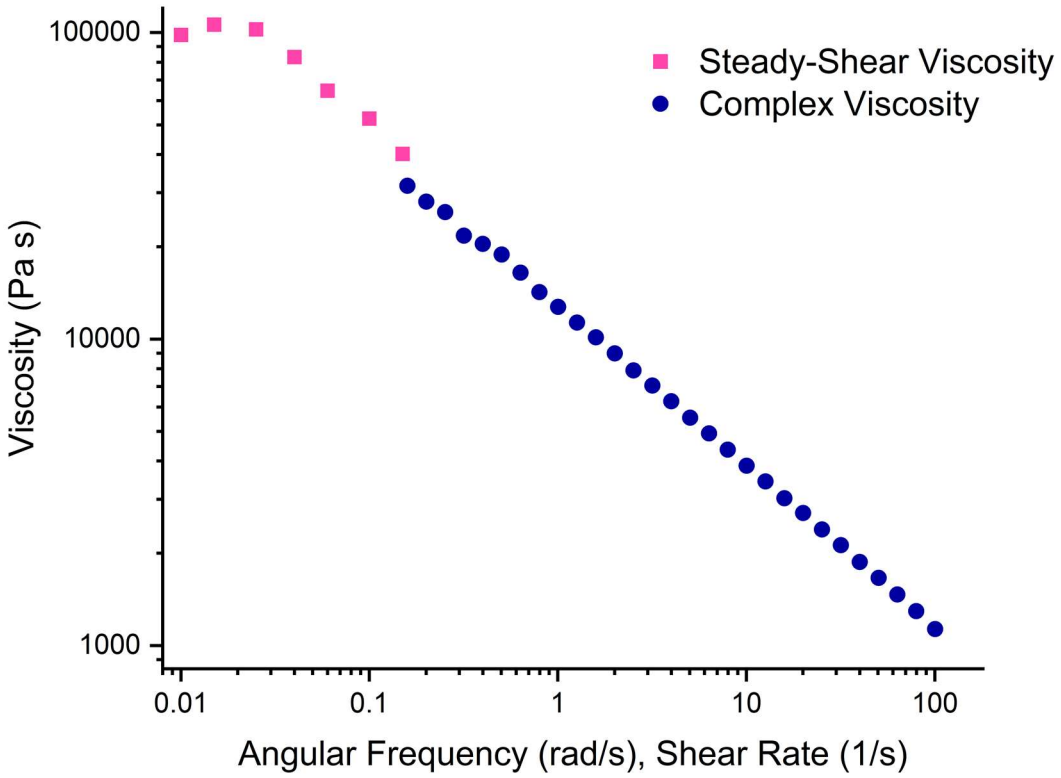

Figure S81: Dynamic viscosity (pink) and steady-state shear viscosity (blue) for **M4** to test the Cox-Merz rule.

- **M5**

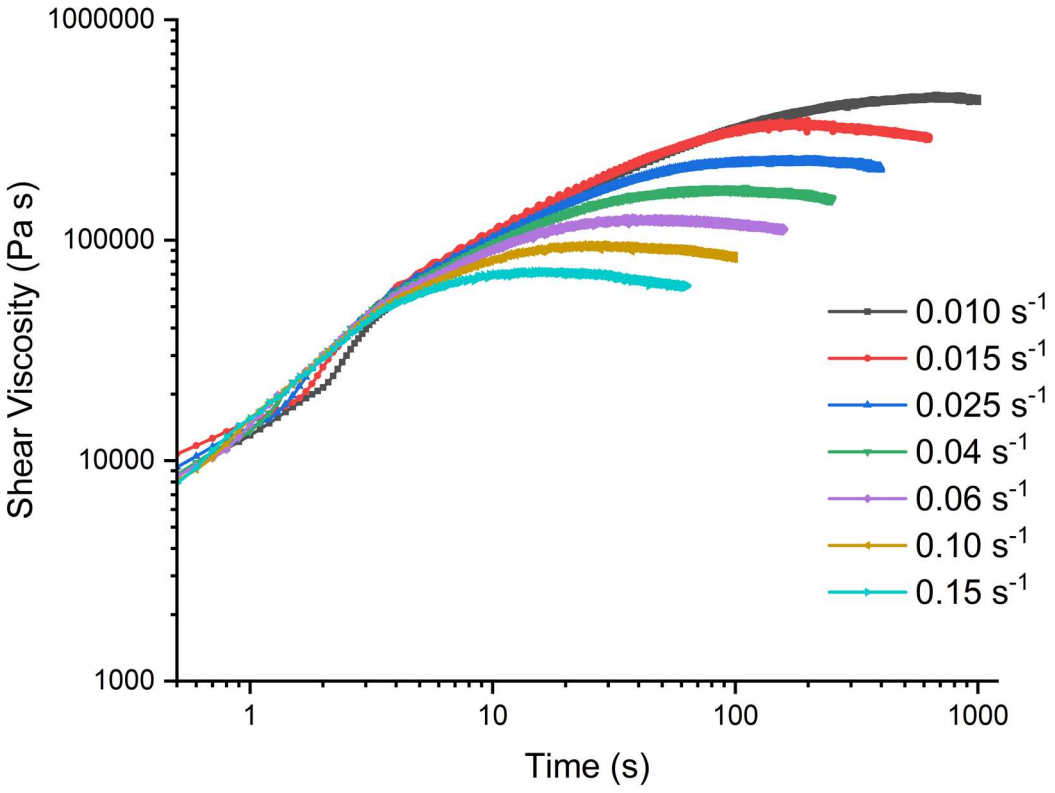

Figure S82: Step-shear non-linear rheology test on **M5** (at 190 °C) at different shear rates.

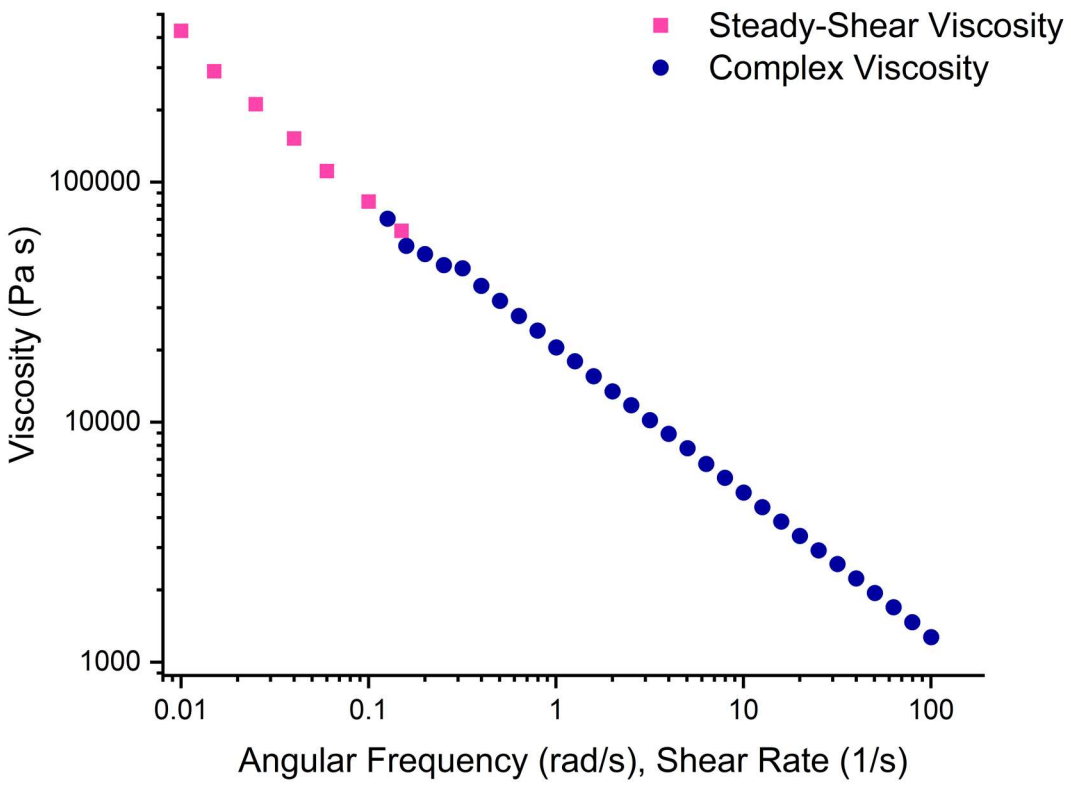

Figure S83: Dynamic viscosity (pink) and steady-state shear viscosity (blue) for **M5** to test the Cox-Merz rule.

4 Size Exclusion Chromatograms of the Modified Samples

- **M1**

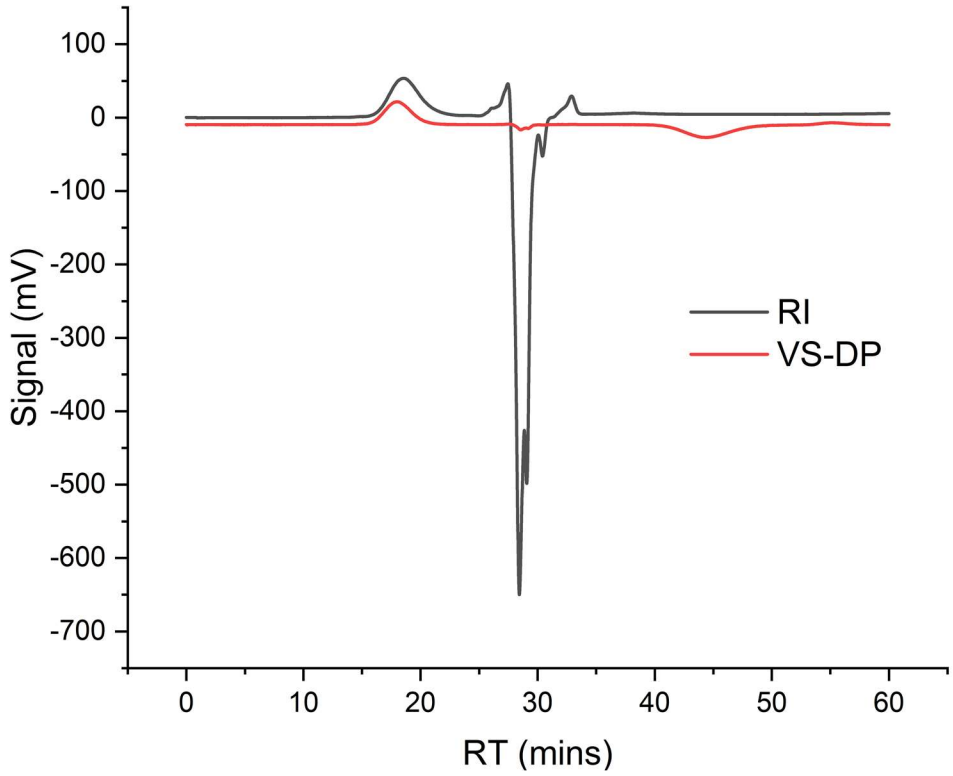

Figure S84: Raw GPC refractive index (RI) and viscometer differential pressure (VS-DP) traces recorded over retention time (RT) for **M1**.

- **M2**

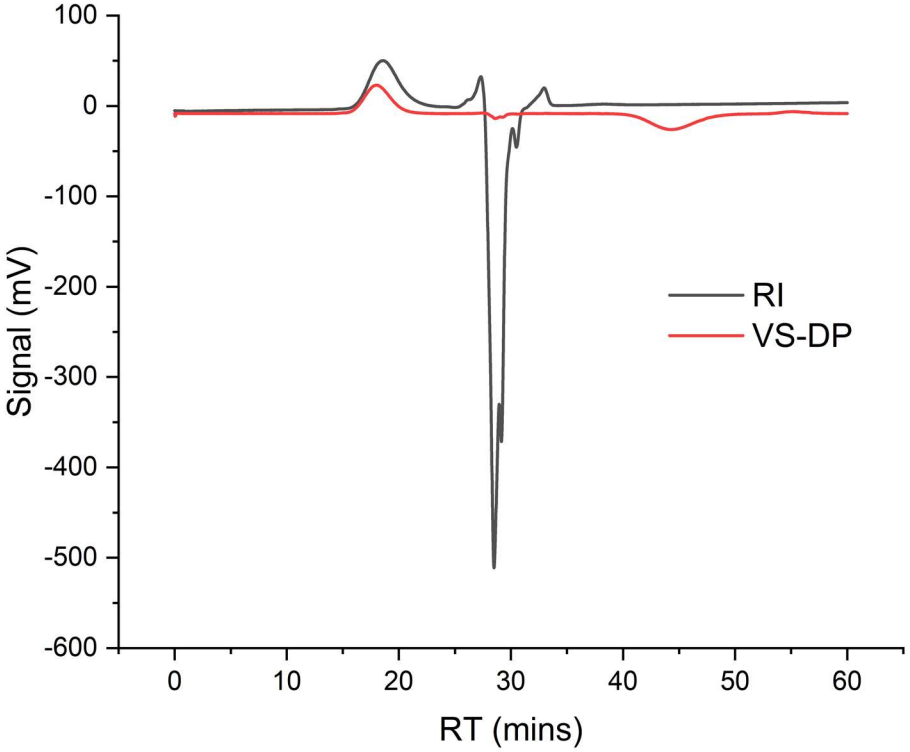

Figure S85: Raw GPC RI and VS-DP traces recorded over RT for **M2**.

- **M3**

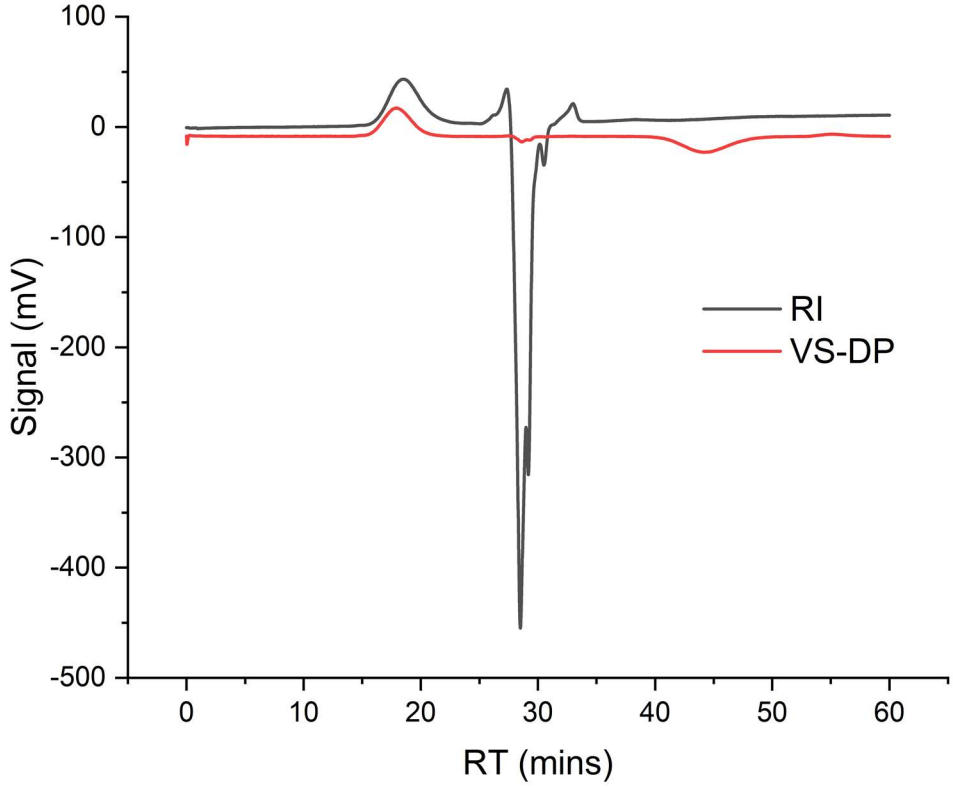

Figure S86: Raw GPC RI and VS-DP traces recorded over RT for **M3**.

- **M4**

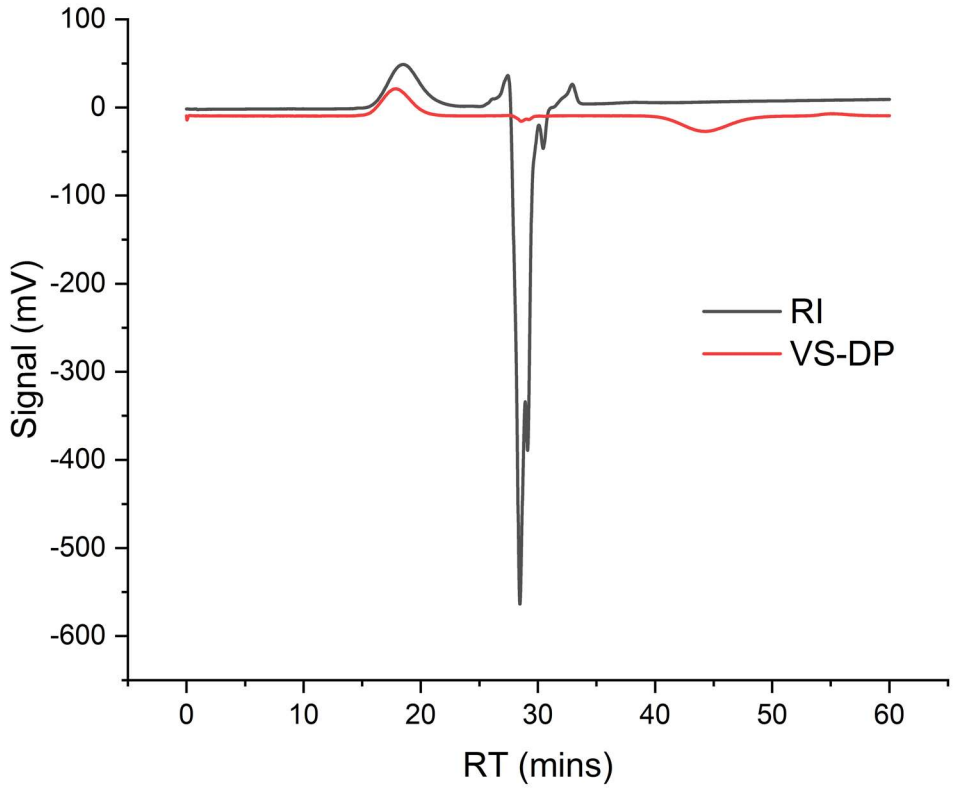

Figure S87: Raw GPC RI and VS-DP traces recorded over RT for **M4**.

- **M5**

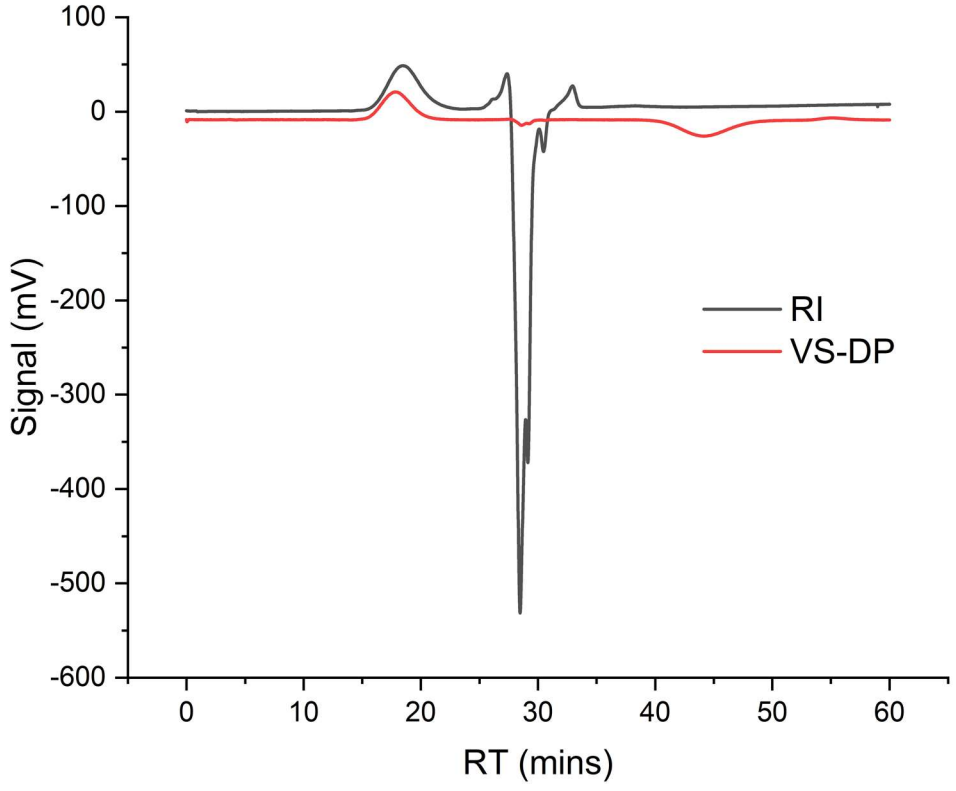

Figure S88: Raw GPC RI and VS-DP traces recorded over RT for **M5**.

- **M15**

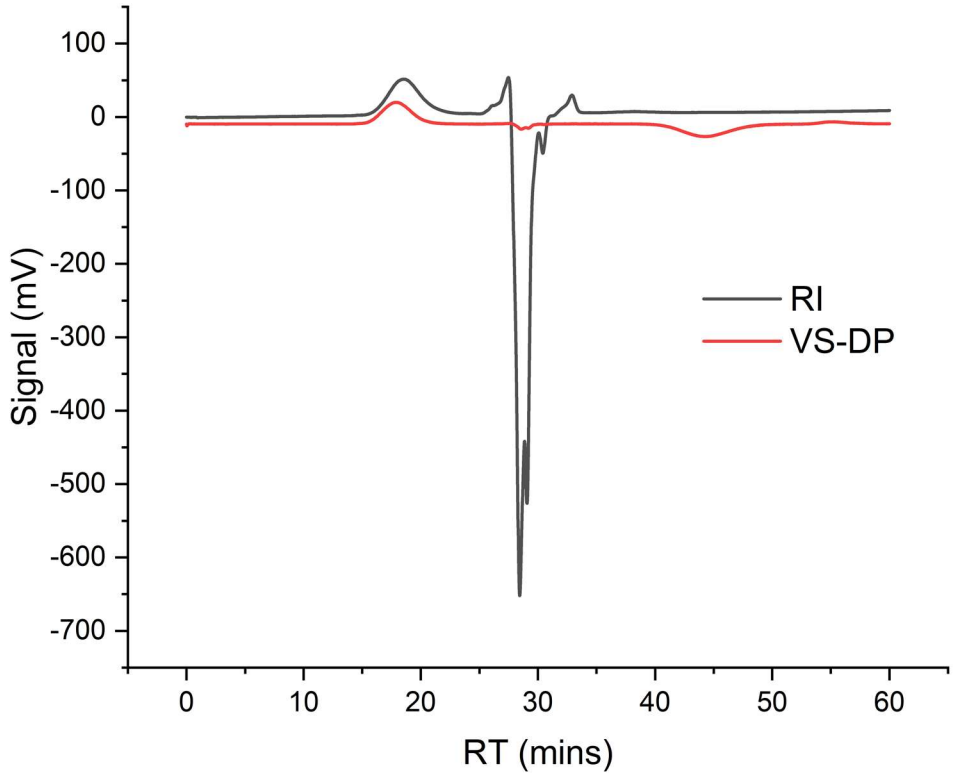

Figure S89: Raw GPC RI and VS-DP traces recorded over RT for **M15**.

- **M16**

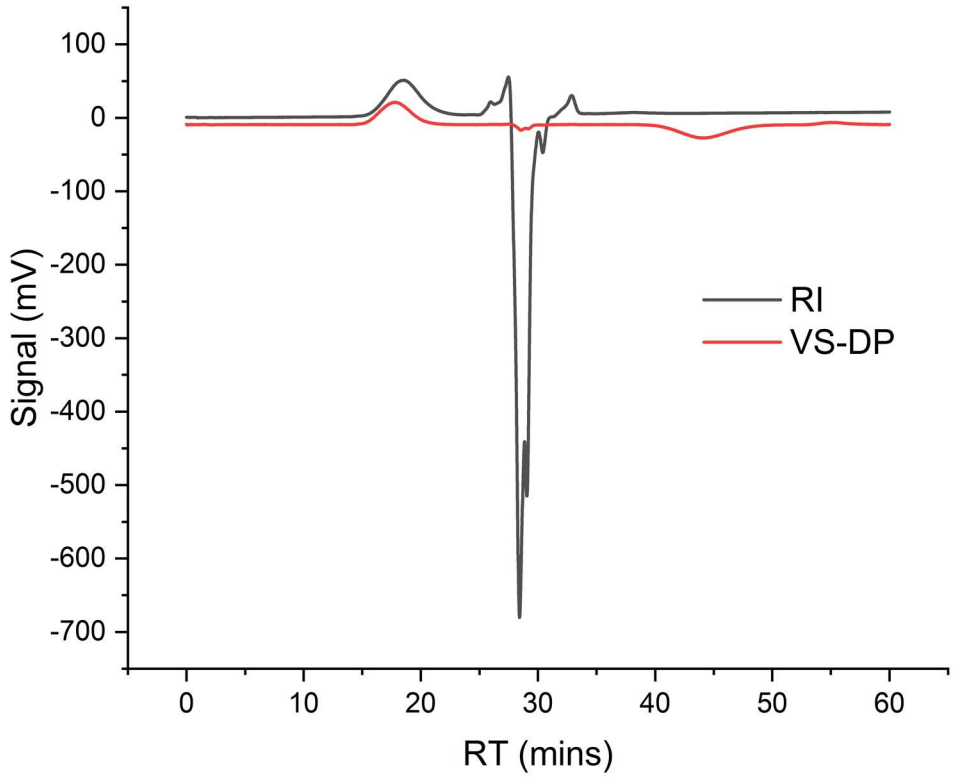

Figure S90: Raw GPC RI and VS-DP traces recorded over RT for **M16**.

5 Differential Scanning Calorimetry (DSC) Results of the Modified Samples

- **M1**

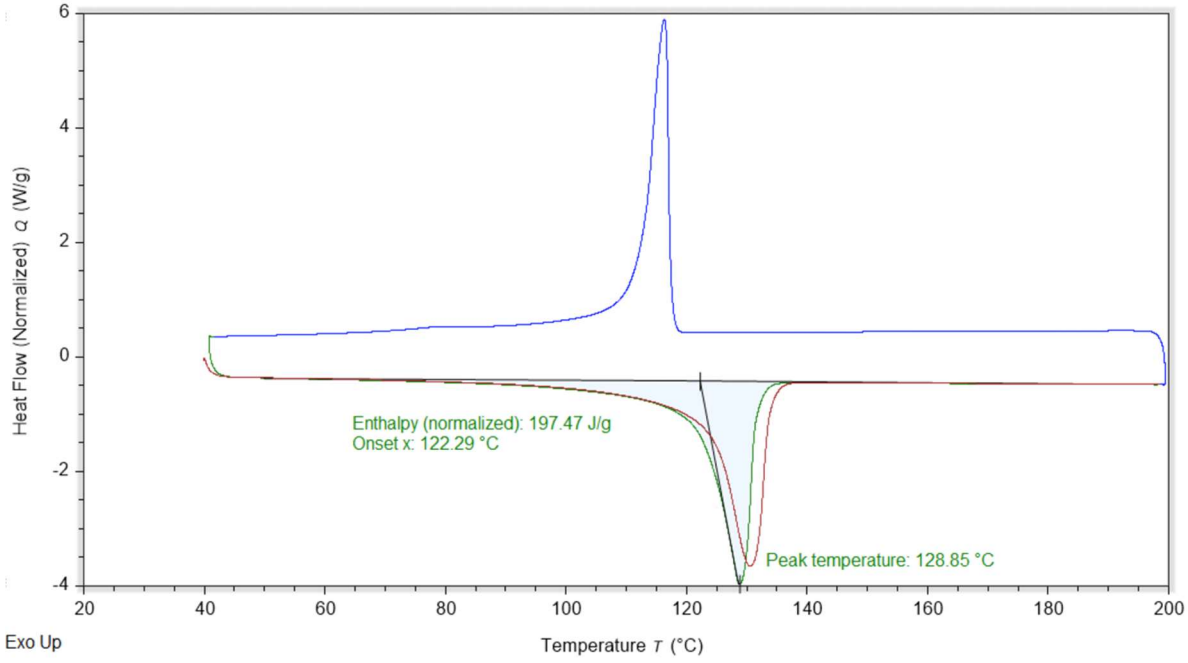

Figure S91: Heat flow traces recorded during the first test of **M1** as per the stated conditions in Experimental. Red, blue and green traces represent the first heating run, the cooling cycle and the second heating run, respectively.

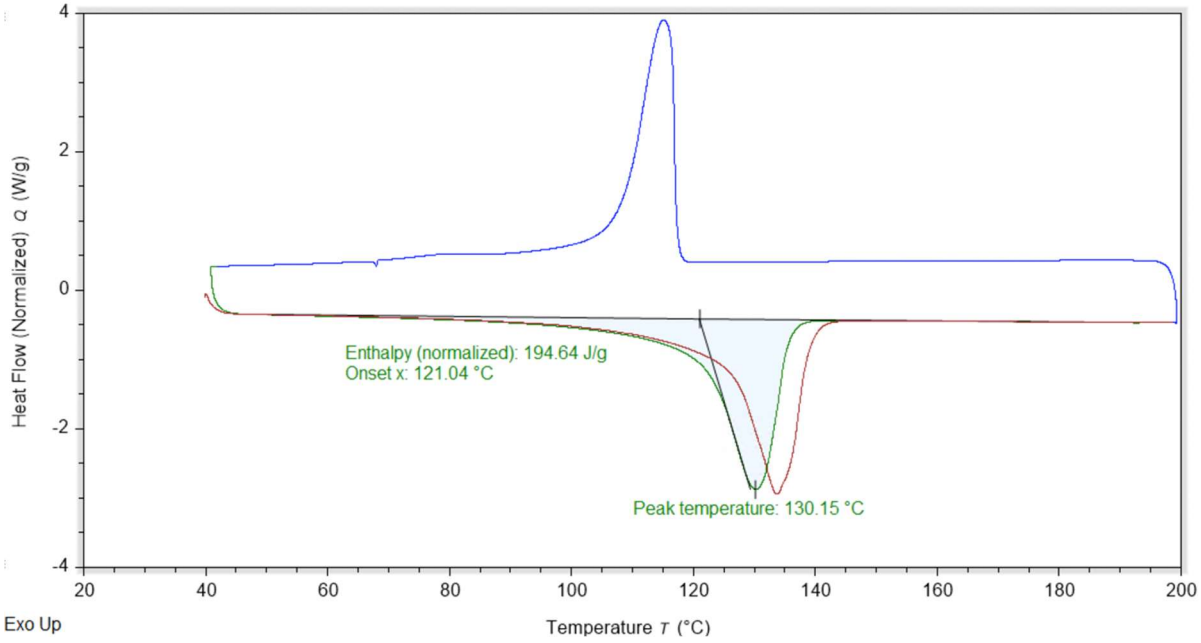

Figure S92: Heat flow traces recorded during the second test of **M1** as per the stated conditions in Experimental. Red, blue and green traces represent the first heating run, the cooling cycle and the second heating run, respectively.

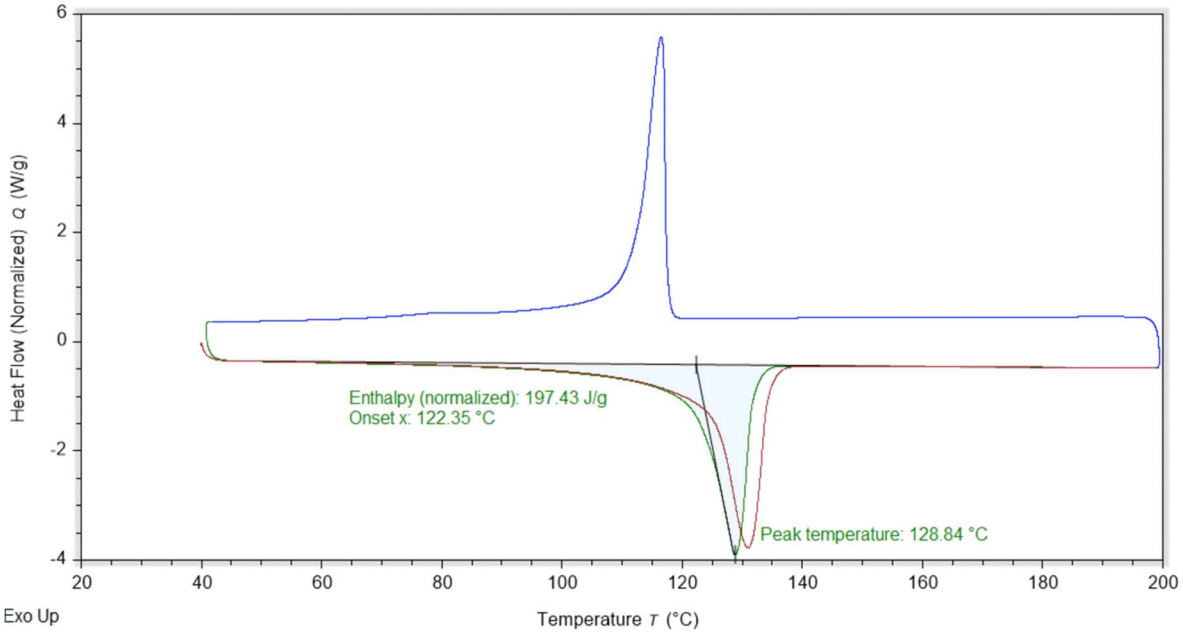

Figure S93: Heat flow traces recorded during the third test of **M1** as per the stated conditions in Experimental. Red, blue and green traces represent the first heating run, the cooling cycle and the second heating run, respectively.

Calculation S2: An example calculation of the polymer sample crystallinity using the energy changes observed with **M1**.

Average energy change = (197.47 J/g + 194.64 J/g + 197.43 J/g) / 3 = 196.51 J/g

Predicted energy change in a 100% crystalline HDPE sample = 290 J/g

%Crystallinity of **M1** = ((196.51 J/g) / (290 J/g)) * 100 = 67.8%

- **M2**

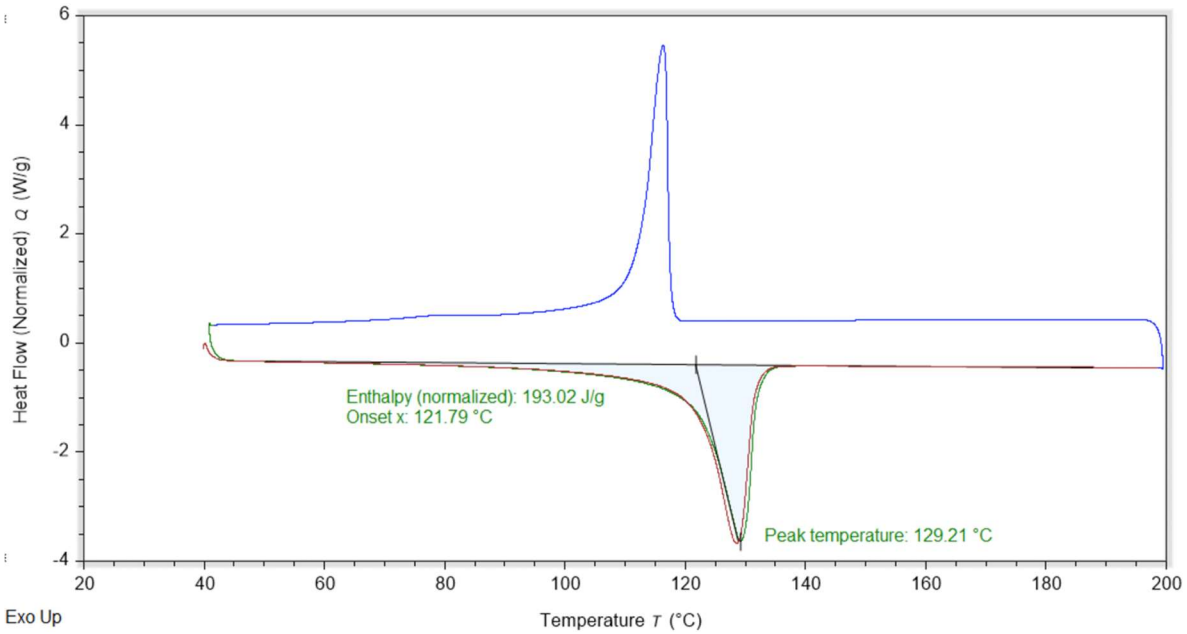

Figure S94: Heat flow traces recorded during the first test of **M2** as per the stated conditions in Experimental. Red, blue and green traces represent the first heating run, the cooling cycle and the second heating run, respectively.

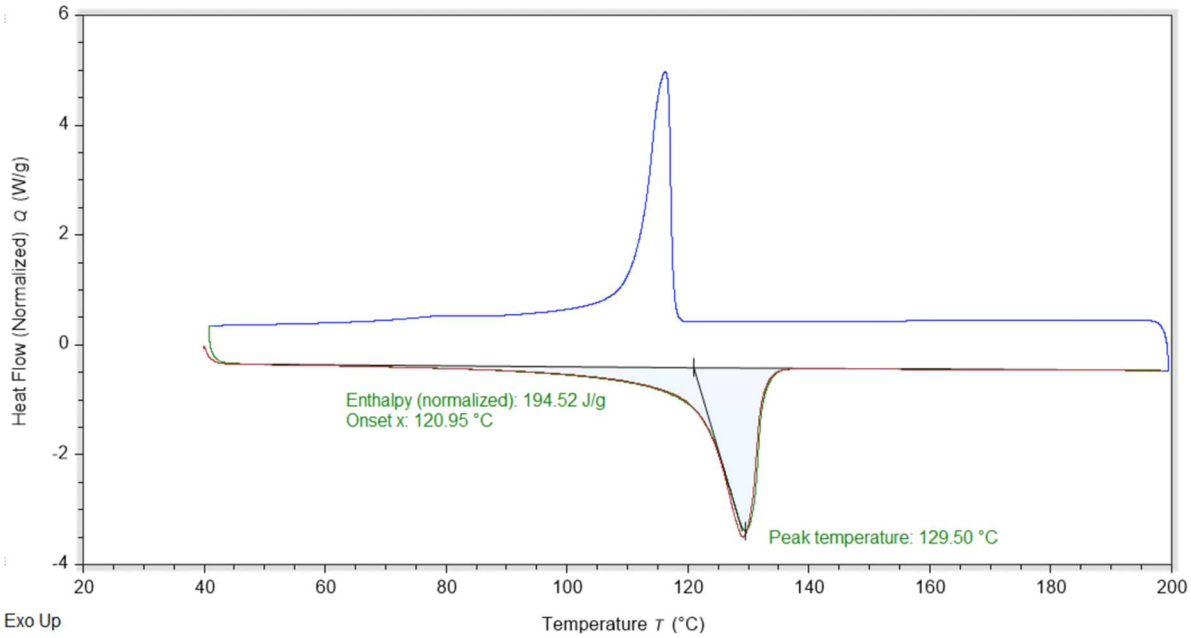

Figure S95: Heat flow traces recorded during the second test of **M2** as per the stated conditions in Experimental. Red, blue and green traces represent the first heating run, the cooling cycle and the second heating run, respectively.

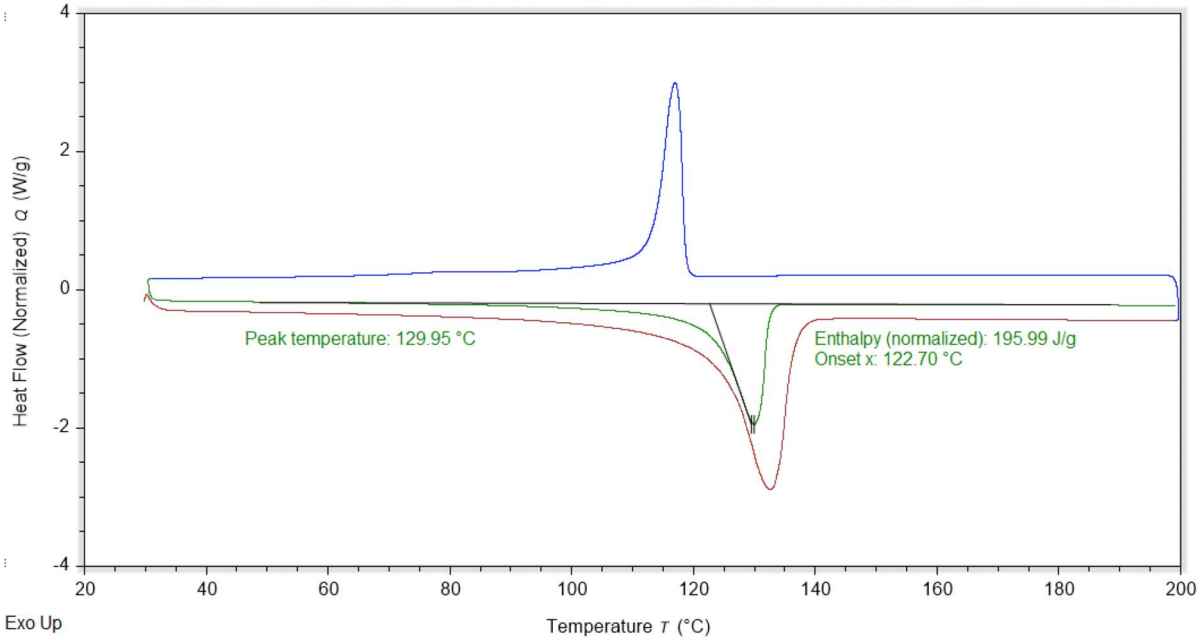

Figure S96: Heat flow traces recorded during the third test of **M2**. The initial heating cycle was run at a rate of 10 °C/min, the others performed at a rate of 5 °C/min. Red, blue and green traces represent the first heating run, the cooling cycle and the second heating run, respectively.

- **M3**

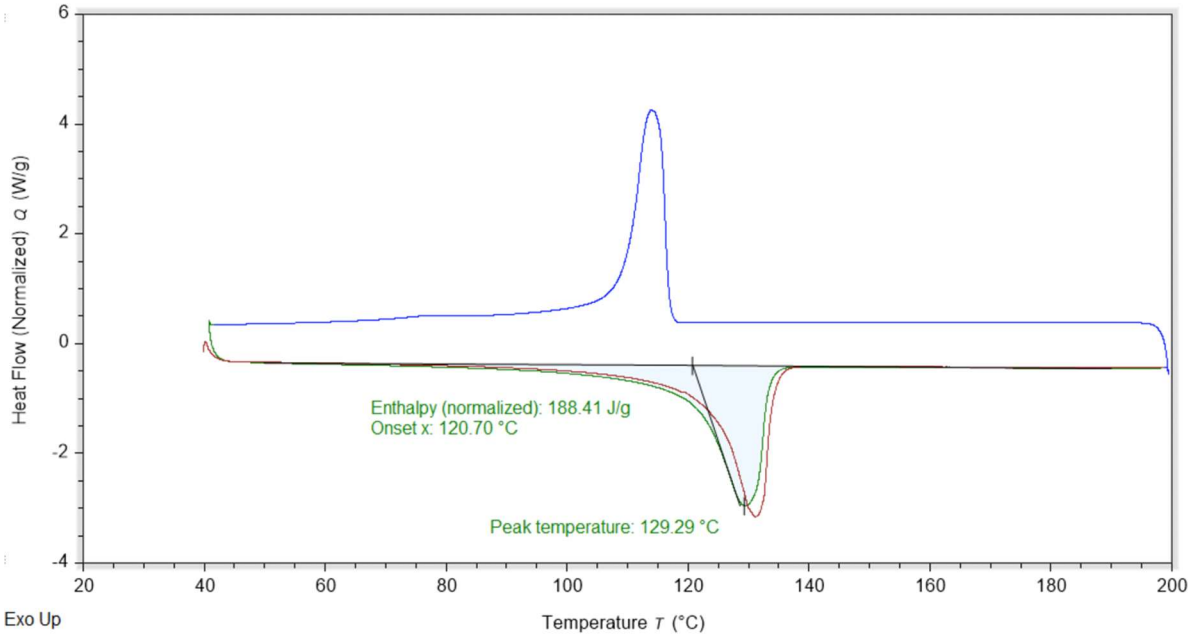

Figure S97: Heat flow traces recorded during the first test of **M3** as per the stated conditions in Experimental. Red, blue and green traces represent the first heating run, the cooling cycle and the second heating run, respectively.

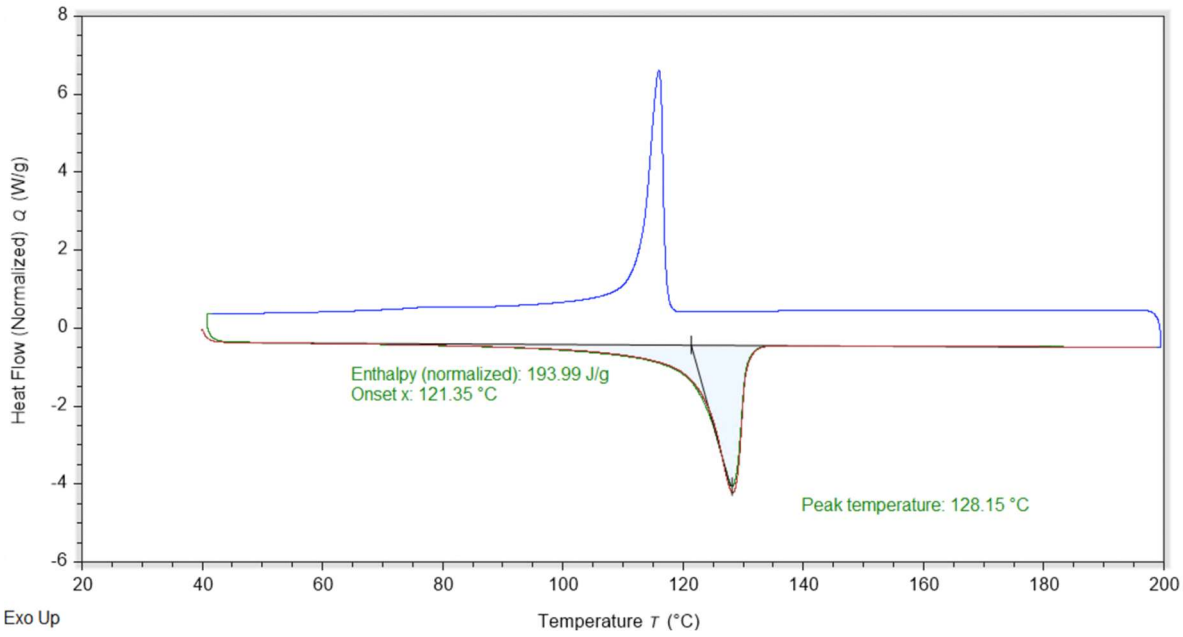

Figure S98: Heat flow traces recorded during the second test of **M3** as per the stated conditions in Experimental. Red, blue and green traces represent the first heating run, the cooling cycle and the second heating run, respectively.

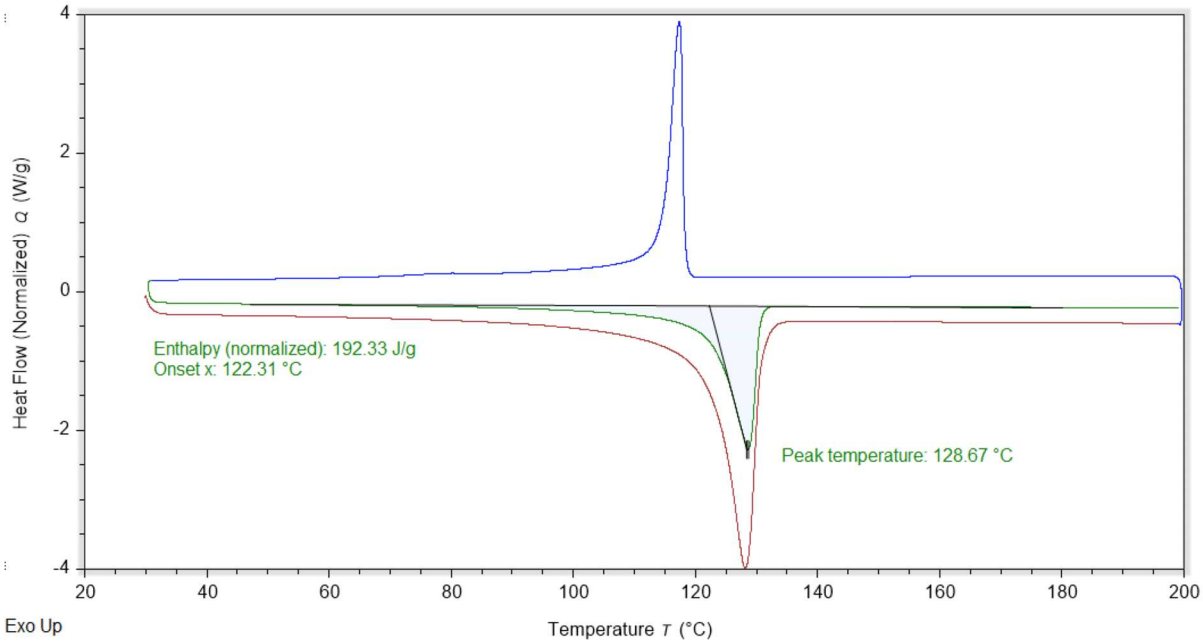

Figure S99: Heat flow traces recorded during the third test of **M3**. The initial heating cycle was run at a rate of 10 °C/min, the others performed at a rate of 5 °C/min. Red, blue and green traces represent the first heating run, the cooling cycle and the second heating run, respectively.

- **M4**

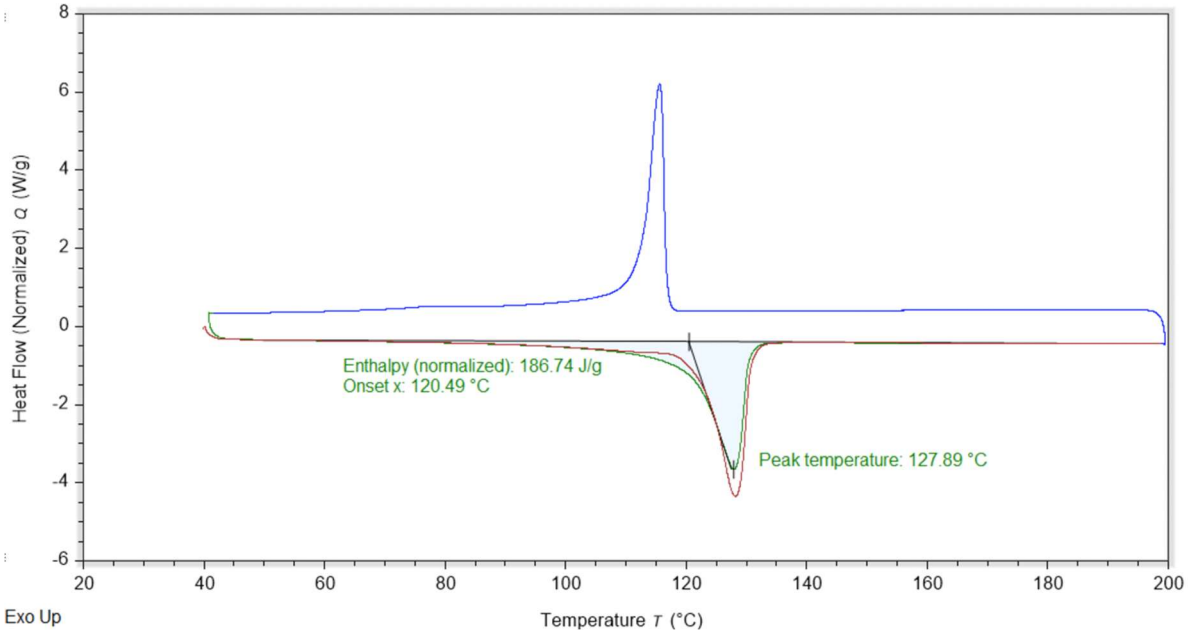

Figure S100: Heat flow traces recorded during the first test of **M4** as per the stated conditions in Experimental. Red, blue and green traces represent the first heating run, the cooling cycle and the second heating run, respectively.

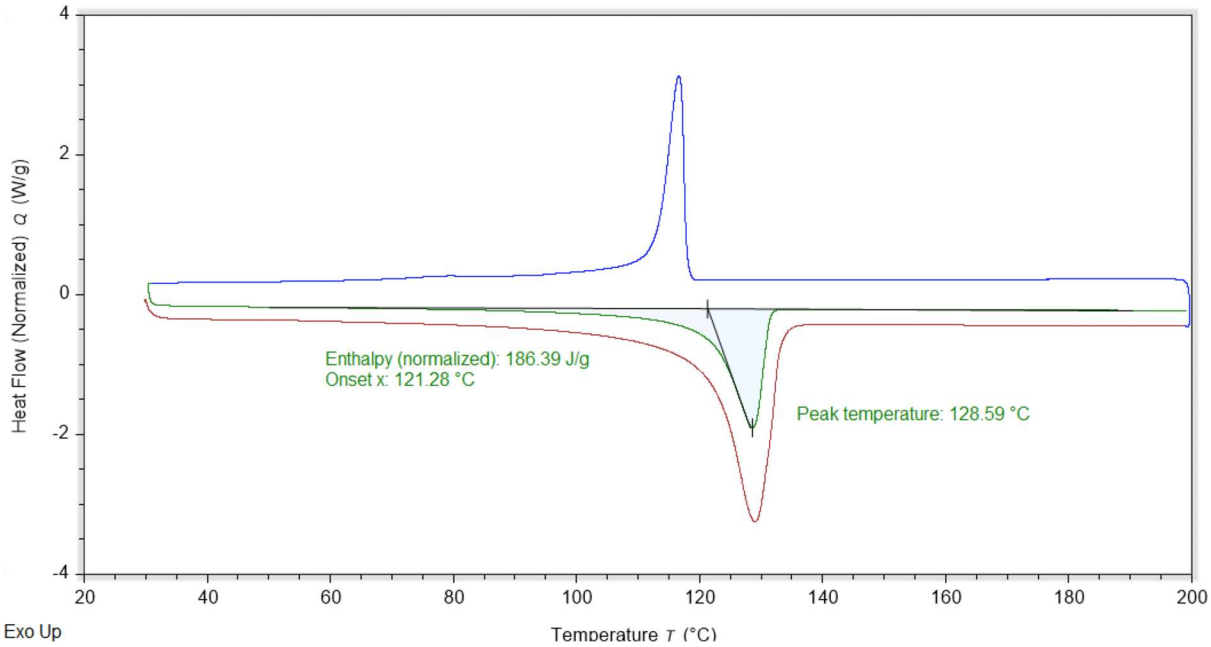

Figure S101: Heat flow traces recorded during the second test of **M4**. The initial heating cycle was run at a rate of 10 °C/min, the others performed at a rate of 5 °C/min. Red, blue and green traces represent the first heating run, the cooling cycle and the second heating run, respectively.

- **M5**

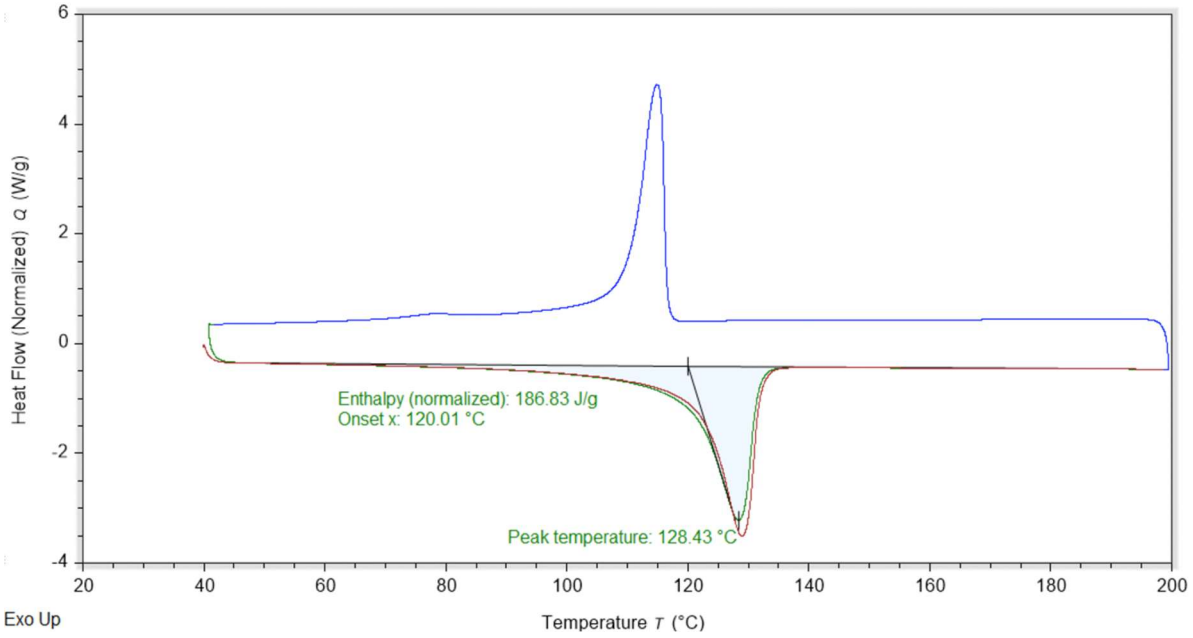

Figure S102: Heat flow traces recorded during the first test of **M5** as per the stated conditions in Experimental. Red, blue and green traces represent the first heating run, the cooling cycle and the second heating run, respectively.

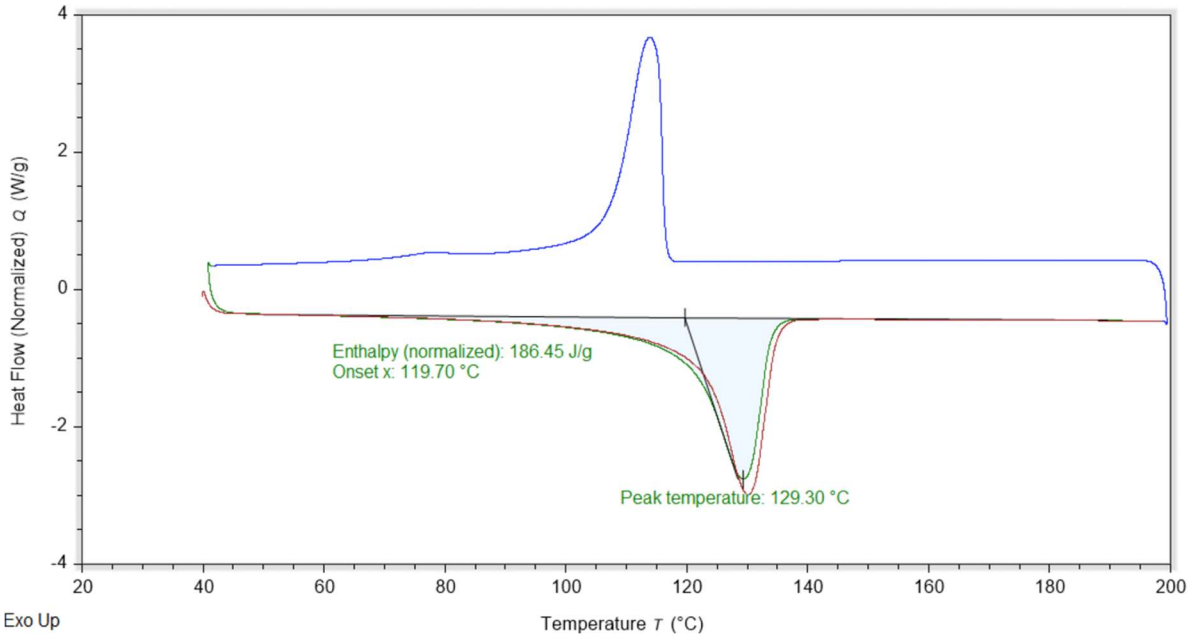

Figure S103: Heat flow traces recorded during the second test of **M5** as per the stated conditions in Experimental. Red, blue and green traces represent the first heating run, the cooling cycle and the second heating run, respectively.

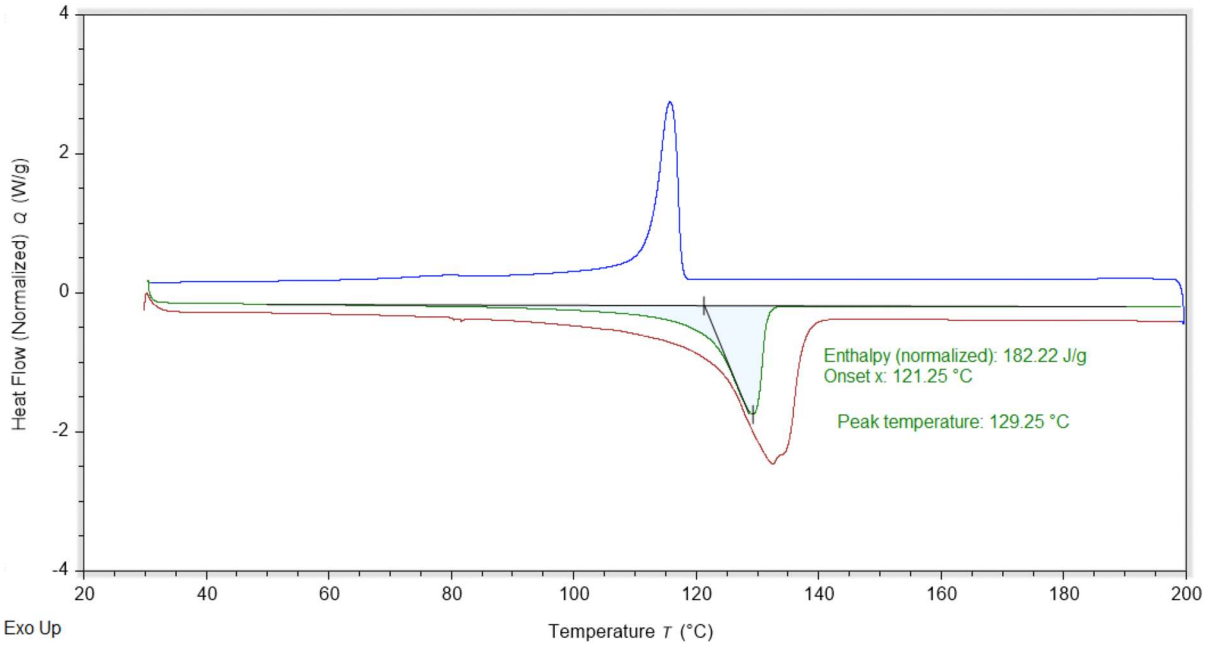

Figure S104: Heat flow traces recorded during the third test of **M5**. The initial heating cycle was run at a rate of 10 °C/min, the others performed at a rate of 5 °C/min. Red, blue and green traces represent the first heating run, the cooling cycle and the second heating run, respectively.

- **M15**

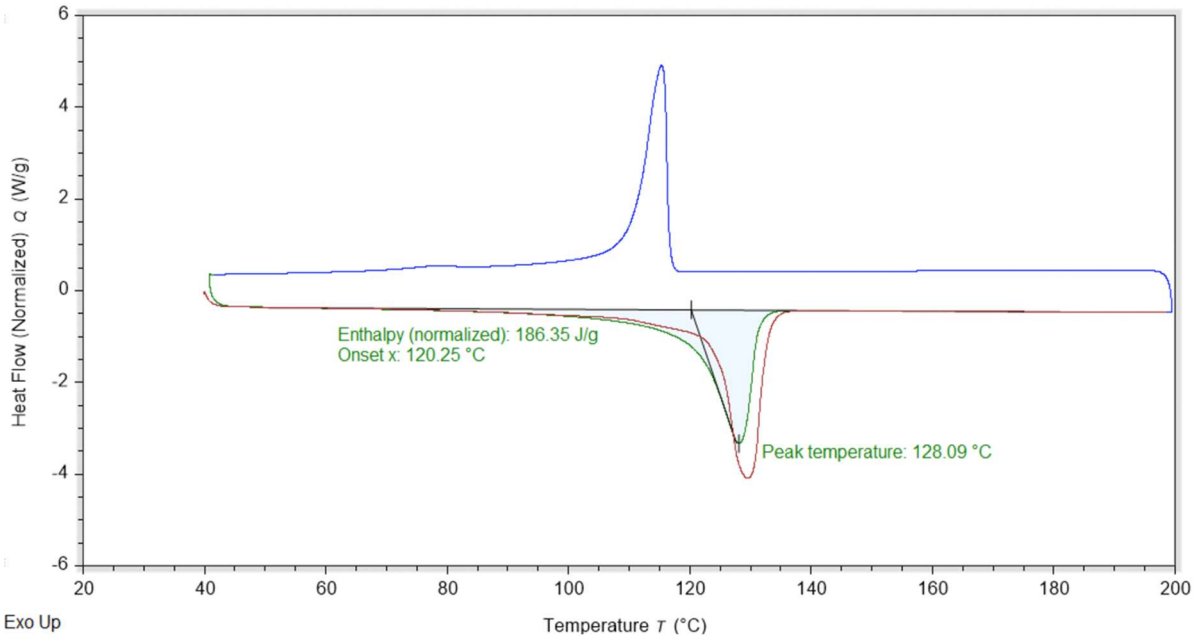

Figure S105: Heat flow traces recorded during the first test of **M15** as per the stated conditions in Experimental. Red, blue and green traces represent the first heating run, the cooling cycle and the second heating run, respectively.

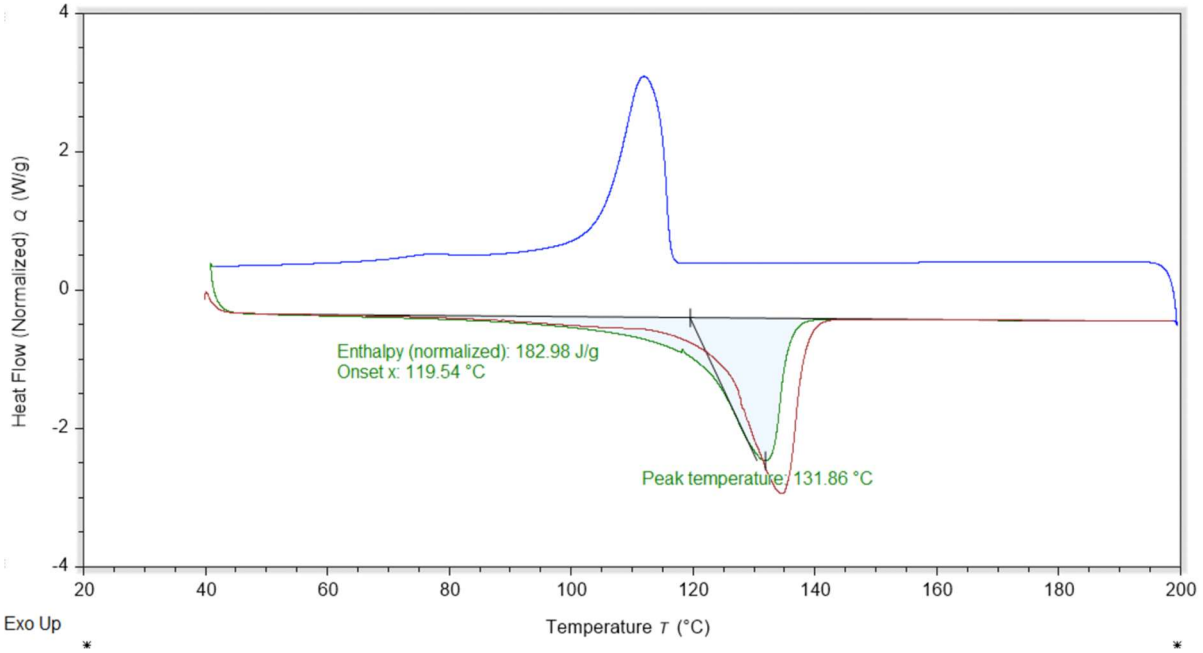

Figure S106: Heat flow traces recorded during the second test of **M15** as per the stated conditions in Experimental. Red, blue and green traces represent the first heating run, the cooling cycle and the second heating run, respectively.

- **M16**

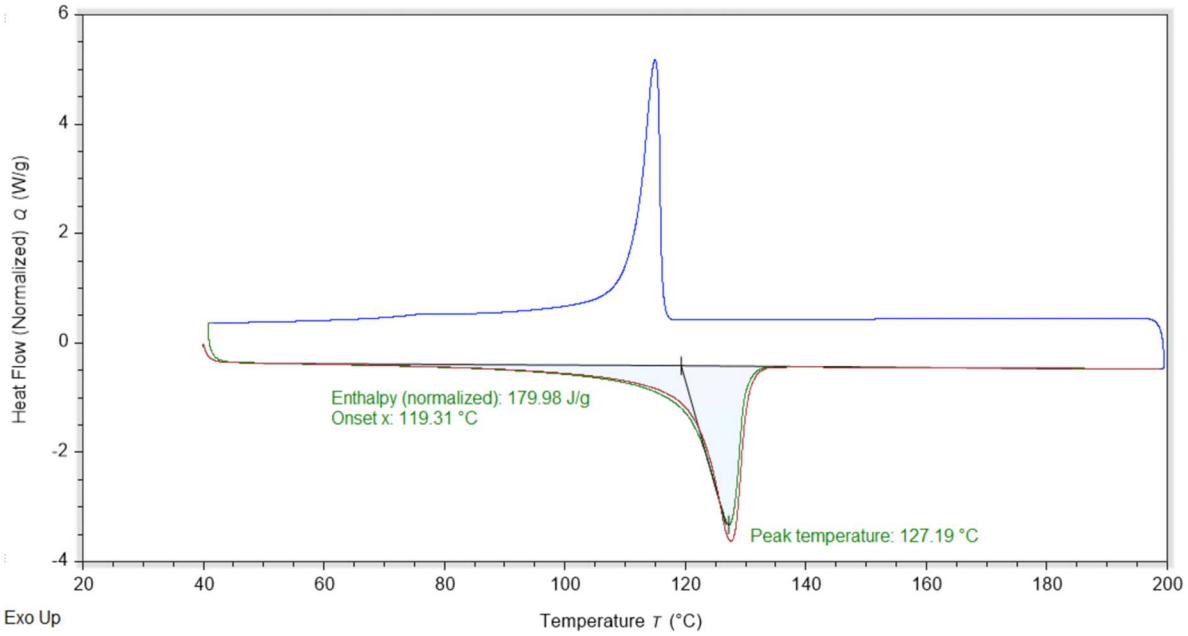

Figure S107: Heat flow traces recorded during the first test of **M16** as per the stated conditions in Experimental. Red, blue and green traces represent the first heating run, the cooling cycle and the second heating run, respectively.

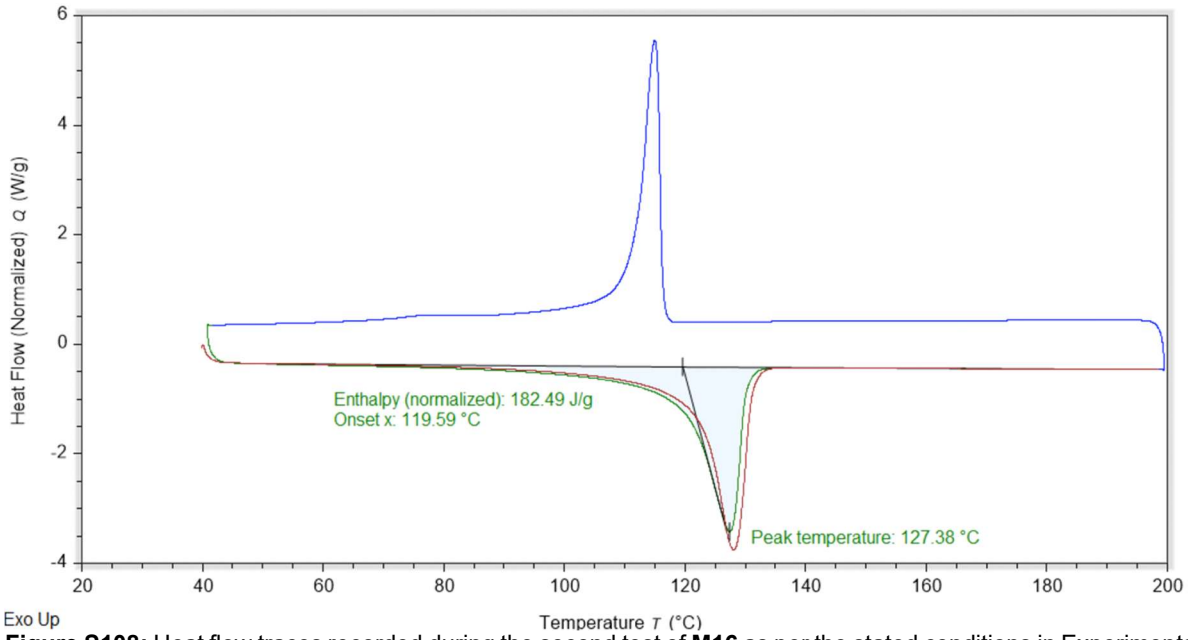

Figure S108: Heat flow traces recorded during the second test of **M16** as per the stated conditions in Experimental. Red, blue and green traces represent the first heating run, the cooling cycle and the second heating run, respectively.

Table S2: A summary of the energy change and crystallinity results from the DSC traces. An example calculation is provided in **Calculation S2**.

Sample	Average Melting Enthalpy (J/g)	Standard Deviation (± J/g)	Crystallinity (%)	Propagated Error (± %)
M1	196.5	1.6	67.8	0.6
M2	194.5	1.5	67.0	0.5
M3	191.6	2.9	66.1	1.0
M4	186.6	0.2	64.3	0.1
M5	185.2	2.6	63.9	0.9
M15	184.7	2.4	63.7	0.8
M16	181.2	1.8	62.5	0.6

6 Wide Angle and Small Angle X-Ray Scattering (WAXS and SAXS) Results

- **WAXS**

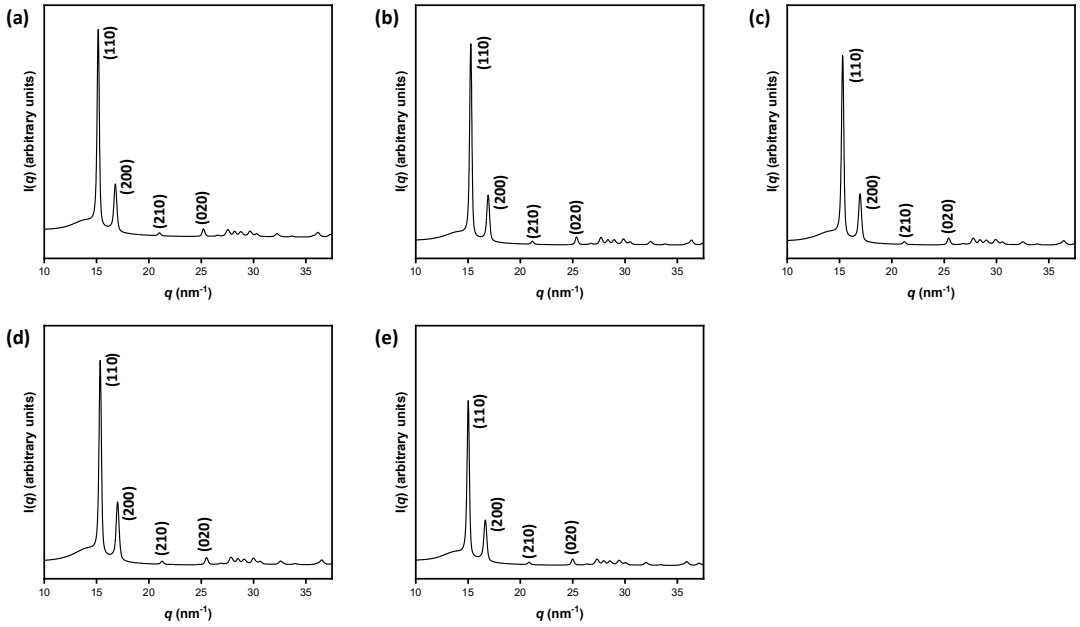

Figure S109: WAXS intensity profiles of polymer films **(a) M1**, **(b) M2**, **(c) M3**, **(d) M4**, and **(e) M5**, where the peaks in each pattern are annotated with the corresponding reflections of an orthorhombic crystalline structure.

- **SAXS**

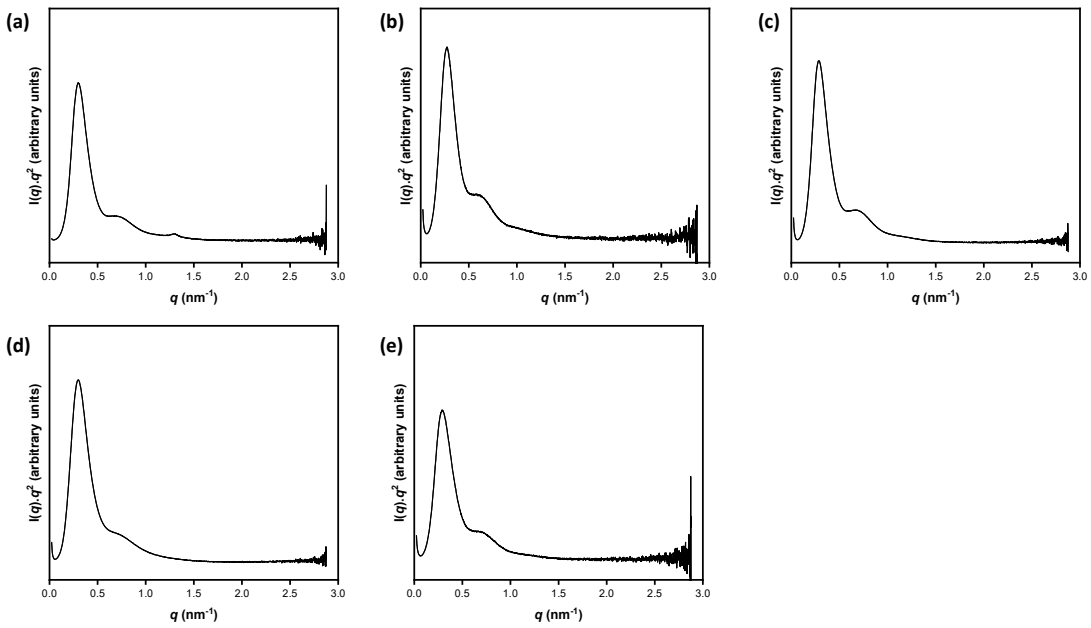

Figure S110: Lorentz-corrected SAXS intensity profiles of polymer films **(a) M1**, **(b) M2**, **(c) M3**, **(d) M4**, and **(e) M5**.

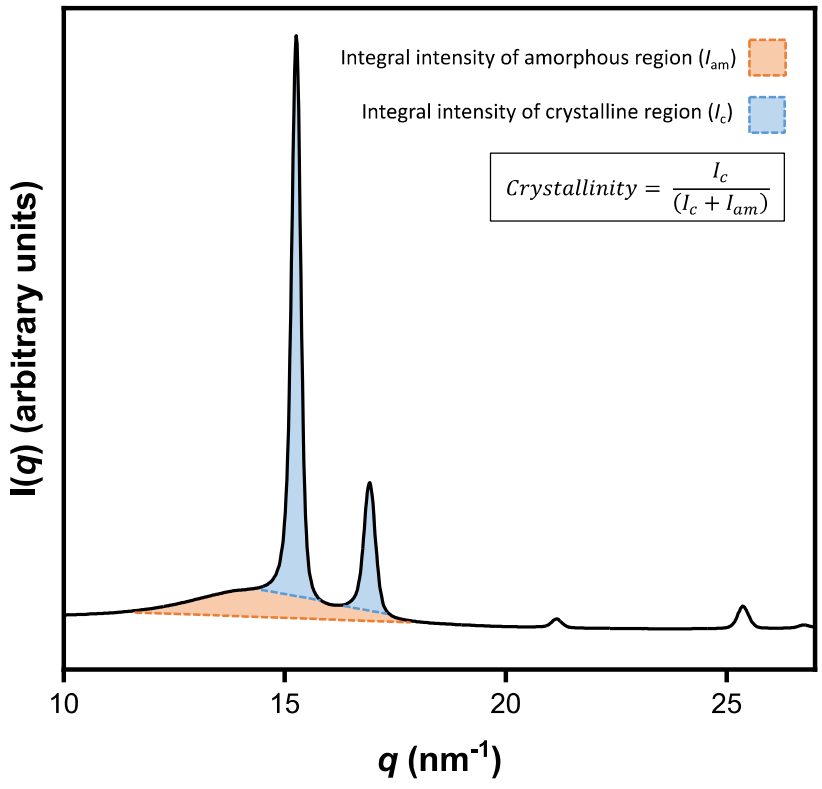

Figure S111: Example degree of crystallinity calculation using the WAXS intensity profile for **M2**.

7 NMR Spectroscopy Results of the Modified Samples

- **M1-M5**

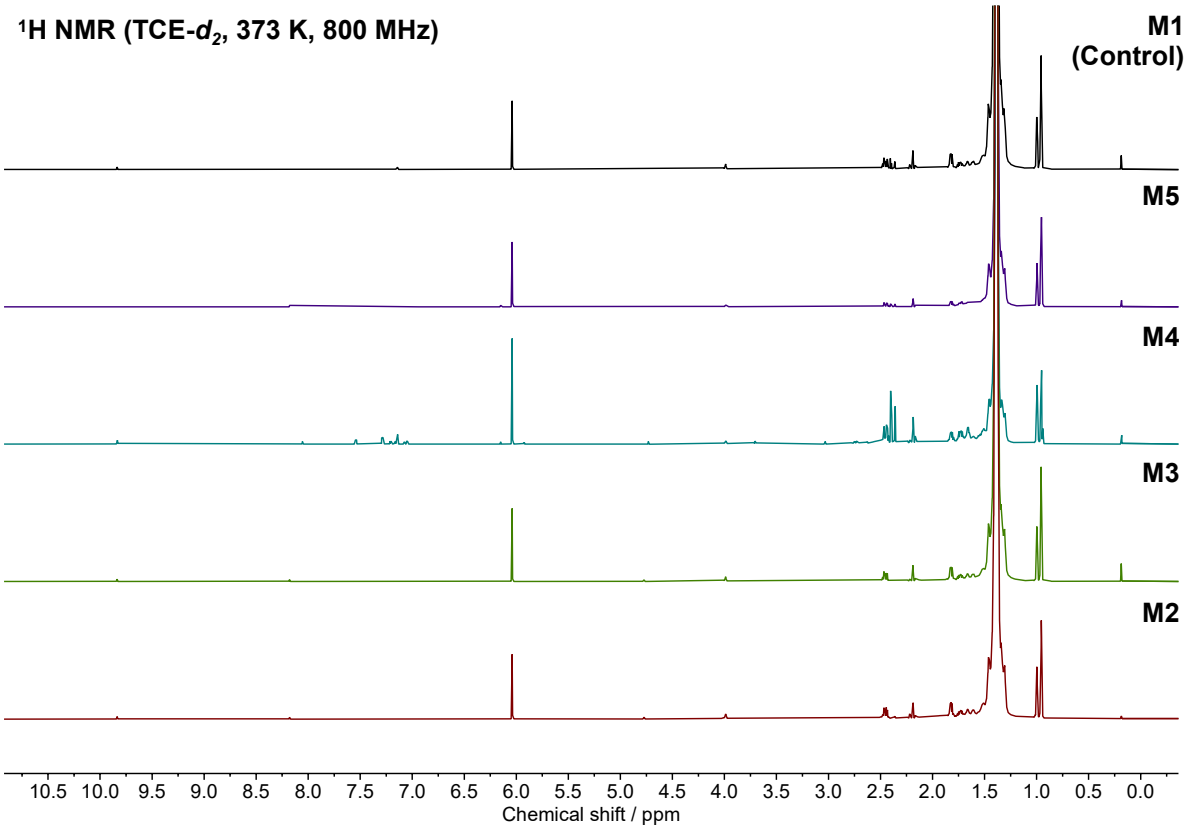

Figure S112: Stacked ^{1}H NMR spectra of **M1-5**.

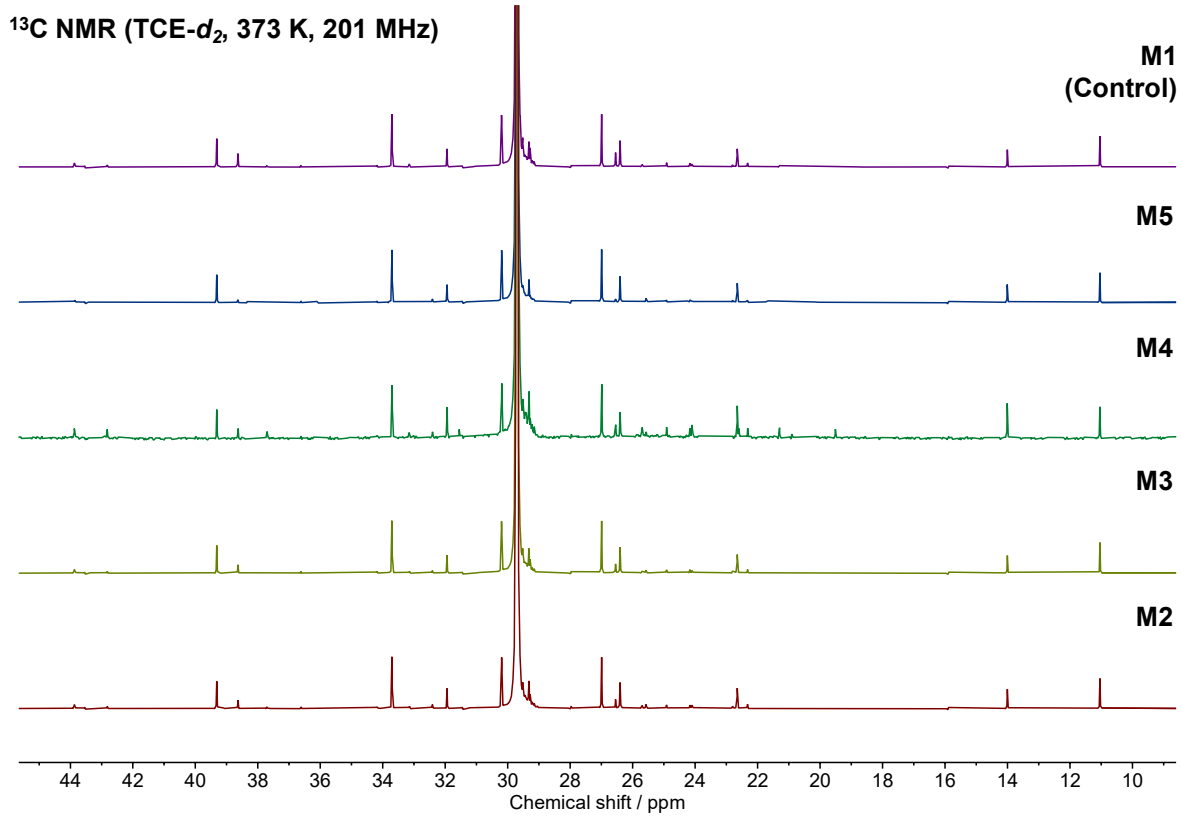

Figure S113: Stacked ^{13}C NMR spectra of **M1-5**.

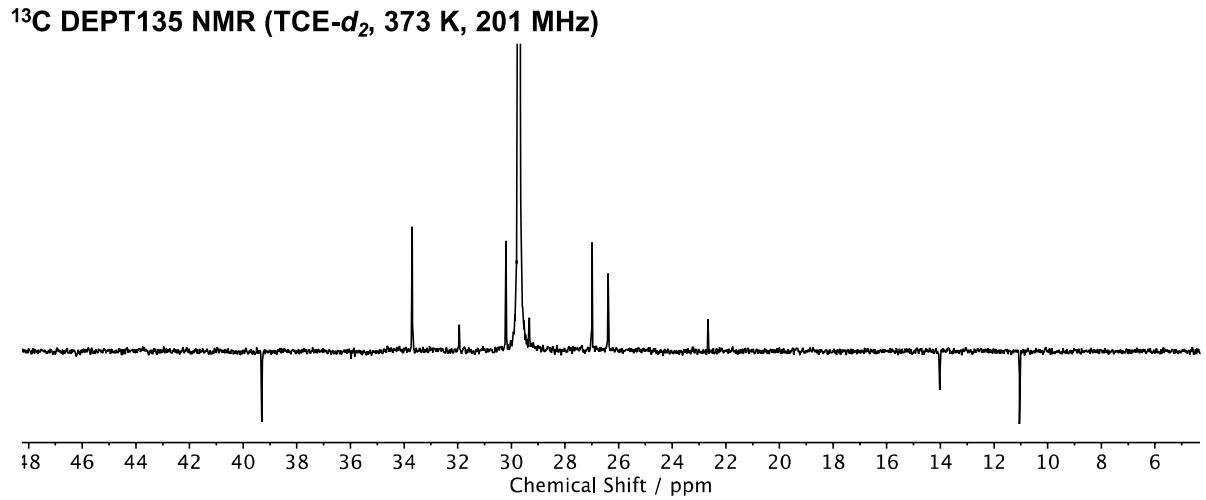

Figure S114: The ^{13}C distortionless enhancement by polarisation transfer (DEPT) NMR spectrum of **M5**.

- **M15 and M16**

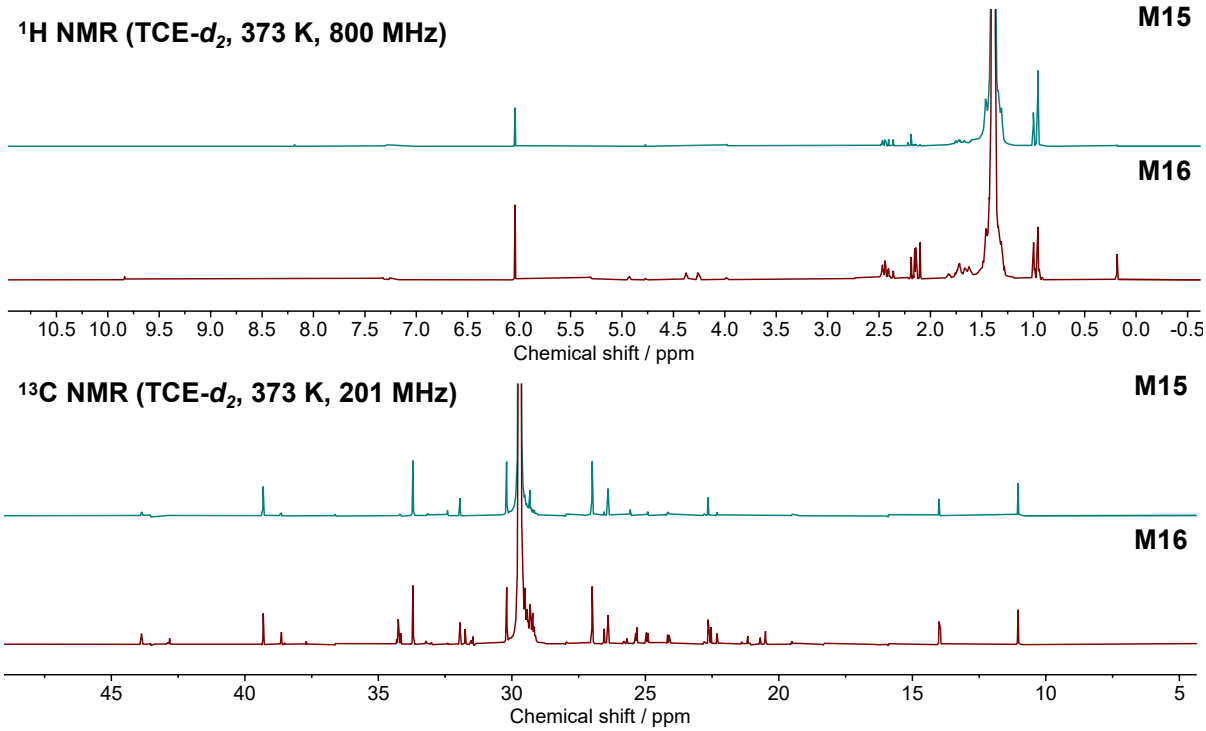

Figure S115: ^{1}H and ^{13}C NMR spectra of **M15** and **M16**.

8 Small Molecule Reactivity Studies on *n*-Dodecane

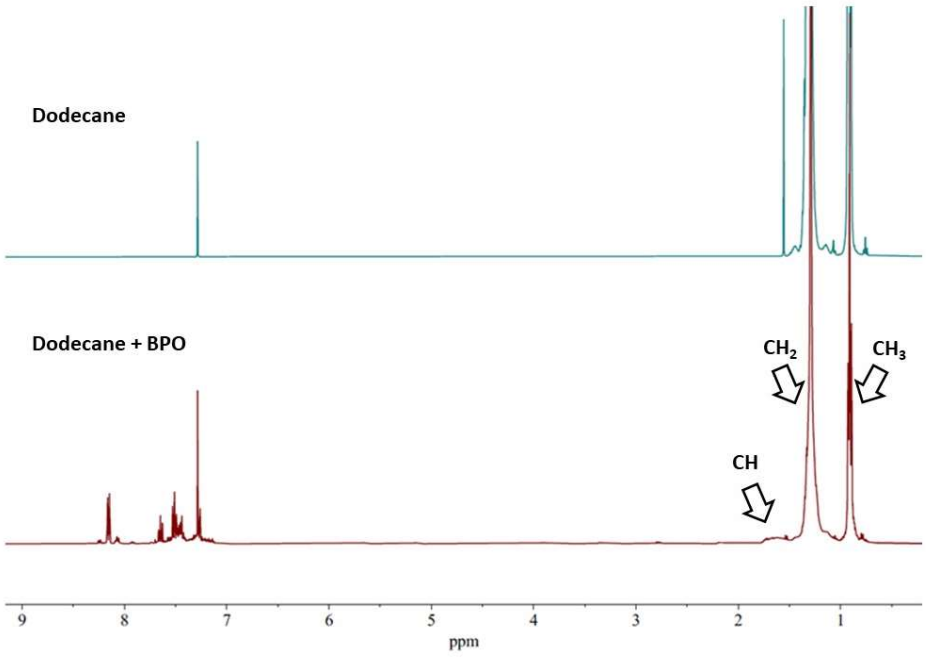

Figure S116: Overlaid ^{1}H NMR spectrum showing dodecane before (top) and after (bottom) reaction with benzoyl peroxide.

9 FT-IR Analysis

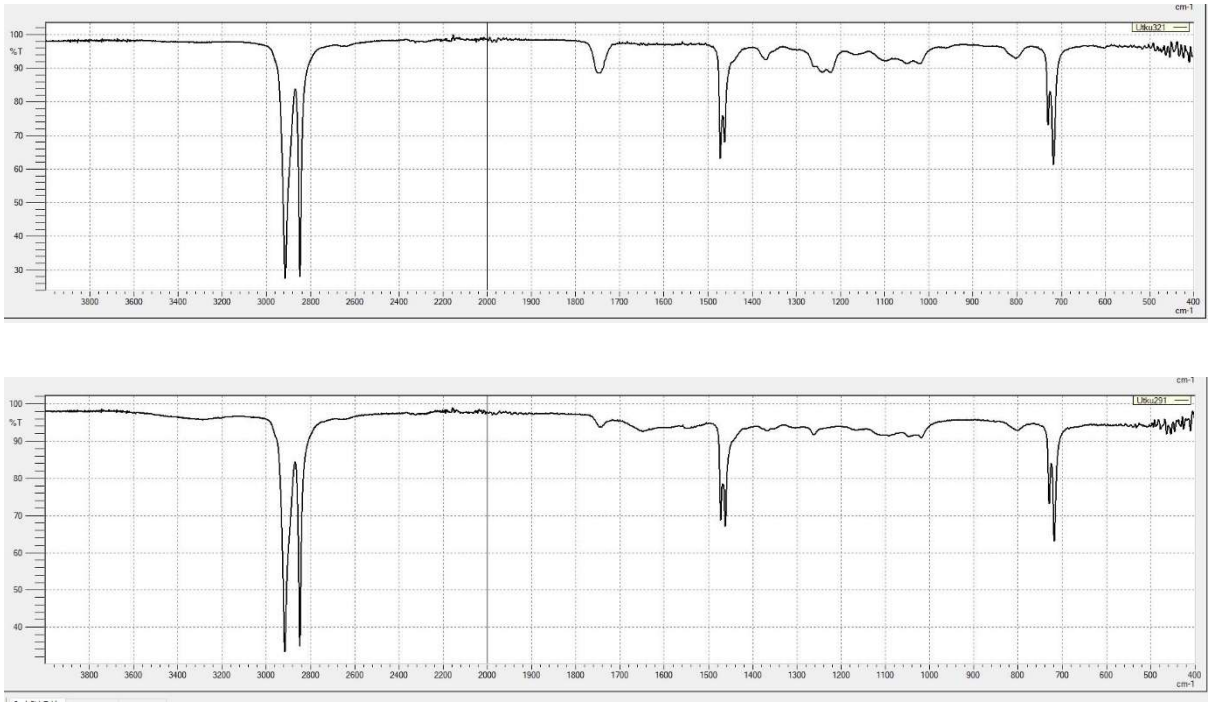

Figure S117: FT-IR analysis of sample **M1** (control reaction, top) and sample **M5** (6 wt% DLP, bottom), showing the lack of significant oxidation following peroxide modification under N_2 atmosphere. Sample **M5** was selected for comparative purposes as it has the highest peroxide loading of all samples tested.

10 References

1. Randall, J. C., A Review of High Resolution Liquid 13Carbon Nuclear Magnetic Resonance Characterizations of Ethylene-Based Polymers. *Journal of Macromolecular Science, Part C* **1989,** *29* (2-3), 201-317.